

TABLE OF CONTENTS

ACKNOWLEDGEMENTS	iii
TABLE OF CONTENTS	iv
LIST OF TABLES	vi
LIST OF FIGURES	viii
ABSTRACT	xii
CHAPTER 1 INTRODUCTION	1
1.1 Overview	1
1.2 Research Objectives and Organization of the Dissertation	2
CHAPTER 2 ALKALI SILICA REACTION AND RECYCLED CONCRETE AGGREGATE	4
2.1 Alkali Silica Reaction (ASR)	4
2.1.1 ASR essentials	4
2.1.2 ASR mechanisms	5
2.1.3 ASR test methods review	7
2.1.4 Potential mitigation methods	9
2.2 Recycled Concrete Aggregate (RCA)	11
2.2.1 Recycled aggregate preview	11
2.2.2 RCA with ASR distress	13
2.2.3 RCA alkali contribution and alkali leaching	17
CHAPTER 3 PORE SOLUTION	19
3.1 Pore solution extraction	19
3.1.1 Instrumental introduction and description	19
3.1.2 Sample preparation	24
3.1.3 Extraction method and load scheme	25
3.2 Pore Solution Chemical Analysis	27
3.2.1 Alkali evolution process in pore solution	27
3.2.2 Pore solution test schemes and methods	29
3.2.3 Test results and analysis	32

CHAPTER 4	RCA ASR MITIGATION USING MINERAL ADMIXTURES	35
4.1	Fly Ash Mitigation	35
4.1.1	Fly ash as a concrete admixture	35
4.1.2	Mortar bar expansion test	38
4.1.3	Expansion results and comparison	42
4.1.4	Pore solution analysis	45
4.1.5	Mitigation mechanism analysis	49
4.2	Ground Granulated Blast Furnace Slag (GGBFS) Mitigation	54
4.2.1	Slag production and use in concrete	54
4.2.2	Expansion test results and comparison	55
4.2.3	Pore solution analysis and TGA	57
4.3	Silica Fume Mitigation	59
4.3.1	Expansion results and comparison	60
4.3.2	Pore solution analysis and TGA	65
4.3.3	Particle size issue	66
4.4	Glass as a Potential Admixture for ASR Mitigation	69
4.4.1	Glass chemical composition	70
4.4.2	Glass powder for ASR mitigation	71
CHAPTER 5	ASR MITIGATION OF RCA CONCRETE AND EXISTING CONCRETE BY LITHIUM	76
5.1	Lithium as an Admixture for ASR Mitigation	76
5.1.1	Lithium basic chemistry	76
5.1.2	Lithium compounds as concrete admixtures	78
5.1.3	Mechanisms of lithium ASR mitigation	79
5.2	Lithium Effectiveness Evaluation	83
5.2.1	ASTM C 1293 results and analysis	84
5.2.2	ASTM C 1260 modification, results and analysis	86
5.3	Pore Solution Analysis	92
5.4	Mitigation of Existing Concrete with ASR	98

5.4.1 Concrete prism test	99
5.4.2 Simulated mortar bar test	102
5.4.3 Pavement block test	105
CHAPTER 6 SUMMARY AND CONCLUSIONS	115
REFERENCES	118

LIST OF TABLES

1	Summary of ASR test methods	8
2	Aggregate grading for ASTM C 227, 441, 1260 and 1567	8
3	Coarse aggregate grading for ASTM C 1293	9
4	Different applications of recycled PCC	13
5	Blue Rock RCA material properties for minus #4	17
6	Blue Rock RCA material properties for plus #4	17
7	Material properties comparison between RCA and Blue Rock	17
8	RCA alkali content, flushed and soaked	18
9	Ottawa sand grading	24
10	Chemical composition of the type II cement	24
11	Pore solution extraction ratios of different samples	26
12	The instant release of the cement alkalis	28
13	Effect of alkali interaction on Na, K and Li measurements	30
14	Alkali interaction effect and its reduction by matrix matching	30
15	Pore solution evolution for high alkali cement paste samples	32
16	Pore solution evolution for high alkali cement mortar samples	33
17	Pore solution evolution for low alkali cement mortar samples	33
18	The beneficial uses of fly ash	36
19	Chemical composition of the Brayton Point fly ash	38
20	Comparison between crushed RCA and ASTM C1260 standard grading	39
21	Mix proportions for BR, RCA ASTM C 1260 samples, with/without fly ash	43

22	Comparison of ASTM C 1260 and ASTM C 1293 for fly ash	45
23	Pore solution evolution for Ottawa sand mortar with 25 percent fly ash	46
24	Pore solution evolution for BR mortar with 25 percent fly ash	47
25	Pore solution evolution for RCA mortar with 25 percent fly ash	47
26	Alkali concentration in solution before and after RCA soaking	49
27	Mix proportions for mechanism analysis mortar samples	50
28	Typical US slag oxide composition	55
29	Comparison of ASTM C 1260 and ASTM C 1293 for GGBFS	57
30	Mix design for ASTM C 1293 BR, RCA concrete prisms with silica fume	60
31	Comparison of ASTM C 1260 and ASTM C 1293 for silica fume	65
32	Sieve analysis of silica fume as received	67
33	Typical commercial glass oxide composition by weight percentage	70
34	Window glass powder grading	72
35	Basic ionic characteristics of Li, Na and K	77
36	Solubility products of lithium salts and their calcium counterparts	78
37	Volume changes for silica gel slurries (ml)	82
38	Lithium nitrate modification of soaking solution (LN)	88
39	Lithium hydroxide modification of soaking solution (LH)	88
40	Comparison of ASTM C 1260 and ASTM C 1293 for lithium	91
41	Alkali evolution for Ottawa sand samples with lithium	94
42	Alkali evolution for BR mortar bars with lithium	94
43	Alkali evolution for RCA mortar bars with lithium	94
44	Comparison on alkali and lithium concentration, before/after RCA soaking	98

LIST OF FIGURES

1	Blue Rock RCA samples	15
2	ASTM C 1260 expansion comparison between blue rock and recovered rock	15
3	Total assembly of the pore solution extraction device	20
4	Base adapter with the compression plate	21
5	Top adapter with the piston	22
6	The spacer	22
7	The compression chamber	23
8	The extractor claws	23
9	Alkalis evolution in pore solution for cement mortar	34
10	Microphotograph of fly ash	37
11	ASTM C 1260 expansion error at 14 days as a function of the number of mortar bars	41
12	ASTM C 1260 expansion error at 28 days as a function of the number of mortar bars	41
13	ASTM C 1260 expansions for BR and RCA samples	44
14	ASTM C 1260 expansions for BR control samples, with/without fly ash	44
15	ASTM C 1260 expansions for RCA control samples, with/without fly ash	45
16	Pore solution alkalis evolution for Ottawa sand mortar samples, with/without fly ash	48
17	Pore solution alkalis evolution for BR/RCA mortar samples, with/without fly ash	48

18	Effect of spiked Ca(OH) ₂ and NaOH on fly ash mitigation	51
19	ASTM C 1260 expansions for BR samples with high fly ash substitution and NaOH spike	51
20	TGA of Ca(OH) ₂ , cement paste and cement paste with different fly ash substitution	53
21	ASTM C 1260 expansions for BR control samples, with/without GGBFS	56
22	ASTM C 1260 expansions for RCA control samples, with/without GGBFS	57
23	Pore solution alkalis evolution for Ottawa sand mortar samples, with/without GGBFS	58
24	TGA of Ca(OH) ₂ , cement paste and cement paste with GGBFS	59
25	ASTM C 1293 expansion error as a function of the number of samples at 95% confidence level	61
26	ASTM C 1260 expansions for BR control samples with/without silica fume	62
27	ASTM C 1260 expansions for RCA control samples, with/without silica fume	63
28	ASTM C 1293 expansions for BR and RCA samples	63
29	ASTM C 1293 expansions for BR control samples, with/without silica fume	64
30	ASTM C 1293 expansions for RCA control samples, with/without silica fume	64
31	Pore solution alkalis evolution for Ottawa sand mortar samples, with/without silica fume	66
32	TGA of Ca(OH) ₂ , cement paste and cement paste with silica fume	67
33	ASTM C 1260 expansions for BR control, with/without 5% silica fume substitution of aggregate	68
34	Expansions of paste bars, with/without 5% silica fume cement substitution under ASTM C 1260 condition	69
35	ASTM C 1260 expansions for BR control samples, with/without E-glass powder	73

36	ASTM C 1260 expansions for RCA control samples, with/without E-glass powder	73
37	ASTM C 1260 expansions for BR control samples, with/without window glass powder	74
38	ASTM C 1260 expansions for RCA control samples, with/without window glass powder	74
39	ASTM C 1260 expansions for BR control samples, with/without crushed waste glass powder	75
40	ASTM C 1260 expansions for RCA control samples, with/without crushed waste glass powder	75
41	Container for measuring silica gel slurry volume change	82
42	BR mortar bar expansions in 1N different alkali hydroxide solutions	84
43	ASTM C 1293 expansion of BR control concrete prisms, with/without lithium	85
44	ASTM C 1293 expansion of RCA concrete prisms, with/without lithium	86
45	Standard ASTM C 1260 expansions for BR control mortar samples, with/without lithium	87
46	LN Modified ASTM C 1260 expansions for BR control mortar samples, with/without lithium	89
47	LH Modified ASTM C 1260 expansions for BR control mortar samples, with/without lithium	89
48	LN Modified ASTM C 1260 expansions for RCA control mortar samples, with/without lithium	90
49	LH Modified ASTM C 1260 expansions for RCA control mortar samples, with/without lithium	90
50	Soaking solution effects on Blue Rock mortar samples ASTM C 1260 expansion	92
51	Lithium to alkali ratio evolution for Ottawa sand mortar samples with lithium	93

52	Lithium to alkali ratio evolution for BR mortar samples with lithium dosage 0.74	95
53	Lithium to alkali ratio evolution for BR mortar samples with lithium dosage 1.0	95
54	Lithium to alkali ratio evolution for RCA mortar samples with lithium dosage 0.74	96
55	Lithium to alkali ratio evolution for RCA mortar samples with lithium dosage 1.0	96
56	Comparison of lithium to alkali ratio evolution for RCA and BR mortar	97
57	Sketch of the 1/4 inch studs	100
58	Expansion of existing concrete prisms, control versus ASTM C 1260	101
59	Expansion of existing concrete prisms, control versus NaCl, lithium treatment	101
60	Continuing expansion of pre-crack mortar samples, with/without treatment	104
61	Continuing expansion of post-crack mortar samples, with/without treatment	104
62	Sketch of the 4-inch studs (not to scale)	106
63	Positioning of the studs	107
64	Schematic sketch of wood box holding blocks	108
65	Picture of wood box holding blocks	108
66	Surface Expansion Comparison of concrete pavement blocks, with/without treatments	111
67	Inside Expansion Comparison of concrete pavement blocks, with/without treatments	111
68	Expansion difference between inside and surface of concrete pavement blocks, with/without treatments	112
69	Lithium alkali ratio profile of concrete pavement blocks, with/without treatments	113

ABSTRACT

MITIGATING ALKALI SILICA REACTION IN RECYCLED CONCRETE

by

Xinghe LI

University of New Hampshire, December, 2005

Concrete made with recycled concrete aggregate (RCA) that had shown alkali silica reaction (ASR) distress was evaluated. It was found that ASR mitigation was needed to prevent continued expansion. Several mitigation methods were evaluated and compared to conventional concrete using the testing procedures of ASTM C 1260/1567 and ASTM C 1293. Pore solution analysis and Thermal Gravimetric Analysis (TGA) were also conducted.

It was found that fly ash, silica fume and ground granulated blast furnace slag (GGBFS) were effective in mitigating ASR in RCA concrete. Compared to conventional concrete, slightly higher dosages were typically required. The ASTM C 1260/1567 test correlated well with ASTM C 1293 with few exceptions.

Pore solution and TGA revealed that calcium hydroxide and alkalis are reduced by fly ash, silica fume and GGBFS substitution. Calcium depletion during the pozzolanic reaction is a sufficient condition for ASR arrest, but the alkali reducing effect appears to

be more pivotal than calcium depletion.

Lithium, as well as the other mitigation strategies, required higher dosages with RCA concrete than conventional concrete. The pore solution lithium to alkali ratio was found to be lower and at one year, reaching equilibrium at approximately 50 to 60 percent of the original dose.

Modifying the soak solution of ASTM C 1260 resulted in higher levels of lithium in the test samples and made the test less conservative.

Topical application of lithium nitrate solution showed reduced surface expansion of pavement blocks however there was no effect on inside expansion. Lithium was found to penetrate about 25mm.

CHAPTER ONE

INTRODUCTION

1.1 Overview

Concrete is widely used as a material in the modern world and its history can be traced back hundreds if not thousands of years. It is fair to say that our modern civilization has somewhat depended on concrete, though people tend to take concrete for granted because of its commonness. It is the most used material in construction, approximately 2 tons of concrete were used per capita in the US in the year of 2000 (1).

Concrete is a composite material, consisting of aggregates (coarse and fine) and paste. Paste is a continuous phase matrix, in which granular aggregates are embedded. The concrete properties are dependent on the aggregate, the paste and their interface. Strength and durability are two predominant properties of concern.

Alkali silica reaction (ASR) is one of the most important concrete durability issues; in fact it is only second to reinforcement corrosion. It was first observed in the early 1940s (2). ASR is the reaction between alkali hydroxide in pore solution and reactive siliceous aggregate. ASR forms a gel, which expands upon absorption of water.

Tremendous work has been done on ASR since 1940. However, the understanding of ASR is far from perfect. Although it is likely ASR exists in all 50 states

and every continent in the world (3). The ages of affected concrete range from as early as 5-10 years to over 100 years. Deterioration of concrete can be minor; many times its functionality is still acceptable despite the ASR distress. Some concrete with advanced ASR must be removed and replaced. Treatment of existing concrete with ASR distress and reuse of old demolished concrete as aggregate for new concrete construction will be discussed.

1.2 Research Objectives and Organization of the Dissertation

The work described herein is a part of the Recycle Materials Research Center (RMRC) initiative to promote recycling of industrial by-products and waste materials within the civil engineering highway infrastructure. The main goals of this research were to study the feasibility of using ASR distressed recycled concrete aggregate (RCA) in new concrete, evaluate different mitigation strategies, conduct treatments of existing concrete with ASR distress to extend service life and evaluate the effectiveness. This dissertation is organized as follows:

Chapter 1 serves as an introduction.

Chapter 2 starts with an overview of ASR fundamentals and recycled concrete aggregate (RCA). This chapter provides information on the ASR mechanism, mitigation approaches, test methods, RCA usage as well as technical challenges.

Chapter 3 presents the pore solution extraction machine, test scheme and concrete pore solution chemistry evolution test results. The pore solution analysis also serves as an

important tool for evaluating the mitigation effect of various admixtures.

Chapter 4 presents mineral admixture mitigation techniques such as fly ash, silica fume and ground granulated blast furnace slag (GGBFS) for RCA and natural aggregate concrete. Different ASR expansion test results are presented. Pore solution chemistry and Thermogravimetric Analysis (TGA) are used to help evaluating the mitigation techniques. Mitigation potential of waste glass is also evaluated.

Chapter 5 presents chemical admixture mitigation for existing concrete and RCA concrete. The mitigation effect of lithium salts, both internally in RCA concrete and topical application on existing concrete, is evaluated. Different expansion test results are presented and pore solution analysis is used to explain the mitigation mechanism.

In chapter 6, conclusions are summarized and technical issues for future research are presented.

CHAPTER 2

ALKALI SILICA REACTION AND RECYCLED CONCRETE

AGGREGATE

2.1 Alkali Silica Reaction (ASR)

2.1.1 ASR essentials

ASR refers to the reaction between the alkali hydroxide in pore solution and reactive siliceous aggregate and it is a complex physical-chemical process. There are quite a few schools of thought on the mechanism, but it is well accepted that there are three basic requirements for ASR to occur.

The first one is the presence of alkali, and the main source is usually from the portland cement. Other sources may include: mineral admixtures such as fly ash, slag and silica fume; chemical admixtures; air-entraining admixture and even some aggregates (4, 5). The alkalis in the concrete are mainly potassium and sodium. The alkali content is described as equivalent sodium oxide, $Na_2O_{eq} = Na_2O + 0.658K_2O$, where 0.658 is the ratio of the molecular weight of Na_2O to the molecular weight of K_2O . Compared to other oxides such as CaO or SiO_2 , the percentage of Na_2O_{eq} is relatively low and in the range of 0.2 to 1.5% of cement weight. In concrete pore solution, calcium hydroxide (CH) is saturated or supersaturated due to its high quantity as a result of the hydration of

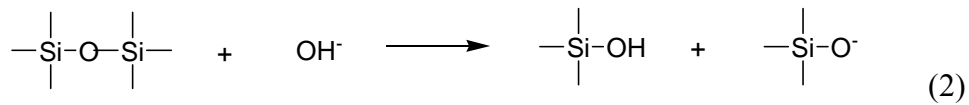
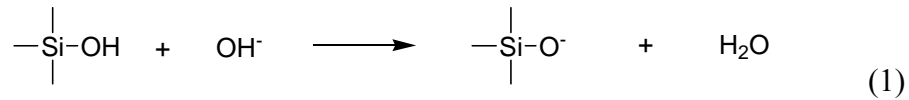
tricalcium silicate (C_3S) and dicalcium silicate (C_2S). The pH of saturated CH is around 12.4 at 25°C (6). Since most of the alkalis end up in pore solution, it renders the pH even higher, in the range of 13 and up. The alkali level to sustain ASR adopted in ASTM C 150 is 0.6% of cement weight (7). Below that level the ASR is unlikely to occur, although recently more research results suggest that the criteria may be inappropriate without taking consideration of other alkali contributing factors (8, 9).

The second one is reactive aggregate. Most reactive aggregates contain amorphous silica in their mineral composition. The difference between reactive and non-reactive aggregates lies in their crystal structures (10, 11). Alkali attack on well crystallized silica like quartz is very slow and only occurs on the limited aggregate surface. On the other hand, the reactive aggregates are less ordered and prone to alkali attack because of higher surface area. It is much easier for hydroxyls to penetrate amorphous silica than well crystallized silica. The main reactive minerals with amorphous structures are: opal, obsidian, cristobalite, tridymite and cherts.

The third one is moisture. It is well accepted that below a threshold relative humidity (RH) ASR and accompanying expansion can not occur. The threshold RH for external moisture is around 80-90% (12, 13).

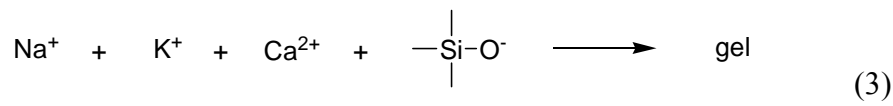
2.1.2 ASR mechanisms

Technically, the term ASR is misleading, since the first step of the reaction is the attack of hydroxyls (not alkalis) on the silica in the aggregate. These reactions can be represented by the following two equations:



These reactions account for the dissolution and destruction of the tetrahedron silica network of aggregates, which is the main skeleton of silica. Provided enough hydroxyls are available, the reaction continues and produces alkali silicate solution.

Following or even concurring with the dissolution process, there is a gel-forming process. The gel formation reaction can be represented by the following equation, in which the calcium ion is from dissolution of the hydration product CH.



The aforementioned reactions are well agreed upon in the ASR research community (12, 14). However, there are several gel expansion mechanism theories.

Hansen proposed an osmotic theory by in 1944 (15). In this theory, pressure develops because cement paste surrounding the reactive grains acts as a semi-permeable membrane which blocks large ions like silicate but allows the smaller ions to pass. Water is drawn into the reacting grain, which increases the pressure and eventually cracks the paste.

McGowan and Vivian proposed an absorption theory and Tang concurred with it (16, 17). In this theory, the expansion is the result of water absorption and accompanying volume increase of gel.

There is also a theory of compromise between the two, which suggests both mechanisms contribute to the pressure and expansion (18). Recently a double layer theory has been proposed based on surface chemistry (19, 20, 21). A double layer, which is composed of sodium, potassium, calcium ions and some anions, develops at the silica surface to offset its negative charge. The excessive positive charges and the surface negative charge create an electrical field. The gel expansion is a result of a pressure gradient, which balances the force created by electrical field.

Calcium is essential in the creation of ASR gel (14). Without calcium, the ASR gel process stops because alkalis are mono-valent and there is no way to crosslink with silica. This is proposed by Diamond and more recently concurred by Hou et al (22, 23).

There is still no consensus on why and how the gel expands, however, it is well accepted that gel needs to have both alkali and calcium in order to be potentially expansive (14).

2.1.3 ASR test methods review

There are many standard tests for assessing ASR and most of them are specified by ASTM. The related ASTM standard tests are: ASTM C 227, C 441, C 1260, C 1293 and C 1567 (*See references 24, 25 26, 27 and 28*). These five methods are summarized in tables 1 through 3.

The ASTM C 441 is used less frequently because the glass aggregate does not represent real practice. Also the Pyrex glass itself is difficult to obtain and contains alkali which is released to the system. The most widely used tests are ASTM C 1260/C 1567

and C 1293. The C 1260 test is a screening test at best and due to its harsh environment can have false positives. The ASTM C1293 has the best field performance correlation, but the time frame is one year and 2 years if supplemental cementitious materials (SCMs) have been used in the proposed mix. The ASTM C 1567 test is nothing more than the ASTM C 1260 test to evaluate the effectiveness of the SCMs mitigation. The ASTM C

Table 1. Summary of ASR test methods

	ASTM C 227	ASTM C 441	ASTM C 1260/ C 1567	ASTM C 1293
Sample Dimensions (mm)	25 x 25 x 285	25 x 25 x 285	25 x 25 x 285	75 x 75 x 285
Water cement ratio	Water required to obtain a flow of 105 to 120	Water required to obtain a flow of 100 to 115	0.47	0.42-0.45
Aggregate	Table 2 grading	Pyrex Glass Table 2 grading	Table 2 grading	Table 3 grading
Aggregate cement ratio	2.25	2.25	2.25	Cement 420kg/m ³
Environmental condition	38 °C near 100% RH	38 °C near 100% RH	80 °C 1N NaOH solution	38 °C near 100% RH
Cement alkali level	>0.6 % Na ₂ O _{eq}	0.95-1.05 % Na ₂ O _{eq}	Not specified	1.25 % Na ₂ O _{eq}
Time ranges	14 days		16/30 days	1 year/2 years
Linear expansion criteria	None	None	0.10 % marginal 0.20 % reactive	0.04%

Table 2. Aggregate grading for ASTM C 227, 441, 1260 and 1567

Passing	4.75mm	2.36mm	1.18mm	0.6mm	0.3mm
Retained on	2.36mm	1.18mm	0.6mm	0.3mm	0.15mm
Mass (%)	10	25	25	25	15

Table 3. Coarse aggregate grading for ASTM C 1293

Passing	19.0mm	12.5mm	9.5mm
---------	--------	--------	-------

Retained on	12.5mm	9.5mm	4.75mm
Mass (%)	33.3	33.3	33.3

227 lies in between as regards to time frame, but it does not have specific expansion criteria and for some aggregates it yields poor results. In this research, the ASTM C 1260/1567 test, its modified version and the ASTM C 1293 test are the main test methods employed.

2.1.4 Potential mitigation methods

Based on the three requirements for ASR to occur, there are different options to potentially consider for controlling ASR in concrete.

Reducing the alkalis in the concrete is an option. Much research has been done on this aspect and ASTM C 150 specifies low alkali cement as cement that has an alkali content ($\text{Na}_2\text{O}_{\text{eq}}$) less than 0.6 percent of cement weight (1, 7, 12). Some researchers reported that a 0.6 percent is not conservative criteria and some structures showed ASR distress even with cement alkali level below 0.6 percent (8). Recently a more appropriate measurement to prescribe alkali mass in a unit volume of concrete, e.g. $\text{Kg Na}_2\text{O}_{\text{eq}}/\text{m}^3$ concrete, has often been used as low alkali criteria. It is a better indicator because it takes other alkali sources as well as cement content in the concrete into consideration. The threshold ranges from three to five $\text{Kg Na}_2\text{O}_{\text{eq}}/\text{m}^3$ concrete dependent on aggregate reactivity (9). There is no consensus on the effectiveness of this approach. Cement alkali contents are on the rise due to the increase of environmental criteria during cement production. This is the result of recycling the kiln dust back to the clinker, causing the average alkali content to go up. Low alkali cement is becoming more and more expensive

and usually is locally unavailable.

The second obvious option is to use innocuous aggregate. This is a good option, but a resource dependent issue. If enough innocuous aggregates, proved by long term performance, are locally available, ASR will not be an issue. But still many sources of “acceptable” aggregates used across the country are slowly reactive and eventually cause ASR. Strict quality control and frequent testing is needed to ensure the non-reactivity of aggregates. Many states have consumed all of their innocuous aggregates and economy prevents long distance transportation from other states. In this case other ASR mitigation methods must be considered.

The third option is to reduce the moisture content below approximately 80 percent relative humidity, a threshold for the reaction to sustain itself. Limiting the availability of external moisture is an effective way to stop ASR however for most structures it is extremely difficult to lower the internal moisture to such a low level. This option may be viable for some unique structures, but not for infrastructures such as concrete pavement (11, 13).

In most situations, innocuous aggregates are not available and moisture control is not practical. The option left is either to use low alkali cement or more likely use mitigation by mineral and/or chemical admixture, which will be discussed in details in the following chapters.

2.2 Recycled Concrete Aggregate (RCA)

2.2.1 Recycled aggregate preview

Aggregates are indispensable components in concrete construction, which provide bulk, strength and wear resistance. Aggregates consumption in the US is around 70 percent of the total raw materials demand (29). Two billion tons of aggregate are produced each year in the US and the number is expected to reach 2.5 billion tons per year by the year 2020 (30). On the other hand, many old infrastructures in the US have become or are becoming obsolete. As many roads and structures are torn down or demolished, large amounts of demolished waste are generated. The construction waste from building demolition alone is estimated to be 123 million tons per year (30). Demolished infrastructure waste faces two options: landfill or recycling.

In recent years, concrete communities have become more aware and have begun to follow the trend of sustainable development and will continue to do so in the future (31). It would be prudent on their part to continue addressing sustainability before it is forced on them by society. ACI has recently become very active in sustainability of concrete and several of its committees such as Committee 555, Concrete with Recycled Material, are expected to provide leadership in this area (32). The basic premise of sustainability is that material use should be designed so as to be easily recycled into new products at the end of its design life. This reduces disposal and decreases consumption of nonrenewable natural materials (33). Europe has been very active in recycling and a high percentage of waste concrete is recycled. In some countries such as the Netherlands and Denmark, the percentage is as high as 90 percent. In the US, 20 to 30 percent of

construction and demolition waste is recovered for recycling (33, 34). Concrete recycling will increase in the US if for no other reason than the economics of doing so. Established in 1998 in close coordination with FHWA's Pavement Management Coordination Group, the RMRC works on the national level to promote the appropriate use of recycled materials in the highway environment (33).

Concrete recycling has several potential uses currently in practice. Currently there are 38 states recycling concrete as aggregate base and 39 states which have or are presently recycling concrete as aggregate for portland cement concrete (PCC) (30). The different applications of recycling PCC are presented in table 4. When used as base and subbase materials, RCA performs better than virgin aggregates due to presumably recementing of the old paste as well as its high angularity. As shown in table 4, the high-value usage of recycled concrete, which includes PCC, asphalt hot mix and riprap, is fairly low. The US currently produces approximately 100 million tons of recycled aggregate annually. Increased usage of recycled concrete in new concrete construction has the potential of saving our natural resources. Compared to landfill, recycling concrete, especially in high value applications such as new concrete, can conserve natural resources, spare landfill space and also make concrete a more sustainable material (29).

Unlike in low-value applications, such as road base, recycled concrete in new concrete construction needs to meet higher standards. The main concerns are their potential detrimental effect on strength and durability. The strength of RCA concrete is comparable to natural aggregate concrete with medium to high water cement ratio (35). It

has been reported that with silica fume, RCA concrete can achieve a compressive strength of 50 to 60 MPa and the durability is also comparable to natural aggregate concrete (36).

Table 4. Different applications of recycled PCC

Recycled aggregate usage	Percentage
Road Base	68
New portland cement concrete	6
Asphalt hot mixes	9
High-value riprap	3
Low-value fill	7
Others	7

For a recycled materials utilization application in highway environment, there is an evaluation framework published by the Federal Highway Administration to establish a logical and hierarchical evaluation process. The framework is divided into three stages: stage 1 is screening; stage 2 is engineering and environmental laboratory testing; stage 3 is engineering and environmental field testing. This research focuses on stage 2 of RCA evaluation (33, 37).

2.2.2 RCA with ASR distress

Since ASR is a wide spread problem in US it is reasonable to assume that a considerable amount of the concrete that is available for recycling is affected by ASR. It is possible that a concrete that was made with old lower alkali cement did not contain an alkali loading sufficient to activate ASR in those aggregates that were potentially reactive. These aggregates may very well be reactive in the presences of the increased alkali in modern day cements. There is little information on recycling concrete with ASR. It was reported that a Wyoming highway project with RCA usage had recurrent ASR (38). To

clear the high-value usage barrier, both real and perceived, the potential ASR problem needs to be addressed prior to recycling. This research is focused on recycled concrete made with RCA that showed ASR distress.

The recycled concrete used in this research was from a pavement section of Interstate I-95, near Gardener, Maine. Typical ASR distress was visually observed on the surface of the pavement. Concrete slabs were removed from a section of I-95 during reconstruction of a section of the pavement. The slabs were placed in storage at the contractor's construction site and later were trucked to the University of New Hampshire for evaluation. Petrographic evaluation as well as visual observation confirmed the concrete had deteriorated from ASR caused by the coarse aggregate. The concrete slabs were crushed to create RCA with maximum size of one and a half inches. Some recycled aggregate samples are shown in figure 1. From the construction record, the original coarse aggregate used was a quartzite/quartz-biotite aggregate locally referred to as Blue Rock (BR). Comparison of the current aggregate production from the same source as the original aggregate was done by dissolving the paste portion of the RCA using hydrochloric acid to retrieve the original aggregate. The original aggregate is geologically the same material as is currently under production and has the same texture and appearance as of the present aggregate BR. The recovered original aggregate was crushed for ASTM



Figure 1. Blue Rock RCA samples

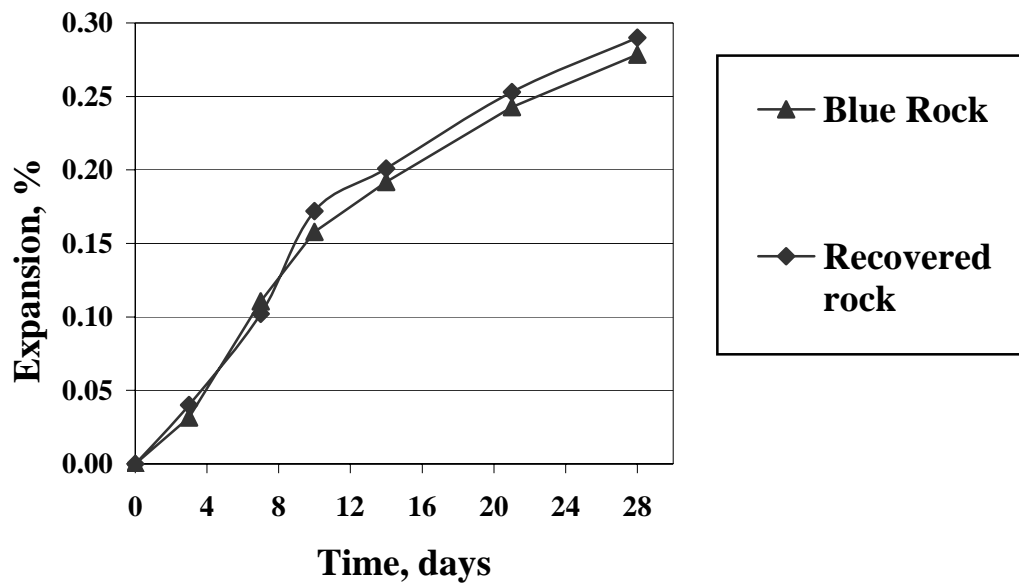


Figure 2. ASTM C 1260 expansion comparison between Blue Rock and recovered rock

C 1260 testing. The average expansion data up to 28 days are shown in figure 2. It can be seen that the expansion curves are almost the same as the currently produced Blue Rock. The expansion differences are all within 0.5 standard deviations, which suggest they are statistically insignificant.

Unlike the natural aggregates, RCA is inhomogeneous at the micro as well as macroscopic level because it contains original aggregate and paste. Many of the material properties depend on particle size due to variable quantities of paste. Table 5 and 6 summarize the properties of BR RCA of several sizes. The specific gravity and absorption were measured according to ASTM C 127 (39). Approximately 500 to 1500 grams of each sieve size were soaked in dilute hydrochloric acid to dissolve the paste and recover the aggregate. The paste content was calculated based on weight loss. The coarse aggregate and sand were not soluble in dilute acid.

It can be seen from tables 5 and 6 that the paste content varies with aggregate particle size and affects specific gravity and absorption as would be expected. With increasing paste content, specific gravity decreases whereas absorption of water increases.

Compared to the natural Blue Rock aggregate, RCA has lower specific gravity (relative density) and higher absorption due to paste as shown in table 7. This trend agrees with other researchers' results (40).

Table 5. Blue Rock RCA material properties for minus #4

Size (retained)	2.36mm	1.18mm	0.6mm
Specific Gravity	2.437	2.289	2.147

Table 6. Blue Rock RCA material properties for plus #4

size (retained)	25mm	19mm	12.5mm	9.5mm	4.75mm
Specific Gravity	2.528	2.640	2.601	2.523	2.497
Absorption (%)	3.18	1.54	2.34	3.36	5.23
Paste content (%)	18	7.3	14	20	27

Table 7. Material properties comparison between RCA and Blue Rock

	Blue Rock	RCA
Specific Gravity*	2.674	2.540
Dry rod unit weight (g/cm ³)	1.513	1.371
Adsorption (%)	0.474	3.64
Paste content (%)	N/A	19.5

* based on ASTM C 1293 grading as in table 3

2.2.3 RCA alkali contribution and alkali leaching

The paste content of the BR RCA test samples were 19.5 percent for the grading used in ASTM C 1293, which was consistent with what is obtained when the BR RCA was produced as shown in table 7. Taking into account that the aggregate is roughly three to four times the weight of cement, there is a considerable amount of old paste in the RCA. It is reasonable to assume that RCA may contain soluble alkali from ASR gel and possible deicing salt. To test the water soluble alkali content, 1000 grams of RCA with an ASTM C 1293 grading was put in a closed container with five liters of de-ionized water. The container was then stocked in an 80°C water bath for 72 hours before sampled.

In a simple flushing test for evaluating alkali leaching, 1000 grams of RCA with an ASTM C 1293 grading was subjected to one flushing of distilled water at a liquid to

solid ratio of 5. This test was performed to evaluate the alkali reduction in RCA in the presence of water. The soaking water and collected flushed water were both analyzed by Inductively Coupled Plasma Optical Emission Spectroscopy (ICP –OES), which is discussed in detail in chapter 3. The results presented in table 8 show that alkalis in the flushed out test is about 10 percent of the amount of soaked test, suggesting water rinsing does not significantly reduce the alkali in RCA.

Table 8. RCA alkali content, flushed and soaked

	Na ₂ O*	K ₂ O*	Na ₂ O _{eq} *
Soaked	0.0138	0.0109	0.021
Flushed	0.00144	0.00106	0.00214

* As percentage of aggregate weight

CHAPTER 3

PORE SOLUTION

Since ASR is a reaction between aggregate and ions in the pore solution, pore solution chemistry plays a very important role. The species in the pore solution are mainly soluble chemicals coming from cement, its hydration product and admixtures.

3.1 Pore Solution Extraction

3.1.1 Instrumental introduction and description

The device used to extract the pore solution as shown in figure 3 was manufactured at University of Cape Town in South Africa.

The device has five basic components: base adapter with compression plate, top adapter, spacer, extractor claws, compression chamber and piston. The bottom of the base adapter has a bolt that can be connected to the Instron testing machine, which is a close-looped hydraulic testing machine with maximum capacity of 220 kips. The top of the base adapter was attached together with the compression plate. The compression plate is a round flat steel disk with a concaved O-ring, to which a drainpipe is attached. The base adapter with compression plate is shown in figure 4. The top adapter, which is shown in figure 5, holds the piston through its bottom and connects to the Instron testing machine through its top. The spacer, as shown in figure 6, is used in removing the sample



Figure 3. Total assembly of the pore solution extraction device from the chamber and has a height of 63 mm (2.5 inch). The compression chamber as shown in figure 7 holds the sample during the test.

The sample is put in the compression chamber, which sits on the compression plate. Pressure is applied to the sample through the piston. The compression chamber of the pore solution extraction machine has an inner diameter of 50 mm (1.97 inch) and height of 122 mm (4.80 inch). Pore solution is collected through the drain pipe shown in

figure 4. After the test, the two pins at the top of compression chamber are connected to the top adapter before the compression chamber is lifted up. The spacer then is placed on the compression plate, secured by two pins before the sample is pushed out of compression chambers into the spacer. Extractor claws, as shown in figure 8, are used to lock the compression chamber to the base adapter, while the piston is pulled out of the compression chamber.



Figure 4. Base adapter with the compression plate



Figure 5. Top adapter with the piston

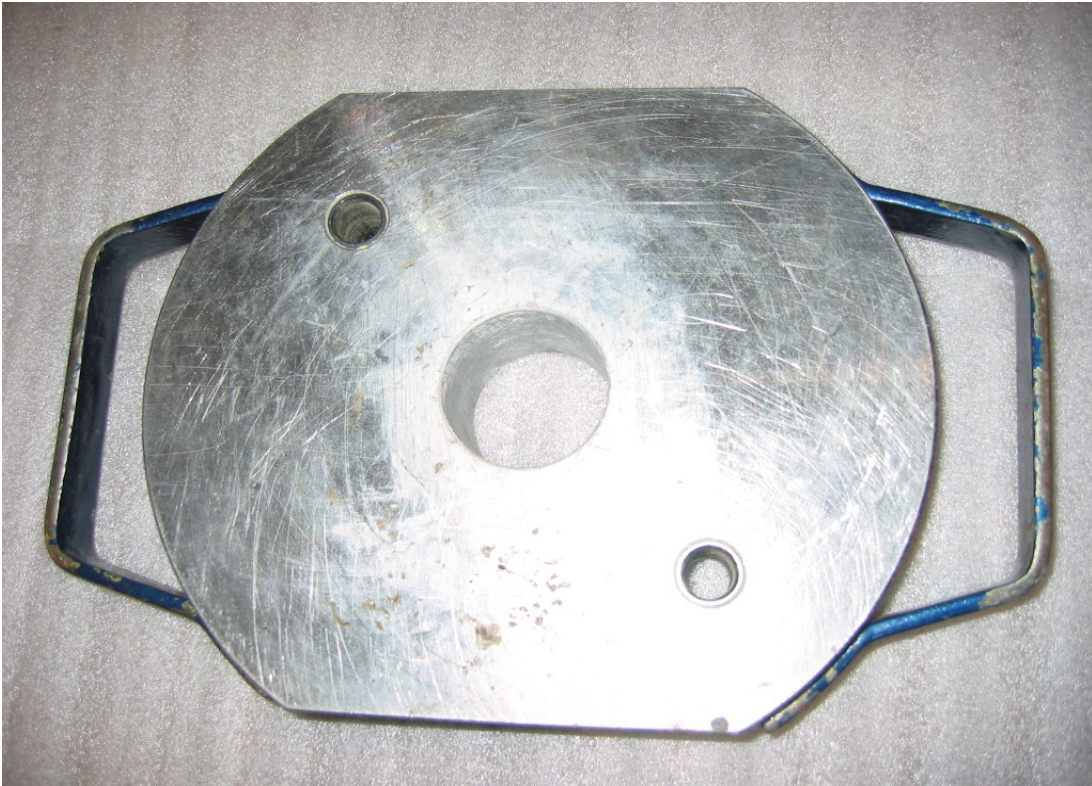


Figure 6. The spacer



Figure 7. The compression chamber



Figure 8. The extractor claws

3.1.2 Sample preparation

A longitudinal split PVC pipe with an inner diameter of 48.5 mm (1.91 inch) was used as a mold to fabricate the specimens. The length of the mold was chosen at 54 mm (2.13 inch) taking the height of spacer into consideration. Both paste and mortar sample were prepared. Six samples were batched from each mix set, vacuum-bagged with 5ml of water and stored at 38 °C. Pore solution was extracted from the samples as a function of time. Ottawa sand from Ottawa, Illinois, with grading shown in table 9, was used as a non ASR reactive fine aggregate. A water cement ratio of 0.47 and a cement aggregate ratio of 1:2.25 were used. For the paste samples, a water cement ratio of 0.4 was used. The low alkali cement used in the mix is from Holnam Inc., Dundee, Michigan, with alkali content of 0.26 percent. The regular high alkali cement is type II cement from Thomaston, Maine with chemical composition as shown in table 10.

Cored concrete samples with 43mm (1.7inch) diameter and variable length from 20mm (0.79inch) to 50mm (1.97inch) were also obtained from the same pavement section as the RCA source.

Table 9. Ottawa sand grading

>600 μm	300 μm (retained)	150 μm (retained)	< 150 μm
0.5%	78%	21%	<0.5%

Table 10. Chemical composition of the type II cement

Components	percent
CaO	62

Table 10. Chemical composition of the type II cement (continued)

SiO ₂	20
Al ₂ O ₃	4.4
Fe ₂ O ₃	2.9
Na ₂ O	0.3
K ₂ O	1.2
Na ₂ O _{eq}	1.09
MgO	3.6
SO ₃	3.9
LOI	2.3
Specific surface	394m ² /kg
Autoclave expansion	0.16

3.1.3 Extraction method and load scheme

The objective was to extract pore solution from the sample for chemical analysis. A test volume of at least 0.5 to 1 ml was needed for analysis. In the preliminary test and instrumental calibration, different load schemes to maximize pore solution extraction efficiency were developed. Alternating cycles of sine and triangle loading was found to squeeze much more pore fluid that sustained constant load of the maximum, 250 kips. A final cyclic loading scheme was used by applying an alternating sine load ranging from 489KN (110 kips) to 934KN (210 kips) at a frequency of 0.2 Hertz. Based on the average sample cross section area of 1963.5 mm² (3.05 in²), the stress profile of the sine wave ranged from 249MPa (36 ksi) to 475MPa (69 ksi) at 0.2 Hertz. This frequency was chosen to maximize extraction efficiency and also extend the fatigue life of the device. Typical samples were loaded for 250-300 cycles. No significant amount of liquid was extracted from most samples beyond 300 cycles. During the development of the loading procedure, some samples were subjected to loading for up to 48 hours.

It was very hard to extract pore solution from any sample beyond the age of 28 days. It was very difficult to obtain pore solution from the cored concrete samples, only one of 21 samples squeezed out more than 0.3ml liquid. Because of this, all samples were vacuumed bagged with 5ml water and stored at 38°C to assure the internal pores approached equilibrium. For pure paste samples, especially at young ages, it was observed that the drain hole tends to clog during the test.

After finishing the extraction test, some samples were heated at 105°C to constant weight to remove all evaporable water (41). The pore liquid extraction ratio for samples tested, expressed as a percentage of total evaporable water, is presented in table 11.

Table 11. Pore solution extraction ratios of different samples

Sample ID	w/c	Age (days)	Liquid extracted (ml)	Loss on 105°C heat (g)	Extraction ratio (%)
Cored 1*	N/A	N/A	0.3	6.56	4.4
Cored 2*	N/A	N/A	0	4.26	0
Mortar 1	0.47	1	7.06	12	37
Mortar 2	0.47	7	5.12	11.4	31
Mortar 3	0.47	28	3.04	5.9	34
Mortar 4	0.47	180	1.35	2.03	40
Mortar 5	0.47	360	0.78	1.57	33.2
Mortar 6*	0.47	28	3.64	3.45	50.6
Paste 1	0.42	1	2.48	14.5	14.6
Paste 2	0.42	7	2.10	17.24	10.9
Paste 3	0.42	28	2.34	18.64	11.2
Paste 4	0.42	180	1.02	10.23	9.1
Paste 5	0.42	360	0.87	9.94	8
Paste 6*	0.42	28	2.87	14.67	16.4

*more than 300 cycles and up to 48 hours loading was applied

From table 11, it can be seen that even for the most aggressive extraction scheme used, there is still 50 percent liquid left in the sample. The extracted liquid and ratio for

paste are lower due to clogging of the drain hole. Based on these data, it appears a more aggressive loading scheme was not warranted because ample volume was obtained for chemical species analysis by the above procedure. It was noted that extracted liquid was not a reliable indicator of evaporable water in the sample.

3.2 Pore Solution Chemical Analysis

3.2.1 Alkali evolution process in pore solution

Although the cement alkalis are represented as Na_2O and K_2O , there are no free alkali oxides in cement clinker due to their high reactivity at the high temperature achieved during cement manufacture. The soluble alkalis are in the form of sulfate. Cement alkali release into the pore solution is not an instant process. Part of the alkali releases immediately when water contact is initiated. Some of it releases gradually during hydration. The instant soluble alkali is mainly in the form of sulfates such as K_2SO_4 , Na_2SO_4 , $\text{K}_6\text{Na}_2(\text{SO}_4)_4$ and $\text{K}_2\text{Ca}_2(\text{SO}_4)_3$ (41).

The alkali instant fraction is defined as the instant soluble alkali percentage based on the total alkali. The alkali instant fraction depends on the sulfur to alkali ratio in cement clinker and is in 50 to 60 percent range for typical cement. It is higher for potassium than sodium (41, 42). The alkali content of cement in a typical mill analysis is analyzed by the hydrochloric acid soluble method and it is the total alkali amount which includes both instant soluble and insoluble (43).

The alkali instant fraction for the cement used in this research was estimated

using a vacuum filter system. One gram of cement was placed on the filter and 10ml water was quickly filtered through with a contact time of less than two minutes. The filtered solution was diluted to 200ml and the Na^+ , K^+ concentrations were measured by ICP-OES. The cement used has 1.2% K_2O and 0.3% Na_2O . The results are shown in table 12. After alkalis enter the liquid phase, they can go back into the solid phase as hydration progresses. It is well known that hydration products, especially C-S-H gel, bind alkali and hydroxyl (44, 45, 46). So not all alkalis released stay in the liquid phase, some are bound into the hydration product. In mature concrete, ionic species in pore solution are in equilibrium with the hydration products (47). From the ASR perspective, only alkalis, calcium and hydroxyls in the liquid phase participate in the reaction.

Table 12. The instant release of the cement alkalis

	Measured (mg/l)	(mmol/l)	Instant fraction (%)
Na^+	3.89	0.169	35
K^+	24.1	0.618	48.4

From the alkali and hydroxyl perspective, there are three main processes going on during hydration which affect their concentration. Alkali release continues; free water decreases and alkali binding into hydration products progresses as a function of hydration. The pore solution is the result of these three processes and their complex interactions.

3.2.2 Pore solution test schemes and methods

In portland cement concrete the main species in pore solution are Na^+ , K^+ , OH^- ,

Ca^{2+} and SO_4^{2-} . The ICP-OES was used to determine sodium, potassium, calcium and sulfur concentration in the pore solution. The analysis was performed using a Varian Vista-Pro Simultaneous ICP-OES at the UNH Analytical Services Laboratory.

The ICP-OES instrument used to measure the ionic concentrations is very sensitive to interaction among alkali ions (48). The pore solution samples contain Na, K and optionally Li (lithium mitigation samples to be discussed in chapter 5) approximately in the same magnitude. Radial view plasma is less susceptible to alkali interaction if proper view height is chosen, but the equipment used in this research can be operated on top view only (48). So Lanthanum was used as a swap agent to eliminate or reduce the alkali interaction. A designed experiment to help distinguish the concentrations is presented in table 13. The error was defined as the difference between known standard value and measured value and expressed as percentage of the standard value.

From table 13, it can be seen that after lanthanum addition the error was reduced significantly as predicted. Only on the potassium measurement, was the error out of the range of five percent. An error of 5 percent is considered acceptable for chemical analysis and research.

To improve the accuracy of the potassium measurement, a matrix matching method was employed. The principle of matrix matching is trying to match the ionic ratios in the standard to those in the sample. Since the potassium to sodium ratio is roughly known through cement composition, the standards were made with the same ratio. The ratio of two, three and four were added to see the effect of the error on

measurement accuracy. In table 14 it can be seen that with both lanthanum addition and matrix matching the potassium error is controlled at lower than five percent.

Table 13. Effect of alkali interaction on Na, K and Li measurements

Known standard (mg/l)	Measured Na (mg/l)	Error (%)	Measured K (mg/l)	Error (%)	Measured Li (mg/l)	Error (%)
Na 50	50.2	0.4	N/A	N/A	N/A	N/A
K 100	N/A	N/A	97.2	2.8	N/A	N/A
Li 50	N/A	N/A	N/A	N/A	50.6	1.2
Na 50 K 100	46.6	7.8	110.9	10.9	N/A	N/A
Na 50 K 100 Li 50	41.8	16.4	77.3	22.7	56	12
Na 50 K 100 La 1000 addition	49.6	0.8	83.3	16.7	N/A	N/A
Na 50 K 100 Li 50 La 1000 addition	48.8	2.4	91	9	51.4	2.8
Na 50 K 100 Li 100 La 1000 addition	47.9	4.2	91.6	8.4	99.0	1

Table 14. Alkali interaction effect and its reduction by matrix matching

Known standard (mg/l)	Measured K (mg/l)	Error (%)
20 Na 40K 1000La	41.2	3
20 Na 60K	63.2	5.33
20 Na 60K 1000La	59.6	0.67
20 Na 80K 1000La	82.4	3
16 Li 20 Na 80K 1000La	81.5	1.9

The pH of pore solution was measured using a glass electrode pH probe. The glass electrode is constructed with pH sensitive glass in the form of dome, bulb or flat surface at the immersing tip. The ion-exchange reactions between external glass of the electrode and solution create the potential (49). The glass electrode used in this research is a MI-410 microprobe from Microelectronics Inc in Bedford, NH, which is capable of measuring a sample size as small as 0.1ml.

For high PH solution measurement that contains sodium, there is a problem of sodium ion error. It is a result of sodium ion penetration into the glass network. This effect is compensated for by adding a standard correction to observed readings (49). After the pH was measured and adjusted for sodium error, the hydroxyl concentration was calculated. By definition, pH is the negative logarithm of the hydrogen ion activity. It can be described mathematically as:

$$\text{pH} = -\log_{10} a_{\text{H}^+} \quad (4)$$

The activity is the effective concentration of hydrogen ions in solution and is the product of concentration and activity coefficient. The activity coefficient is affected by temperature, the ionic strength, the dielectric constant, the ion charge and ionic size. For hydrogen ion, if temperature is set at 25°C, the activity coefficient is mainly affected by the ionic strength I. The ionic strength I is defined as:

$$I = 0.5 \sum C_m Z_i^2 \quad (5) \text{ where } Z_i \text{ is the ion charge and}$$

C_m is molar concentration of corresponded ion (49). The activity coefficient is calculated by the Debye-Huckel equation (50). The concentration of hydroxyl was calculated by the following equation:

$$[\text{OH}^-] = 10^{(\text{pH} - 14 - \log \gamma_{\text{OH}^-})}. \quad (6) \text{ where } \gamma_{\text{OH}^-} \text{ is the activity}$$

coefficient of the hydroxyl.

3.2.3 Test results and analysis

The pore solution test results for the high alkali cement paste, mortar and the low alkali cement mortar are presented in tables 15 through 17, respectively. One sample was

tested at each test age. The error was defined as the difference between anion normal concentration and cation normal concentration expressed as percentage of the anion normal concentration. The alkali evolution comparison is illustrated in figure 9 for low and high alkali mortar. From the test results it can be seen that:

Sulfate and calcium are insignificant beyond 28 days of age, which agrees with other researcher's results (12).

Alkali cations are mainly balanced by hydroxyls in pore solution. In mature paste or mortar without admixtures, alkali concentration is almost the same as the hydroxyl.

Table 15. Pore solution evolution for high alkali cement paste samples

Species Time	Na ⁺ (mmol/l)	K ⁺ (mmol/l)	OH ⁻ (mmol/l)	SO ₄ ²⁻ (mmol/l)	Ca ²⁺ (mmol/l)	Unbalanced error (%)
1 day	240	624	685	80	0.173	2.8
7 days	260	670	759	70	0.14	4.1
28 days	290	645	824	45	0.2	2.5
3 months	200	345	466	29	0.44	4.5
6 months	175	272	396	22	0.84	1.8
1 year	172	266	404	14	1.64	1.5

As shown in table 16, for cement with alkali content of 1.09 percent, the hydroxyl concentration in the pore solution is around 400mmol/l, which means pH is 13.6 and higher.

Table 16. Pore solution evolution for high alkali cement mortar samples

Species Time	Na ⁺ (mmol/l)	K ⁺ (mmol/l)	OH ⁻ (mmol/l)	SO ₄ ²⁻ (mmol/l)	Ca ²⁺ (mmol/l)	Unbalanced error (%)
1 day	221	578	656	60	0.176	3.6
7 days	246	626	754	47	0.146	3.2
28 days	262	603	766	40	0.24	2.5

3 months	155	312	392	30	0.52	4.1
6 months	147	249	356	15	0.88	3.3
1 year	142	242	355	12	1.58	2.3

As shown in table 17, Low alkali cement (0.26 percent $\text{Na}_2\text{O}_{\text{eq}}$) can reduce pore solution pH to around 13. This conclusion agrees with results from other researchers (12, 51). There is little change in pore chemistry beyond 6 months unless there is water loss.

Table 17. Pore solution evolution for low alkali cement mortar samples

Species Time	Na^+ (mmol/l)	K^+ (mmol/l)	OH^- (mmol/l)	SO_4^{2-} (mmol/l)	Ca^{2+} (mmol/l)	Unbalanced error (%)
1 day	55	127	149	14	0.78	4.4
7 days	63	140	180	8	0.59	4.5
28 days	70	162	214	6	0.5	3.3
3 months	41	78	109	3.6	0.47	3.4
6 months	37	72	99.5	3.2	0.62	4.4
1 year	34	68	98.1	1.8	0.7	1.7

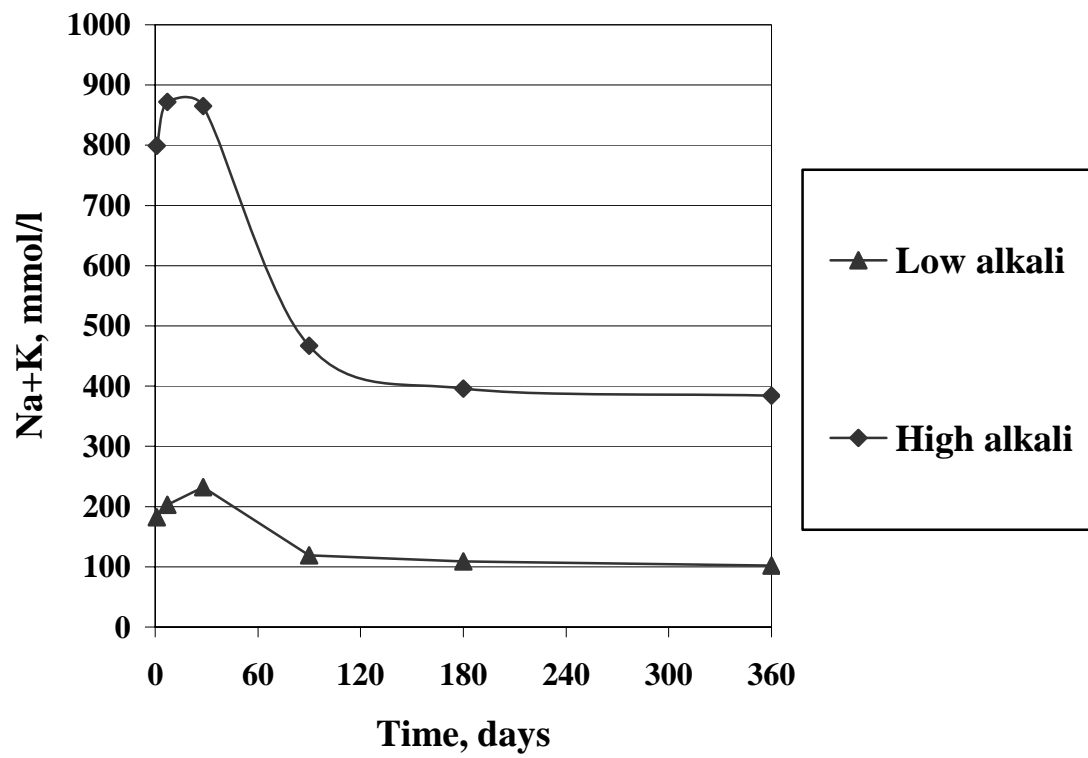


figure 9. Alkalis evolution in pore solution for cement mortar

F

CHAPTER 4

RCA ASR MITIGATION USING MINERAL ADMIXTURES

Since the source concrete of the RCA was known to have ASR, its potential for ASR needed to be addressed. Previous research showed that this RCA concrete must be mitigated (52). In this chapter, different mineral admixtures were tested for ASR mitigation including glass powders. The objective was to control ASR in RCA concrete while promoting usage of industrial by-product and/or waste materials.

4.1 Fly Ash Mitigation

4.1.1 Fly ash as a concrete admixture

Fly ash (FA) is one of the most abundant mineral admixtures used in the concrete industry. Fly ash, also called pulverized fuel ash or coal fly ash, is the finely divided residue that results from the combustion of ground or powdered coal and that is transported by flue gasses (53).

According to the American Coal Ash Association, the 2004 annual production of coal combustion products (CCP) was about 122 million tons, of which fly ash was 70.8 million tons. Examples of the beneficial use of fly ash are as shown in table 18 (54).

As shown in table 18, only around 40 percent of the FA production in 2004 ends up in beneficial usage. There is a great need for improvement. Approximately 90 percent

of the states have power plants that produce significant amount of fly ash, so it is a widely available material. Its price is roughly half the price of the portland cement, so it is economical to replace cement with fly ash in concrete.

Table 18. The beneficial uses of fly ash

Fly ash usage	Percentage of total produced
Concrete/concrete products/grout	19.9
Structural fills/embankment	6.6
Waste stabilization/solidification	3.5
Cement/raw feed for clinker	3.3
Mining applications	1.6
Soil modification/stabilization	0.7
Road base/sub-base/pavement	0.7
Flowable fill	0.25
Mineral filler in asphalt	0.13
Agriculture	0.07
Miscellaneous/other	2.9
Total use	39.65

Its properties and chemical composition mainly depend on the coal and the burning process, both of which vary widely. Fly ash consists primarily of oxides of silicon, aluminum, iron and calcium. Magnesium, sodium, potassium and sulfur also exist to a lesser degree. Fly ash is typically spherical shape and ranges from 10-100 micron in size as shown in figure 10 (55).

Fly ash is classified as Class C or F and it is mainly dependent on its calcium content. Class C fly ash, normally the product of burning sub-bituminous coals, has a higher calcium content, alkali content and it is usually more soluble. Class F fly ash, normally the product of burning bituminous and anthracite coals, has a lower calcium content (53).

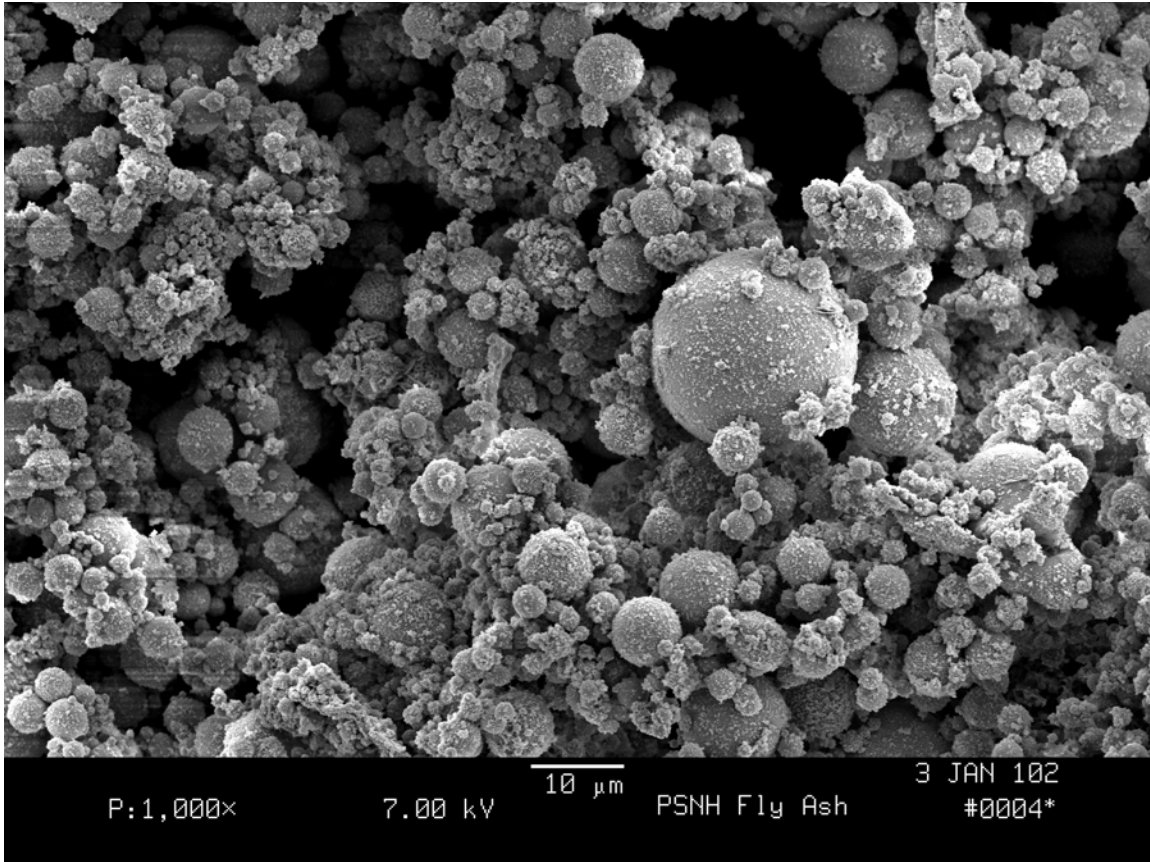


Figure 10. Microphotograph of fly ash

There is a tremendous amount of research available on the use of fly ash as an admixture in concrete (*See references 12, 56, 57 and 58*). It is generally accepted that fly ash can be used to mitigate ASR in concrete (*59*).

Fly ash has many beneficial effects on concrete properties ranging from improved workability to improved durability (*56, 57, 58*). The mechanism of reaction is referred as the pozzolanic reaction and it is quite complex. The main reaction is between calcium hydroxide and reactive silica or alumina. The pozzolanic reaction forms secondary C-S-H gel, which is similar to cement hydration product, but with a lower Ca/Si ratio (*12, 60*).

From the ASR mitigation perspective, fly ash mitigates ASR by lowering the

availability of calcium through calcium hydroxide consumption and alkali binding during the development of a C-S-H secondary gel (45, 46). There can also be an alkali dilution effect if the alkali content of fly ash is lower than that of portland cement. There can be a significant decrease in porosity and permeability due to pore size refinement (12).

A class F fly ash from Brayton Point, MA was used to mitigate ASR in RCA concrete and the Blue Rock control. The chemical composition of the fly ash is shown in Table 19. The cement used was type II commercial cement with chemical composition as shown in Table 10 of Chapter 3.

Table 19. Chemical composition of the Brayton Point fly ash

Components	percentage
SiO ₂	61.8
Al ₂ O ₃	25.2
Fe ₂ O ₃	5.4
CaO	1.2
SO ₃	0.1
Na ₂ O	0.13
K ₂ O	0.5
Na ₂ O _{eq}	0.5
LOI	2.2
Moisture	0.1
#325 sieve retained	17.8

4.1.2 Mortar bar expansion test

Current construction practice uses only the plus #4 fraction of RCA as aggregate when producing recycled concrete. To make ASTM C 1260 mortar bars, RCA needs to be further crushed. Unlike natural aggregates, the chemical and physical properties of RCA depend on its size as shown in tables 5 and 6 of Chapter 2 for Blue Rock RCA. A

decision on what grading to use for ASTM C1260 testing while maintaining a reasonable approximation of the actual grading of RCA was made while not biasing the expansion data. In an effort to maintain the relationship between the paste and aggregate content in the RCA the grading in table 20 was selected for all ASTM C1260 testing. This RCA grading is as crushed and rounded to the nearest 5 percent. This grading was applied to all mortar bar and pore solution samples. The average paste content was measured to be 22 percent by hydrochloric acid dissolution. Compared to the average ASTM C 1293 graded RCA paste content of 19.5 percent in table 7 of Chapter 2, this value is within a reasonable range. The change of paste fraction due to further crushing is insignificant.

Table 20. Comparison between crushed RCA and ASTM C1260 standard grading

Sieve #	#8	#16	#30	#50	#100
Crushed RCA (% retained)	30	25	25	15	5
ASTM C1260 Standard (% retained)	10	25	25	25	15

ASTM C 1260 specifies that at least three specimens need to be tested for each cement aggregate combination. This number needs to be statistically within acceptable marginal error. With exact proportions, 20 standard ASTM C1260 mortar bars with Blue Rock were tested under similar testing conditions. Two expansion data points were used for statistical analysis at 14 days and 28 days.

In this case, the population mean and variance are both unknown. In this condition, with the assumption that the distribution of the population is normal, then

$$\left(\frac{\bar{X} - \mu}{S/\sqrt{n}} \right) \sim t(n-1) \quad (7) \text{ where, } \bar{X} \text{ is the sample}$$

mean, in this case measured average expansion; μ is mean of the population, which is

unknown; S is the sample standard deviation; n is the sample size, in this case number of mortar bars; $t_{(n-1)}$ is Student-t distribution with degree of freedom (n-1) (61). A [100(1- α)] percent confidence interval for the real population mean is given by

$$P(\bar{X} - t_{(n-1), \alpha/2} S / \sqrt{n} < \mu < \bar{X} + t_{(n-1), \alpha/2} S / \sqrt{n}) = 1 - \alpha \quad (8) \quad t_{(n-1), \alpha/2} \text{ is}$$

defined as the value such that

$$P(T > t_{(n-1), \alpha/2}) = 1 - \alpha \quad (9) \text{ where } T \text{ is a random variable}$$

with a distribution of $t_{(n-1)}$.

The marginal error is defined as:

$$\text{Error} = \text{abs}[(\bar{X} - \mu) / \bar{X}] = t_{(n-1), \alpha/2} S / \sqrt{n} / \bar{X} \text{ in percentage} \quad (10)$$

The marginal error is still a random variable and its value can be determined at a specified [100(1- α)] percent confidence level using the expansion data from the 20 mortar bars as follows: $\bar{X} = 0.192\%$, $S=0.01\%$ at 14 days; $\bar{X} = 0.278\%$, $S=0.018\%$ at 28 days.

The marginal error as a function of sample size is presented in figures 11 and 12 for 14 days and 28 days respectively. The confidence levels were chosen at 95 and 90 percent. From figures 11 and 12 it can be seen that with 5 samples, which were adopted for all ASTM C 1260 test in this research, the error is within 8 percent at the 95 percent confidence level. The normal ASTM C 1260 minimum of three samples gives an accuracy of around 15 percent at the 95 percent confidence level.

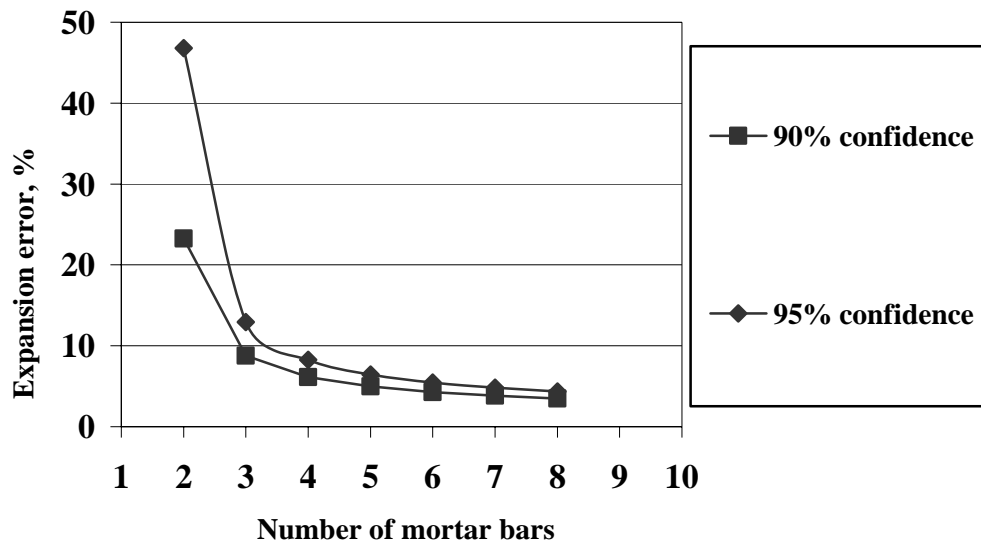


Figure 11. ASTM C 1260 expansion error at 14 days as a function of the number of mortar bars

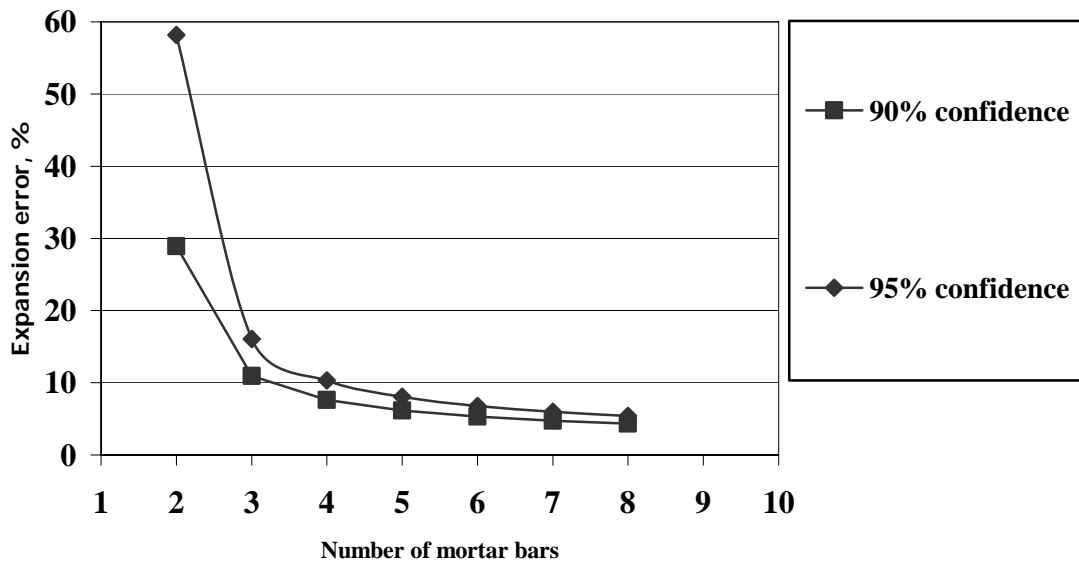


Figure 12. ASTM C 1260 expansion error at 28 days as a function of the number of mortar bars

4.1.3 Expansion results and comparison

As noted in previous research, RCA concrete samples experience early moisture expansion due to moisture equilibrium within the RCA (52). To minimize early expansion of the prism bars due to moisture expansion, the crushed RCA was vacuum soaked for two days before mixing. Typically 10 percent water was added to the four-mill nylon/polyethylene vacuum pouch after samples were put in. The pouch, with sample and water inside, was vacuum sealed by an automatic vacuum sealer and this procedure applied to all vacuum sealing processes in the research. The soaking water was used for mix water to avoid losing soluble alkali. Measured RCA absorption for as crushed grading in table 20 varies from 4.5 to 5.2 percent, with a standard deviation of 0.4 percent (3.6 percent for ASTM C 1293 grading). Absorption mix water in the amount of 5 percent of the RCA aggregate weight was added to address the early expansion.

The mix designs for batches of 5 ASTM C1260 mortar bars are presented in table 21. All mix proportions were the same as required by ASTM C 1260 with the exception of the RCA grading. One RCA batch was not soaked before mixing for comparison. The expansions were measured up to 28 days and are presented in figures 13 through 15. All expansion data are the average of a minimum of five samples. Typical coefficient of variation for ASTM C 1260 expansions ranged from 3 to 5 percent. The worst case was approximately 10 percent, which is typically considered to be reasonably good for research data collection.

Figure 13 shows that ASTM C 1260 expansion data for RCA are almost the same as for Blue Rock up to 28 days and soaking RCA does not make a significant difference

on expansion for the ASTM C 1260 test. The expansion difference between RCA soaked and unsoaked was within 2 standard deviations. One possible reason may lie in that the moisture expansion was almost completed during the 1-day curing and 1-day water soaking period. The other is the smaller size of the particles.

Table 21. Mix proportions for BR, RCA ASTM C 1260 samples, with/without fly ash

Mix Gradients	Blue Rock	RCA	BR Fly ash 15 %	BR Fly ash 25 %	RCA Fly ash 15%	RCA Fly ash 25%
Aggregate (g)	1687.5	1687.5	1687.5	1687.5	1687.5	1687.5
Cement (g)	750	750	637.5	562.5	637.5	562.5
Water (g)	352.5	436.88	352.5	352.5	436.88	436.88
w/c	0.47	0.47	0.47	0.47	0.47	0.47
Fly ash (g)	N/A	N/A	112.5	187.5	112.5	187.5

Figures 14 and 15 show that 25 percent fly ash lowered the ASTM C 1260 expansion for both RCA and Blue Rock mortar bars to less than 0.1 percent at 28 days. Substitution of 15 percent fly ash fails the 0.10 percent criteria at 28 days, but passes at 14 days.

The ASTM C 1260 results are comparable with ASTM C 1293 results from previous research (52). The comparison is presented in table 22. The criteria for ASTM C 1260 and ASTM C 1293 are taken as 0.10 percent and 0.04 percent for 14/28 days and 1/2 years respectively. The two test methods correlate well.

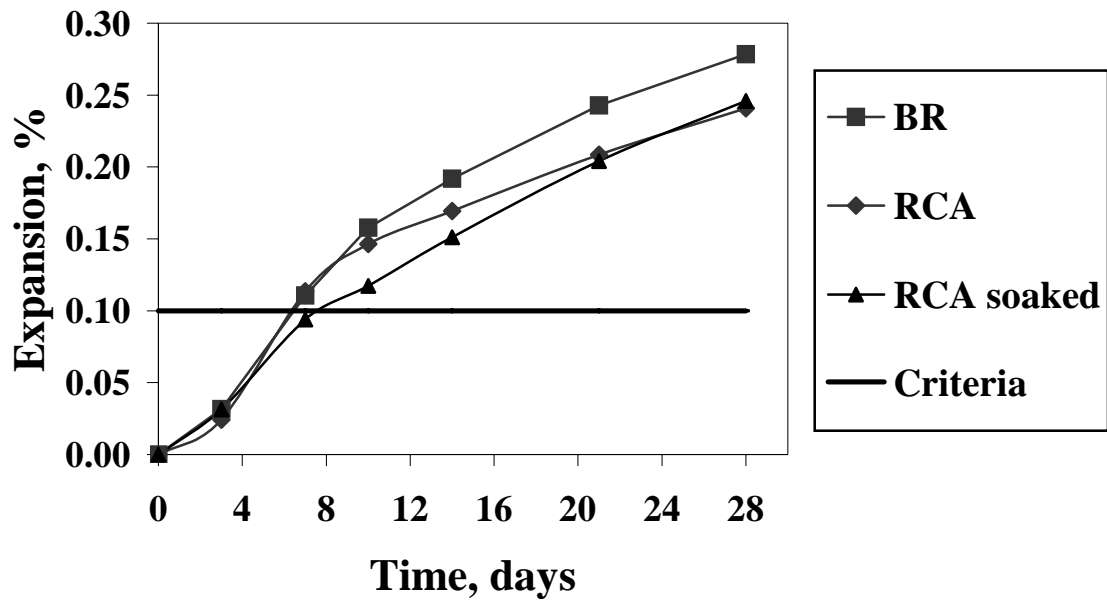


Figure 13. ASTM C 1260 expansions for BR and RCA samples

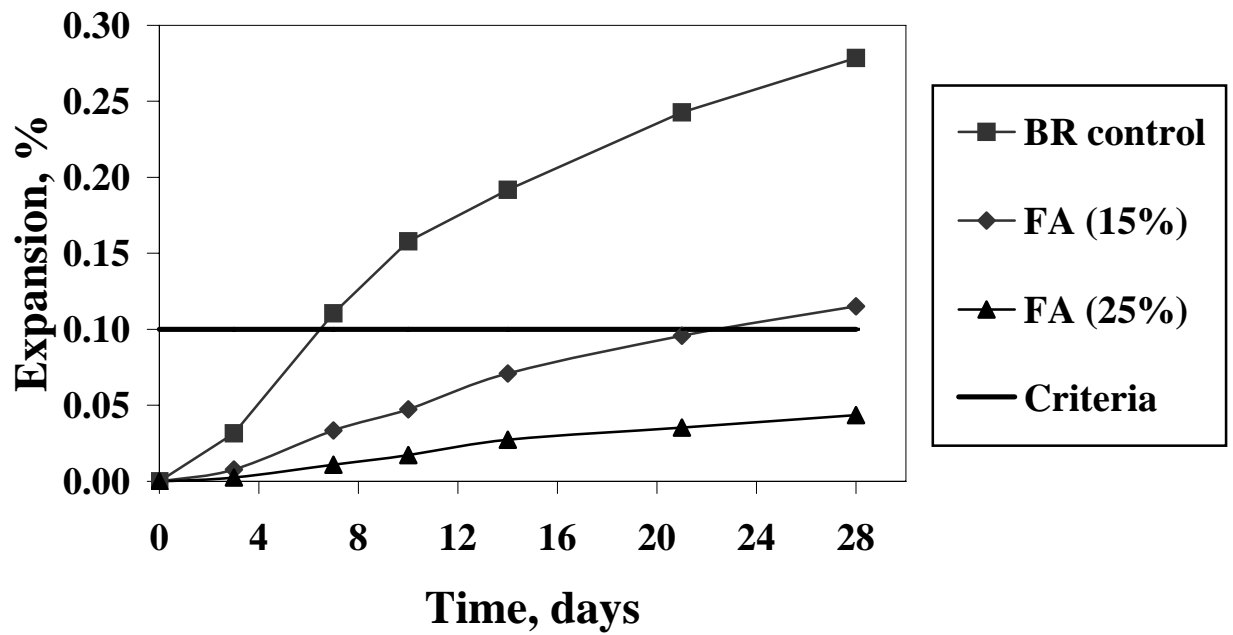


Figure 14. ASTM C 1260 expansions for BR control samples, with/without fly ash

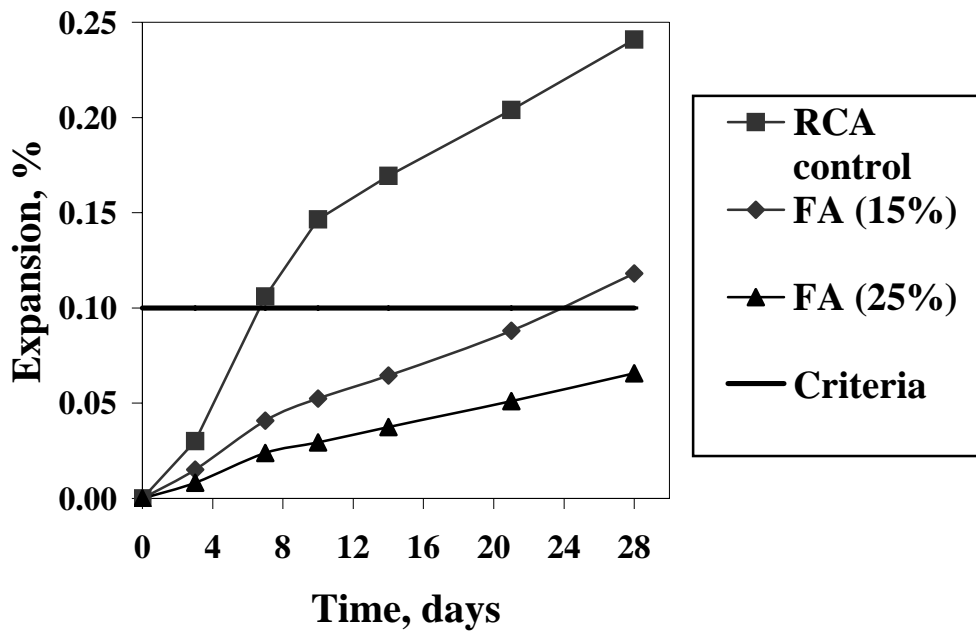


Figure 15. ASTM C 1260 expansions for RCA control samples, with/without fly ash

Table 22. Comparison of ASTM C 1260 and ASTM C 1293 for fly ash

Mitigation methods	ASTM C 1260 14 days	ASTM C 1293 1 year	ASTM C 1260 28 days	ASTM C 1293 2 years
Blue Rock (fly ash 15 %)	Pass	Pass	Fail	Fail
Blue Rock (fly ash 25 %)	Pass	Pass	Pass	Pass
RCA (fly ash 15 %)	Pass	N/A*	Fail	N/A
RCA (fly ash 25 %)	Pass	Pass	Pass	Pass

* data not available

4.1.4 Pore solution analysis

To learn the effect of fly ash on pore solution chemistry, mortar samples with 25 percent of fly ash table were made. A water cement ratio of 0.47 was chosen and

aggregates included Ottawa sand, BR and RCA. Six samples were batched from each mix set, vacuum-bagged with 5ml of water and stored at 38 °C. Pore solution was extracted from the samples as a function of time. The alkali, calcium and sulfate concentration was measured by ICP-OES and pH was measured using the MI-410 probe as described in chapter 3.

The alkali ion and hydroxyl's concentration evolution with time is presented in figure 16, 17 and tables 23 through 25. The hydroxyl concentration is nearly the same as the sum of potassium and sodium. Other ion concentrations are much lower compared to alkali and hydroxyls as shown in pore solution results in chapter 3. For these reasons, only alkali evolution is presented, hydroxyl concentration can be approximated by the sum of alkali.

Table 23. Pore solution evolution for Ottawa sand mortar with 25 percent fly ash

Species Time	Na ⁺ (mmol/l).	K ⁺ (mmol/l).	OH ⁻ (mmol/l).
1 day	173	417	510
7 days	140	290	392
28 days	116	230	332
3 months	92	157	250
6 months	79	144	221
1 year	72	138	200

Compared to the portland cement mortar samples at similar ages, alkali concentrations were significantly lower for the fly ash substitution samples. The hydroxyl concentration at later ages is virtually the same as the sum of alkalis, showing that pH reduction is significant. It is likely that the pH is reduced to below a threshold level and

ASR is mitigated since ASR needs high pH to sustain. Other researchers suggested similar mechanism for fly ash mitigation using different aggregate (62, 63). When used as an ASR mitigation admixture, the fly ash alkali content should be considered as an important factor, the lower the better.

Table 24. Pore solution evolution for BR mortar with 25 percent fly ash

Species Time	Na ⁺ (mmol/l).	K ⁺ (mmol/l).	OH ⁻ (mmol/l).
1 day	199	421	546
7 days	147	307	418
28 days	119	243	343
3 months	86	168	242
6 months	74	137	204
1 year	73	133	200

Table 25. Pore solution evolution for RCA mortar with 25 percent fly ash

Species Time	Na ⁺ (mmol/l).	K ⁺ (mmol/l).	OH ⁻ (mmol/l).
1 day	200	432	564
7 days	147	300	407
28 days	114	234	324
3 months	80	166	228
6 months	70	137	200
1 year	69	131	197

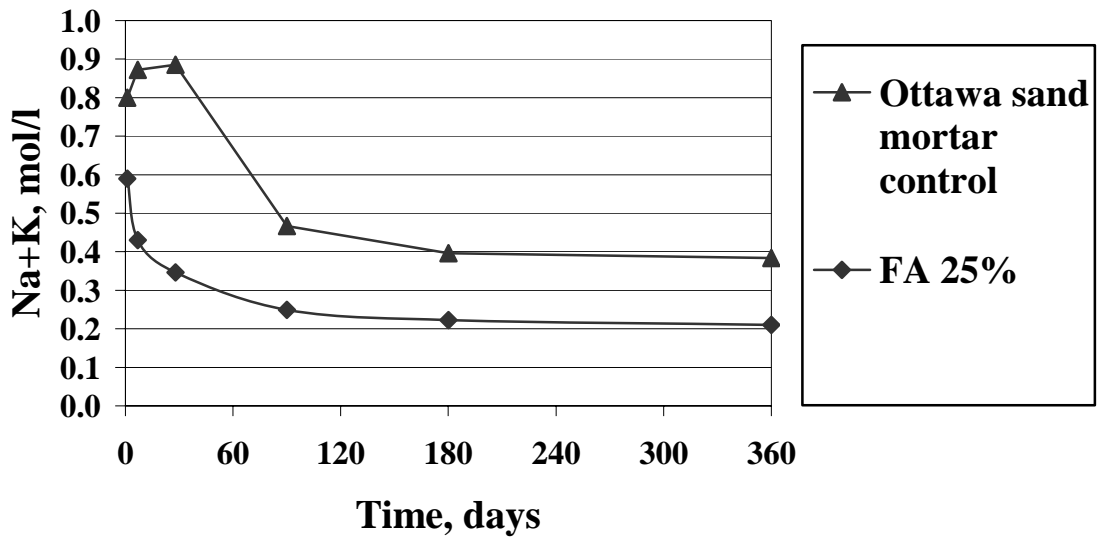


Figure 16. Pore solution alkalis evolution for Ottawa sand mortar samples, with/without fly ash

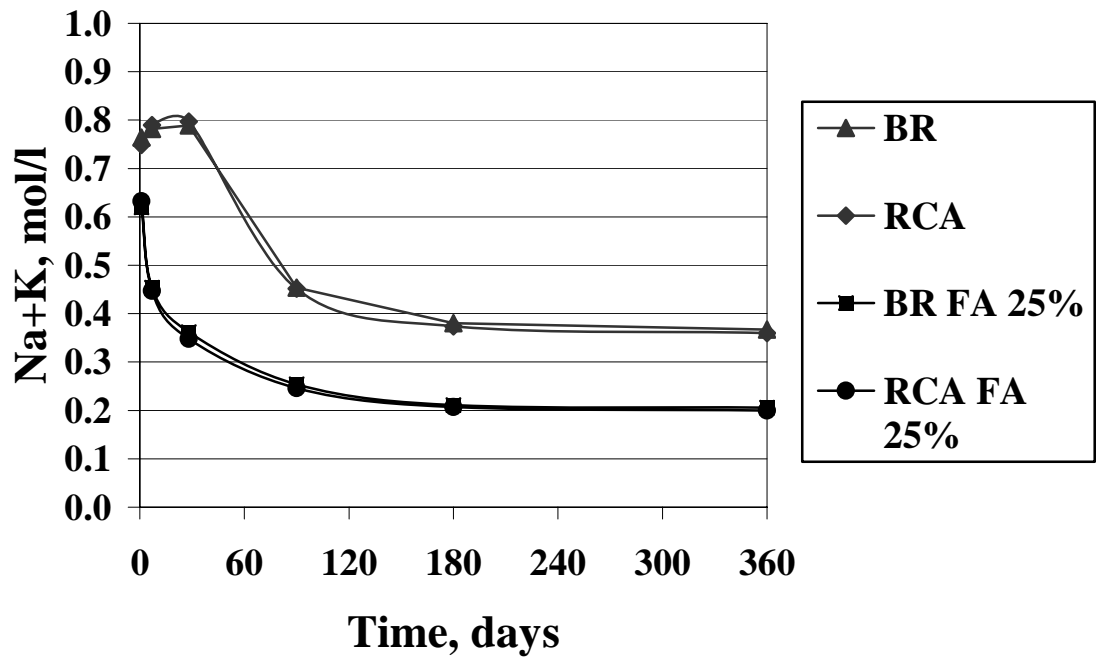


Figure 17. Pore solution alkalis evolution for BR/RCA mortar samples, with/without fly ash

In theory, RCA should contribute alkali to the mortar or concrete system since it has soluble alkali from old paste, but the pore solution does not show the effect on concentration as presented in figure 17. The possible reason may lie in that the pore solution itself is high in alkali concentration from portland cement. To clarify this, RCA was immersed in simulated pore solution (0.1N NaOH+0.2NKOH) for 72 hours. The soaking solution was measured before and after soaking by ICP-OES and it did not show an alkali increase as shown in table 26. The concentration change is negligible and within the ICP-OES measurement error. Compared with the results presented in table 8 in chapter 2, the alkalis leached out to pure water, but not to simulated pore solution with alkalis in it. This suggests the alkalis in RCA may be in equilibrium with the alkalis in the pore solution.

Table 26. Alkali concentration in solution before and after RCA soaking

	Na	K
Before soaking (mg/l)	2240	7678
Post-soaking (mg/l)	2269	7652
Change (%)	1.3	-0.3

4.1.5 Mitigation mechanism analysis

It was clearly shown in the pore solution testing that fly ash substitution reduces the alkalinity of concrete pore solution. To further analyze the fly ash mitigation mechanism and learn the role of alkali and calcium in the gel formation process, six batches of mortar bar samples were made and tested with the mix design shown in table 27. The aggregate used was Blue Rock. Expansions were measured up to 8 weeks and are

presented in figures 18 and 19.

A high dosage of percent fly ash was used to assure the pH of the pore water would fall below the threshold level. The objective of the higher substitutions was to deplete the calcium hydroxide as much as possible. Additional calcium hydroxide and sodium hydroxide was added to the mixes (spiked) to see the effect on expansion.

Figure 18 shows that even with the spiked calcium hydroxide, 40 percent fly ash reduced the ASTM C 1260 expansion to about 0.04 percent at 28 days, effectively mitigating ASR. The expansion differences between the samples with or without spiked calcium hydroxide were within 1.5 standard deviations. Spiked calcium prevented possible calcium depletion suggesting that mitigation is affected by lowered pH and not high doses of calcium. Other researchers also found no correlation between calcium

Table 27. Mix proportions for mechanism analysis mortar samples

Mix Components	FA 40	FA 40 Alkali spike	FA 40 Calcium spike	FA 60 Alkali Spike	FA 70 Alkali Spike	FA 80 Alkali Spike
Aggregate (g).	1687.5	1687.5	1687.5	1687.5	1687.5	1687.5
Cement (g).	450	450	450	300	225	150
Water (g).	352.5	352.5	352.5	352.5	352.5	352.5
w/c	0.47	0.47	0.47	0.47	0.47	0.47
Fly ash (g).	300	300	300	450	525	600
NaOH (g).	N/A	19.35	N/A	43.55	43.55	43.55
Ca(OH) ₂ (g).	N/A	N/A	60	N/A	N/A	N/A

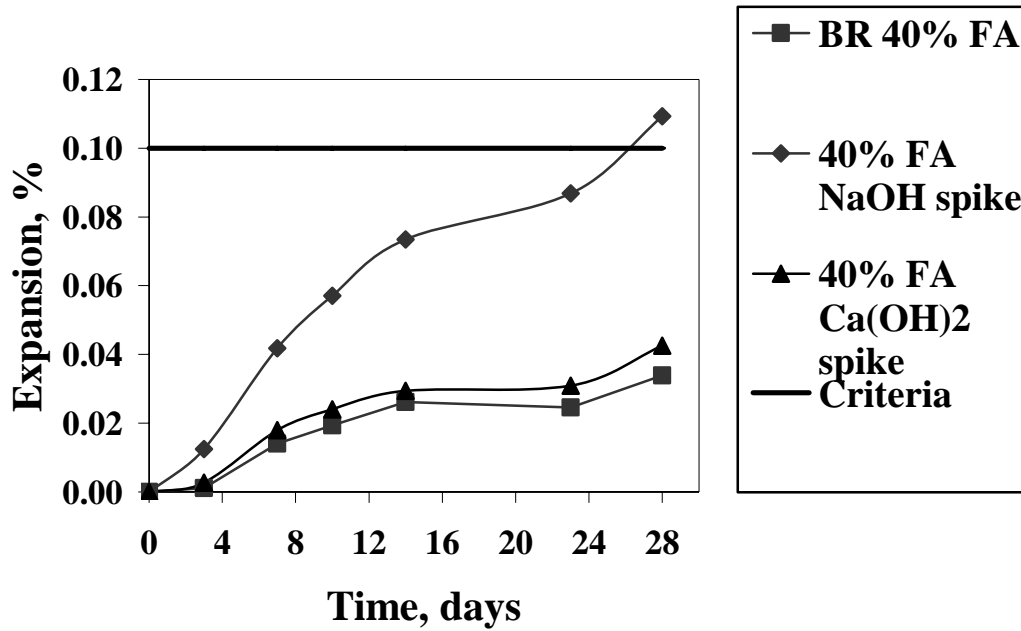


Figure 18. Effect of spiked $\text{Ca}(\text{OH})_2$ and NaOH on fly ash mitigation

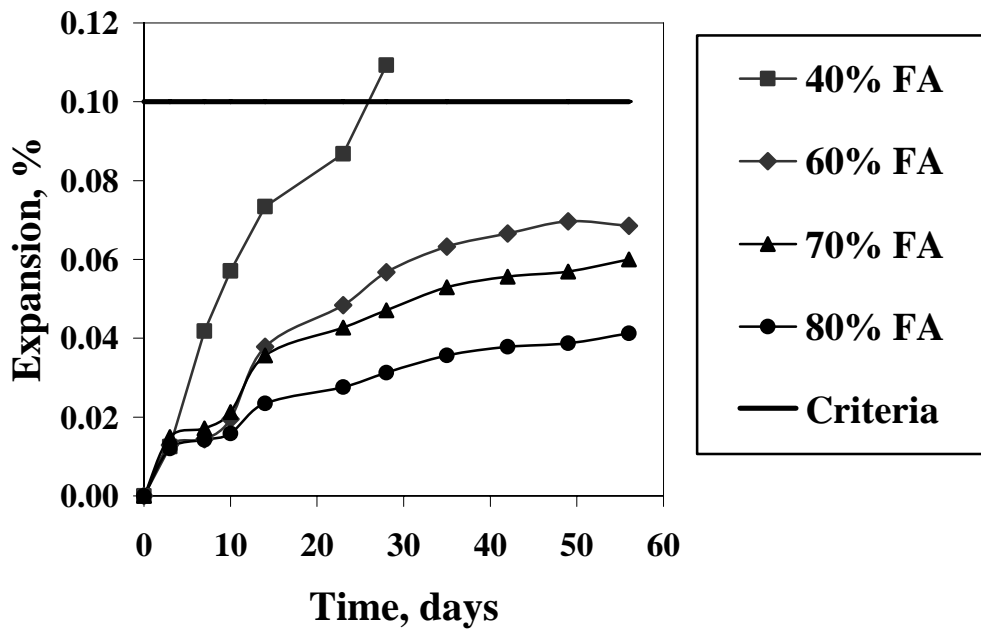


Figure 19. ASTM C 1260 expansions for BR samples with high fly ash substitution and NaOH spike

consumption and expansion reduction unless calcium is near depletion (62, 63). On the other hand, alkali addition counteracts mitigation and increases the expansion significantly. These results were corroborated with pore solution test results that showed alkali and pH reduction is pivotal in fly ash mitigation.

The role of calcium is important in the gel formation and expansion process. Calcium depletion alone may arrest ASR since ASR needs calcium ion, however it is difficult to practically do so (22, 23). The pozzolanic reaction reduces the availability of calcium ions, which are created by dissolution of calcium hydroxide due to cement hydration. If calcium hydroxide is completely depleted, even with high alkalis in the pore solution, ASR gel stops to form. From figure 19 it can be seen even with adding additional sodium hydroxide (as 4.5 percent $\text{Na}_2\text{O}_{\text{eq}}$ of total binder, which is almost five times the normal load), at 60 percent and higher fly ash substitution, the ASTM C 1260 expansion was reduced to less than 0.08 percent even at 8 weeks. The objective of the higher dosage was to consume more calcium hydroxide and deplete it within the short period of the test. All samples were spiked with NaOH, and the usual overwhelming quantity of alkali that exists in the soaking solution (1mol/l NaOH) was constant as in ASTM C 1260.

To evaluate calcium hydroxide consumption by fly ash, a Thermal Gravimetric Analysis (TGA) was performed on several samples containing fly ash. Grounded paste samples and those with fly ash substitution, all of 60 days age, were heated from room temperature to 1000°C at a 20°C/min rate. The results are presented in figure 20. Peaks

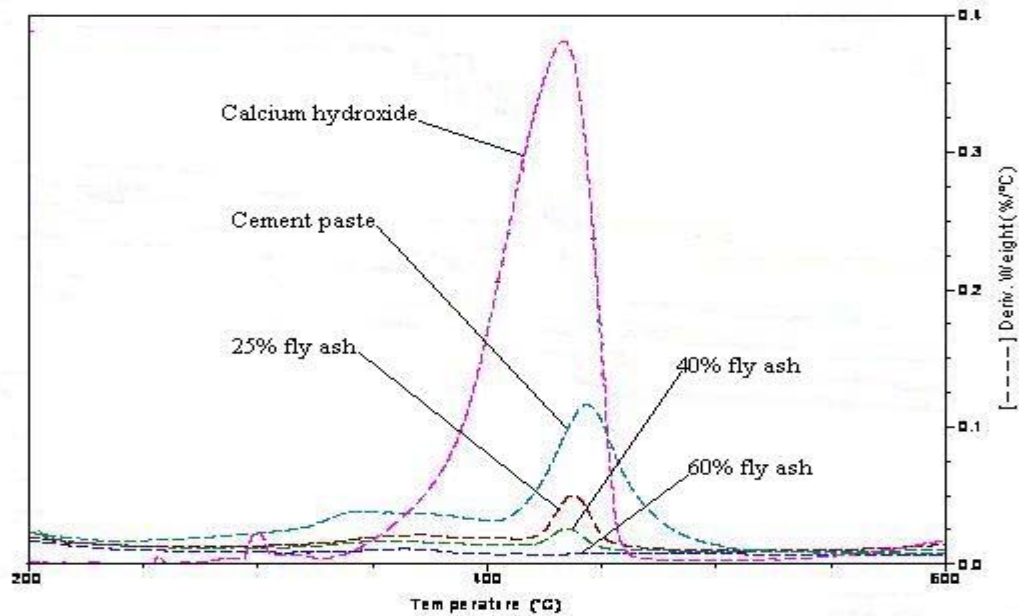


Figure 20. TGA of $\text{Ca}(\text{OH})_2$, cement paste and cement paste with different fly ash substitution

that are present at around 420-430°C are presumably due to decomposition of the calcium hydroxide, which is confirmed by the peak of calcium hydroxide at similar temperature.

It is noted that, with increasing fly ash substitution, the calcium hydroxide content decreases. At the 60 percent fly ash substitution, calcium hydroxide is hardly detectable.

At the 40 percent substitution, there is still considerable calcium hydroxide in the paste system at 60 days. Comparison of the 60 percent and 40 percent sodium hydroxide spiked curves in figure 19 shows the positive impact of calcium depletion on expansion. This is consistent with the work of other researchers in that calcium availability influences the ASR expansion development (64).

It was well known that fly ash has pozzolanic reactivity and the pozzolanic reaction consumes calcium hydroxide and forms a secondary gel (12, 57, 60). The secondary gel, typically C-S-H or C-A-S-H, binds alkali and hydroxyls as the primary gel does (44, 45, 46). It was observed in this case that pH drops below the threshold level to prevent ASR before depletion of the calcium hydroxide. Although calcium depletion alone warrants ASR arrest it would, depending on the cement and fly ash, require approximately 40 percent or more fly ash substitution before calcium depletion could be assured. At 40 percent fly ash substitution, the strength development is much slower than regular concrete. The field properties of such a high dosed mix would restrict its use on most projects that require early strength.

4.2 Ground Granulated Blast Furnace Slag (GGBFS) Mitigation

4.2.1 Slag production and use in concrete

Slag is a by-product of the steel industry. The blast furnace is a huge, steel stack lined with refractory brick, where iron ore, coke and limestone are placed on the top, and preheated air is blown into the bottom. Inside the blast furnace, the materials go through numerous physical changes and chemical reactions while descending to the bottom, where they become the liquid slag and iron. The limestone is melted to become slag which removes sulfur and other impurities during the process (65). The liquid slag then is quickly quenched by pressured water, producing granulated slag with a degree of

vitrification of 95 percent. The quick quench process prevents crystallization, which is the case in air cooling. The quenched slag then is ground to the specific fineness, which is ground granulated blast furnace slag. The composition of GGBFS varies depending on raw materials and the mix proportion. A typical US slag composition is shown in table 28 (12). Slag has been used as a cement substitute in concrete for more than 100 years and it is an effective means of mitigating ASR (66, 67).

Table 28. Typical US slag oxide composition

Oxide	Percentage
CaO	29-42
MgO	8-19
SiO ₂	32-40
Al ₂ O ₃	7-17
SO ₃	0.7-2.2

4.2.2 Expansion test results and comparison

The GGBFS used in this research had specific gravity of 2.85 and alkali content of 0.41 percent as Na₂O_{eq}. The hydraulic activity with NaOH tested per ASTM C 1073 was 8.6MPa (68). ASTM C 1567 mortar bar samples made for BR and RCA with 25 percent and 55 percent GGBFS were evaluated. All mix proportions were as required by ASTM C 1567 with the exception of the RCA grading. Expansions were measured up to 28 days and are presented in figures 21 and 22. Figure 21 and 22 show that 55 percent GGBFS substitution lowered ASTM C 1260 expansions for both RCA and Blue Rock mortar samples to less than 0.1 percent at 28 days. The 25 percent substitution fails the 0.10 percent criteria at 28 days for both RCA and Blue Rock mortar samples. It passes at

14 days for RCA, but not for Blue Rock.

The ASTM C 1260 results are comparable with ASTM C 1293 results from previous research (52). The comparison is presented in table 29. The criteria for ASTM C 1260 and ASTM C 1293 are taken as 0.10 percent and 0.04 percent respectively. The two exceptions of the correlation are as follows: RCA concrete, 55 percent GGBFS substitution failed the ASTM C 1293 at 2 years, but just barely. Blue Rock concrete, 25 percent GGBFS substitution failed the ASTM C 1260 at 14 days, but passed ASTM C 1293 at 1 year.

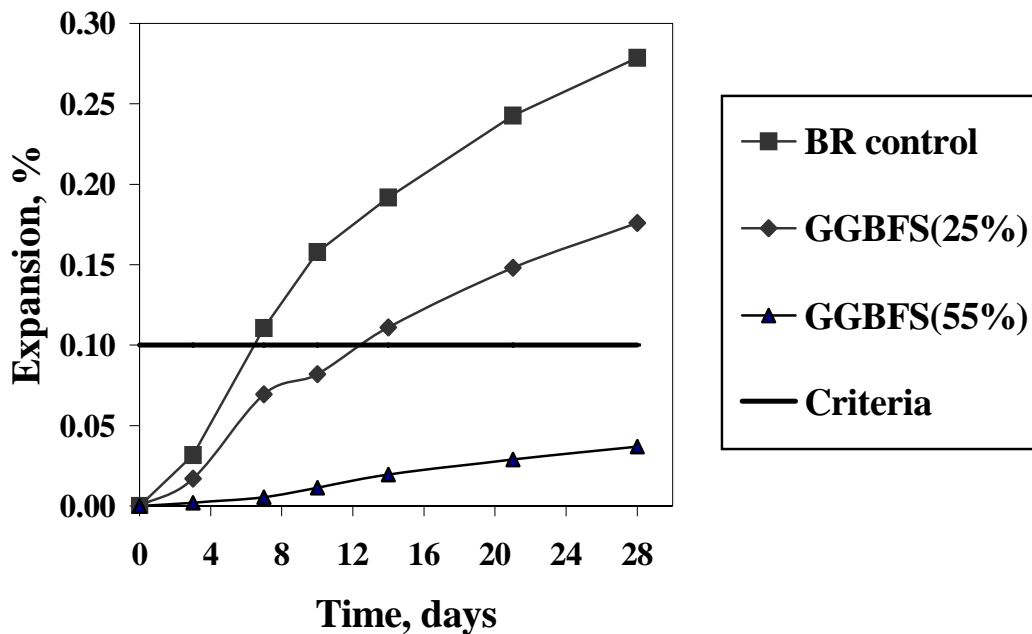


Figure 21. ASTM C 1260 expansions for BR control samples, with/without GGBFS

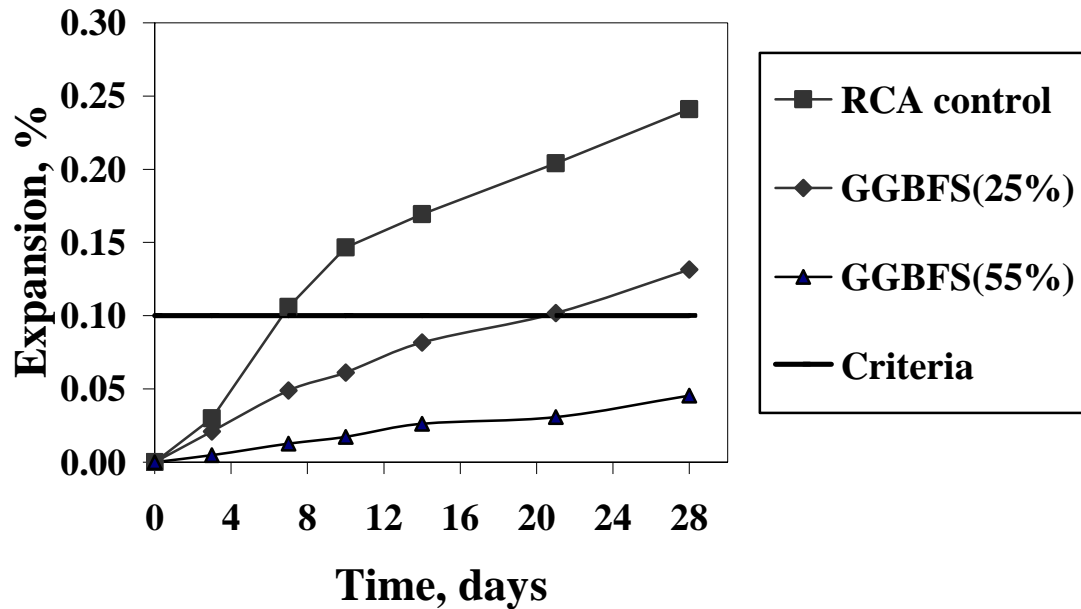


Figure 22. ASTM C 1260 expansions for RCA control samples, with/without GGBFS

Table 29. Comparison of ASTM C 1260 and ASTM C 1293 for GGBFS

Mitigation methods	ASTM C 1260 14 days	ASTM C 1293 1 year	ASTM C 1260 28 days	ASTM C 1293 2 years
Blue Rock (GGBFS 25 %)	Fail	Pass	Fail	Fail
Blue Rock (GGBFS 55 %)	Pass	Pass	Pass	Pass
RCA (GGBFS 25 %)	Fail	Fail	Fail	Fail
RCA (GGBFS 55 %)	Pass	Pass	Pass	Fail (0.0416 %)

4.2.3 Pore solution analysis and TGA

Since the pore solution evolution in fly ash samples suggests that the aggregate does not have much effect on the pore solution, only Ottawa sand mortar samples were used for pore solution analysis for GGBFS. Samples were vacuum-bagged with 5ml of

water and stored at 38 °C. Alkali concentration was measured by ICP-OES as described in chapter 3 for the pore solution. The calcium hydroxide content was measured by TGA for cement paste and those samples with GGBFS substitution at 60 days. The results are shown in figures 23 and 24. Similar to fly ash mitigation, GGBFS substitution reduced alkali concentration in pore solution and calcium content in paste. These are consistent with results from other researchers (69).

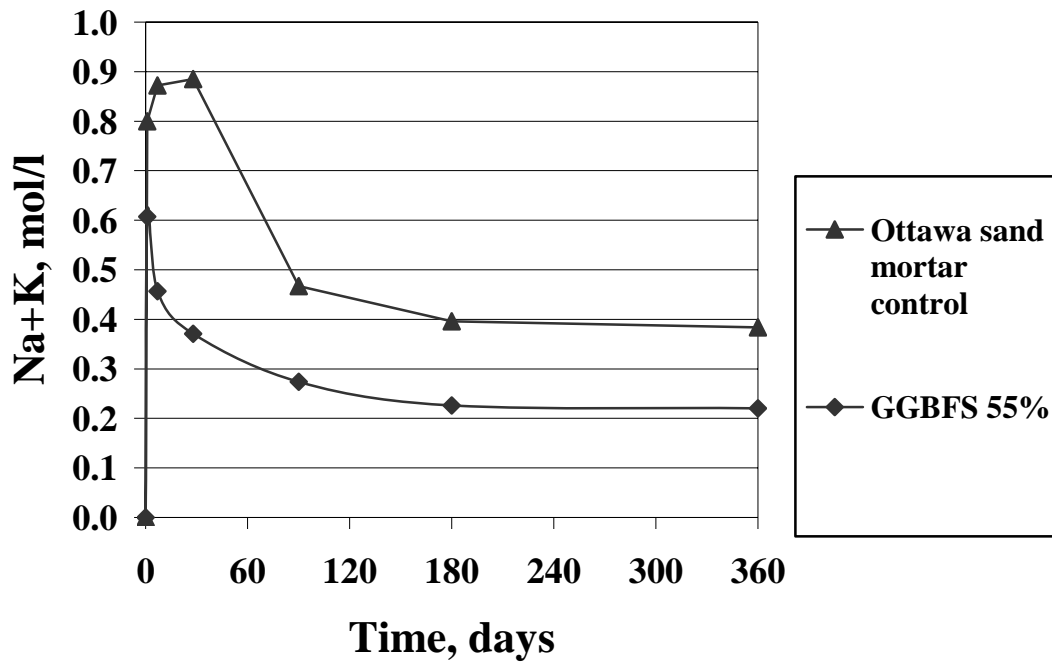


Figure 23. Pore solution alkalis evolution for Ottawa sand mortar samples, with/without GGBFS

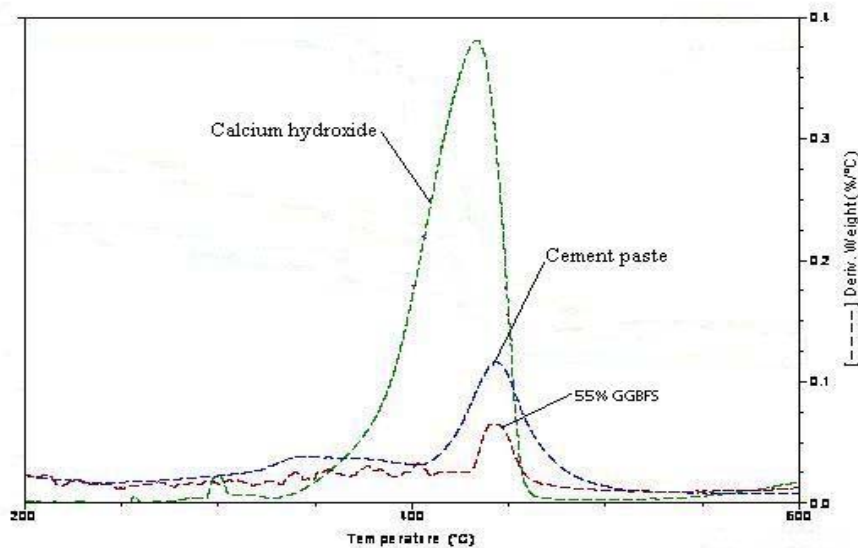


Figure 24. TGA of $\text{Ca}(\text{OH})_2$, cement paste and cement paste with GGBFS

4.3 Silica Fume Mitigation

Silica fume (also called condensed silica fume or micro-silica) is a by-product of silicon and ferrosilicon industries. It precipitates during the condensation of oxidized the silicon monoxide from the gases of silicon and ferrosilicon smelter ovens. The main chemical component of silica fume is SiO_2 , which accounts for around 90 percent of its weight. The major second component is Fe_2O_3 , while other minor components are less than one percent in weight. Since it is formed from gas condensation, the particles are ultra fine and the surface area can be up to $25\text{m}^2/\text{g}$. Compared to portland cement, its average particle size is almost two orders of magnitude smaller (12). Its main commercial

use is in concrete industry and costs approximately 10 times the cost of the portland cement.

Silica fume has been used in concrete for about a half century. It has many beneficial effects on concrete properties and is almost essential for the production of high performance concrete (70). Its pozzolanic reaction is more profound than other admixtures due to its higher amorphous silica content and finer particle size. Silica fume can be very effective in controlling ASR in concrete.

4.3.1 Expansion results and comparison

Silica fume used in this project was obtained from Grace Concrete Products Inc. in Cambridge, MA.

ASTM C 1567 mortar samples were made for BR, RCA with silica fume substitution. All mix proportions were as required by ASTM C 1260 with the exception of the RCA grading. ASTM C 1293 concrete prisms were made according to the mix design in table 30 for BR and RCA. Fine aggregate, which was Ossipee sand from Ossipee NH, has an ASTM C 1260 14 days expansion of 0.04 percent and is characterized as non-reactive.

Table 30. Mix design for ASTM C 1293 BR, RCA concrete prisms with silica fume

w/c	Cement (kg/m ³)	Coarse Aggregate (kg/m ³)	Fine Aggregate (kg/m ³)	NaOH (g/m ³)	Silica fume Substitution level
0.45	420	1050	650	867	8 %, 12%

ASTM C 1293 specifies that three specimens to be tested for each batch of

concrete and it was adopted for all ASTM C 1293 testing. The marginal error, shown in figure 25, was calculated by equation 10 based on the following expansion data of the BR samples:

$$\bar{X} = 0.0892\%, S=0.0029\% \text{ at 1 year; } \bar{X} = 0.108\%, S=0.0031\% \text{ at 2 years.}$$

The error is around 8 and 7 percent at the 95 percent confidence level for expansion at 1 year and 2 years, respectively. This can be considered adequate for research data analysis.

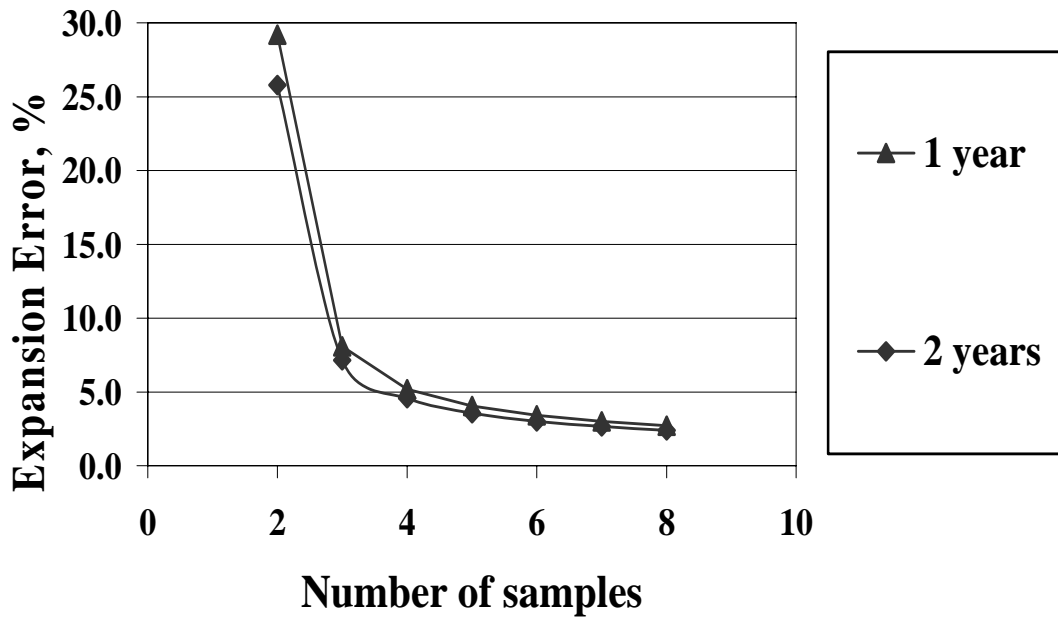


Figure 25. ASTM C 1293 expansion error as a function of the number of samples at 95% confidence level

The expansions of ASTM C 1260 samples were measured up to 28 days and those of ASTM C 1293 samples up to 2 years. The results are presented in figures 26 through 30. All expansion data are the average of a minimum of three or five samples for ASTM

C 1293 and C 1260 respectively.

As shown in figures 26 and 27, 12 percent silica fume substitution lowered ASTM C 1260 expansion of RCA and Blue Rock to less than 0.1 percent at 28 days. The 8 percent silica fume fails the 0.10 percent criteria at 28 days, but passes at 14 days.

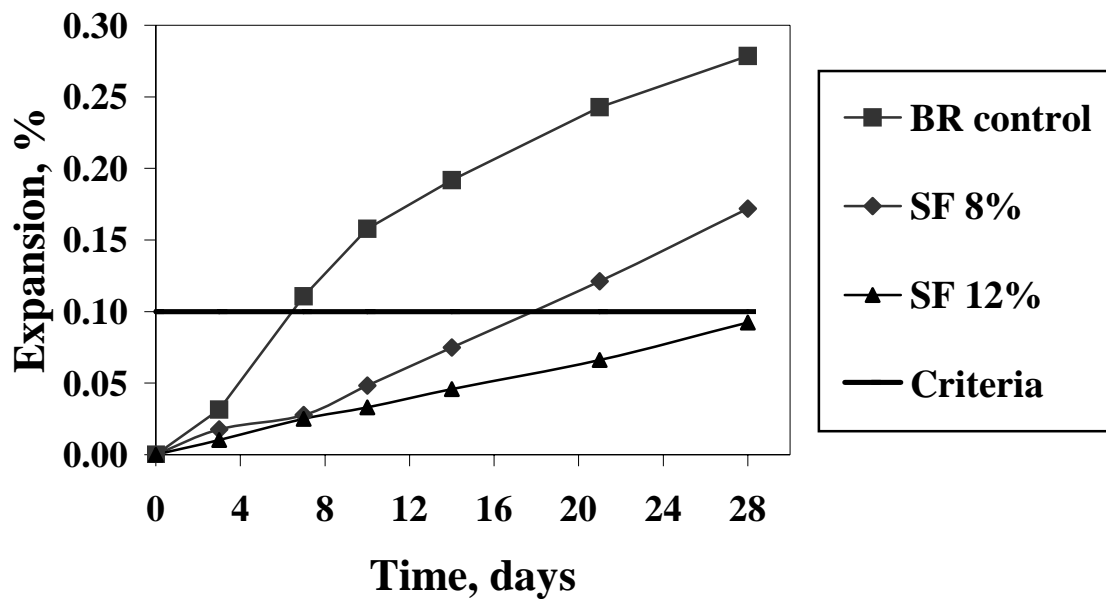


Figure 26. ASTM C 1260 expansions for BR control samples, with/without silica fume

As seen in figure 28, soaking RCA before mixing has significant effect on ASTM C 1293 expansion especially at early ages. Even with soaking technique, RCA expansions are still greater than BR at similar ages. The possible reason may lie in the swelling of the old gel in RCA, reactivation of old reaction product and increased alkali loading.

Figures 29 and 30 show that 12 percent silica fume substitution lowered ASTM C 1293 expansion for both RCA and Blue Rock to less than 0.04 percent at 2 years. The

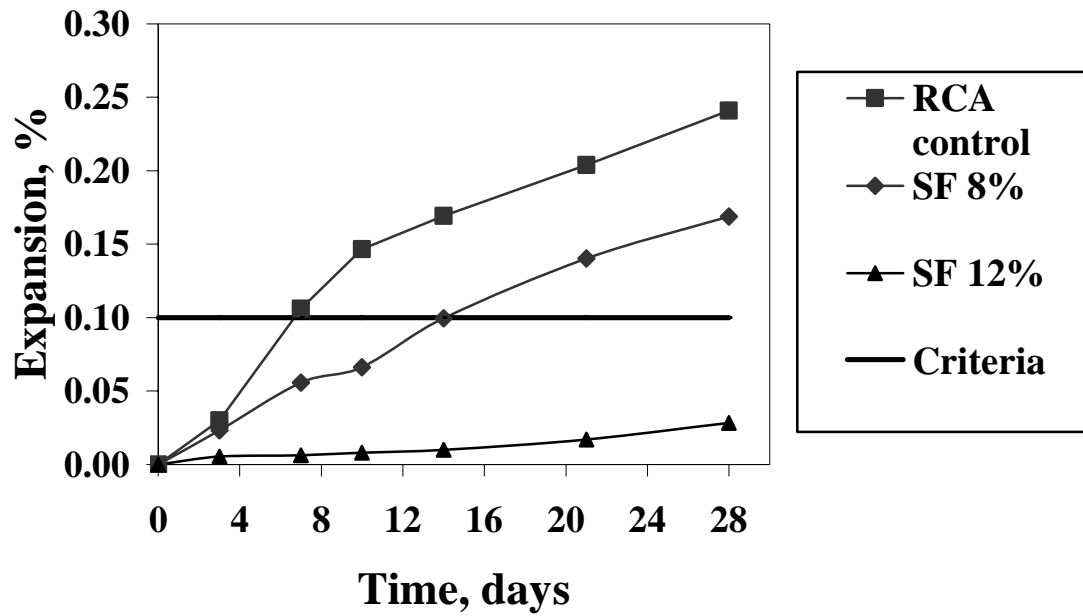


Figure 27. ASTM C 1260 expansions for RCA control samples, with/without silica fume

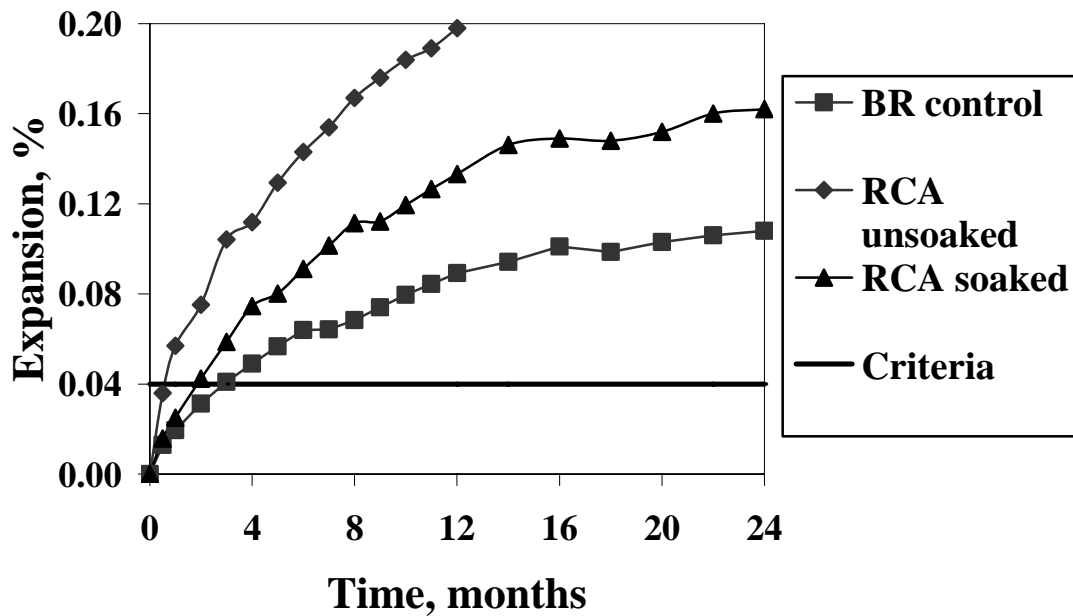


Figure 28. ASTM C 1293 expansions for BR and RCA samples

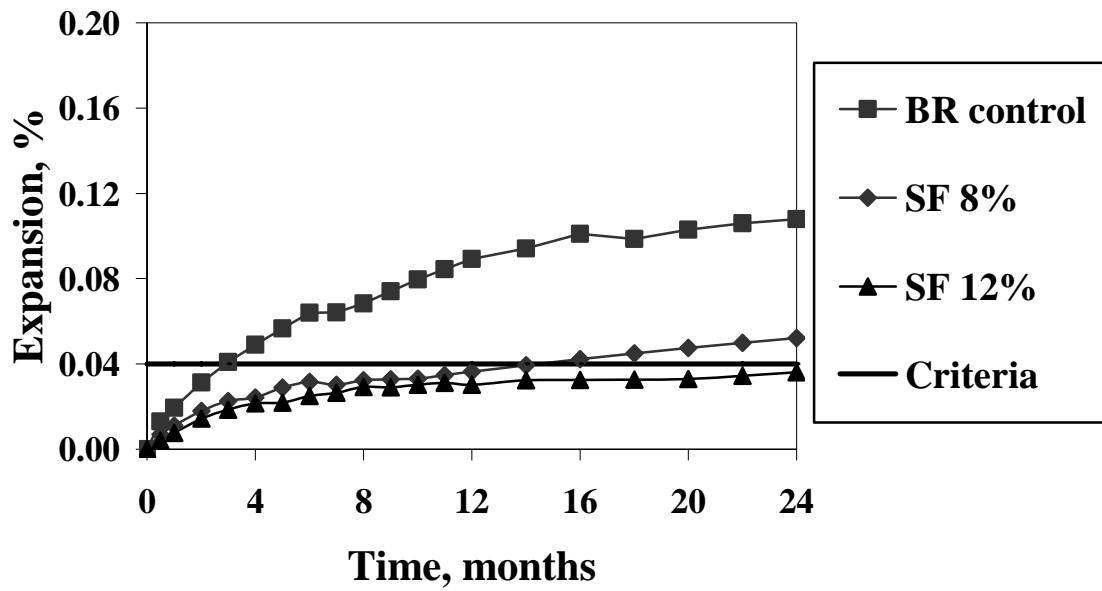


Figure 29. ASTM C 1293 expansions for BR control samples, with/without silica fume

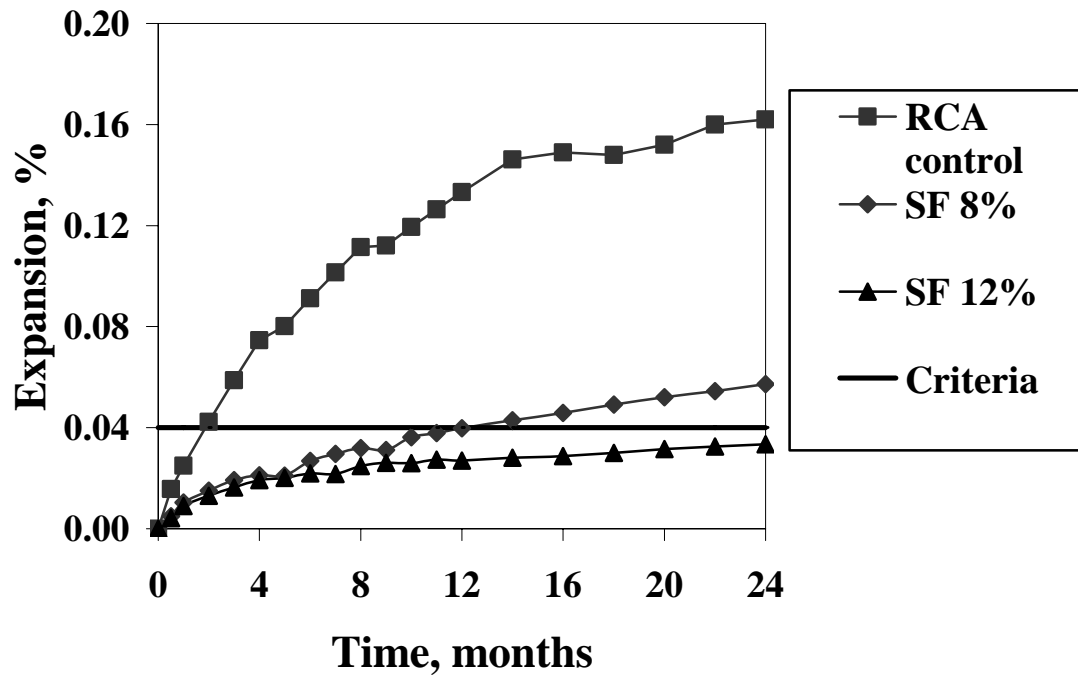


Figure 30. ASTM C 1293 expansions for RCA control samples, with/without silica fume

eight percent silica fume fails the 0.04 percent criteria at 2 years, but passes at 1 year.

The ASTM C 1260 results correlated well with ASCTM C 1293 results and the comparison is presented in table 31.

Table 31. Comparison of ASTM C 1260 and ASTM C 1293 for silica fume

Mitigation methods	ASTM C 1260, 14 days	ASTM C 1293, 1 year	ASTM C 1260, 28 days	ASTM C 1293, 2 years
Blue Rock (silica fume 8 %)	Pass	Pass	Fail	Fail
Blue Rock (silica fume 12 %)	Pass	Pass	Pass	Pass
RCA (silica fume 8 %)	Pass	Pass	Fail	Fail
RCA (silica fume 12 %)	Pass	Pass	Pass	Pass

4.3.2 Pore solution analysis and TGA

The effect of silica fume on pore solution, using Ottawa sand mortar samples, was evaluated. Samples were vacuum-bagged with 5ml of water and stored at 38 °C. The results are shown in figure 31.

The calcium hydroxide content was measured by TGA for cement paste with or without silica fume. As shown in figure 32, similar to fly ash and GGBFS mitigation, silica fume substitution reduced alkali concentration in pore solution. The calcium hydroxide content also decreased significantly due to silica fume. The alkali reduction in the silica fume pore solution, as was the finding with fly ash, is the primary ASR arresting mechanism. These are consistent with results from other researchers (69).

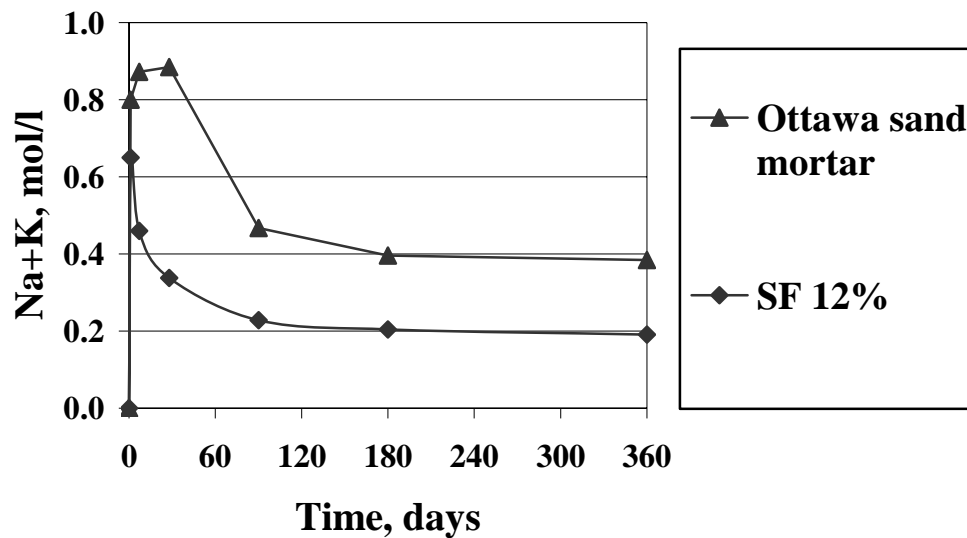


Figure 31. Pore solution alkalis evolution for Ottawa sand mortar samples, with/without silica fume

4.3.3 Particle size issue

It has been widely reported that silica fume agglomerates can cause ASR instead of mitigating it (71, 72). As shown in table 32, the silica fume did have some lumps and conglomerations as large as 0.6mm. It should be noted that the lumps and conglomerations typically break up during mixing, but there has been cases where the large particles did not break completely during the mixing process (69, 72). The silica fume particles were sieved and divided to three size groups: SF30, SF50 and SF200. SF30 includes all the particles retained on sieve #30 and above. SF50 includes all the particles retained on sieve #50 and #100. SF200 includes all the particles passing sieve #200. All silica fume used in the aforementioned mitigation for Blue Rock and RCA concrete was SF200.

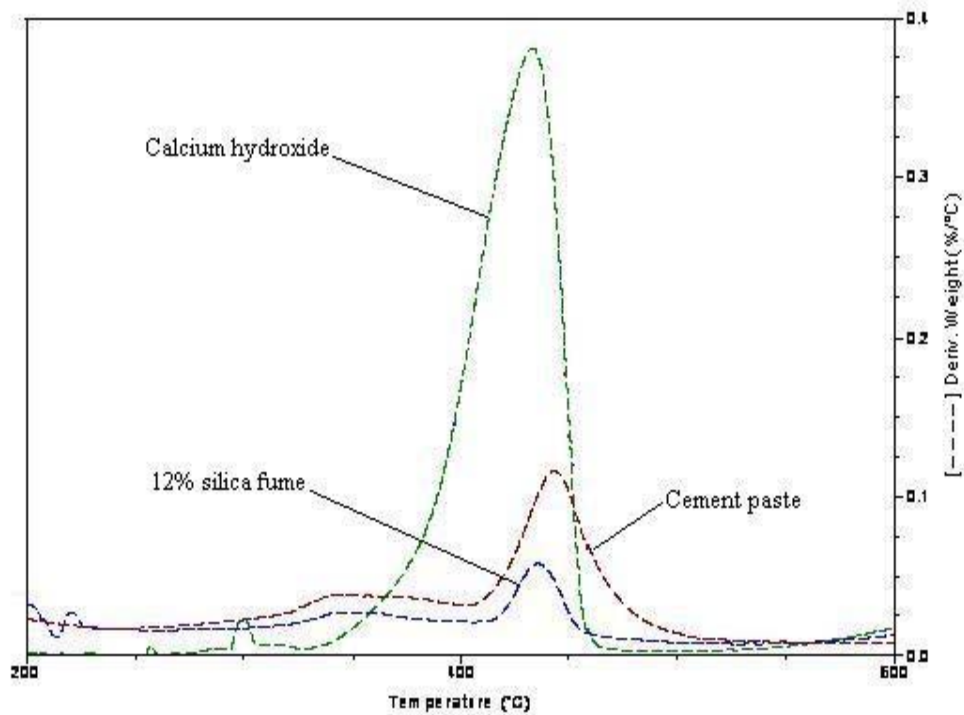


Figure 32. TGA of $\text{Ca}(\text{OH})_2$, cement paste and cement paste with silica fume

Table 32. Sieve analysis of silica fume as received

Passing	1.18mm	0.6mm	0.3mm	0.15mm	75 μm
Retained on	0.6mm	0.3mm	0.15mm	75 μm	pan
Mass (%)	5.5	19.4	26.3	26.8	22

To study the effect of silica fume particle size on ASR mitigation, ASTM C 1260 mortar samples were made with Blue Rock and pure paste samples. The samples were divided into two groups. One group consisted of regular Blue Rock mortar bars with different particle sizes of silica fume. The silica fume was substituted for five percent of

the BR to evaluate the reactivity of silica fume as if it were an aggregate. Other mix proportions follow the ASTM C 1260 standard. The ASTM C 1260 expansions up to 28 days are shown in figure 33. The second group samples were cement paste bars with five percent silica fume with a water cement ratio of 0.37. This was to evaluate the reactivity of silica fume. The expansions up to 28 days are shown in figure 34.

From figures 33 and 34, it can be seen that silica fume particle size had a significant effect on ASR mitigation. With increasing particle size, mitigation is less effective. But even the largest particles still have some mitigation effect on ASR for Blue Rock aggregate. If considered as reactive aggregate, silica fume has much less expansion potential than Blue Rock as shown in figure 33. In the paste samples, silica

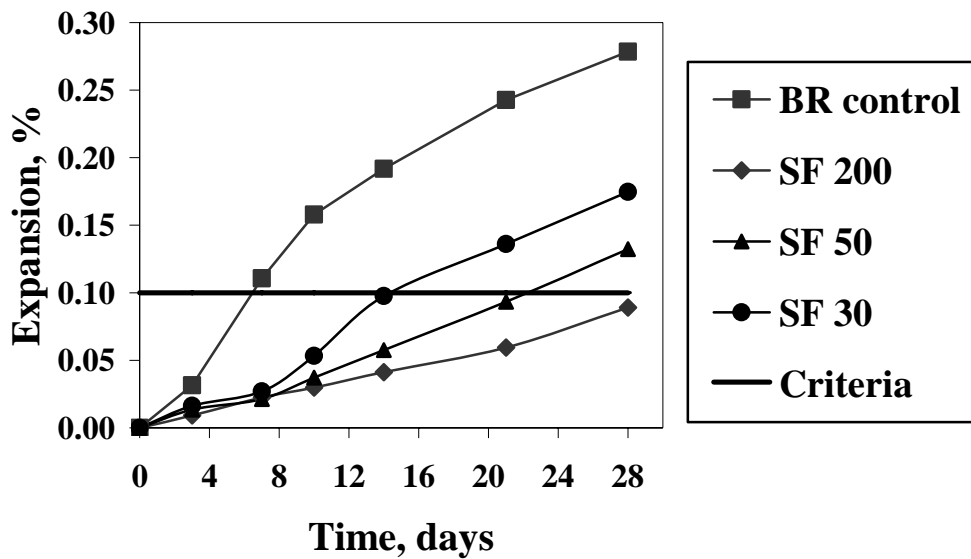


Figure 33. ASTM C 1260 expansions for BR control, with/without 5% silica fume substitution of aggregate

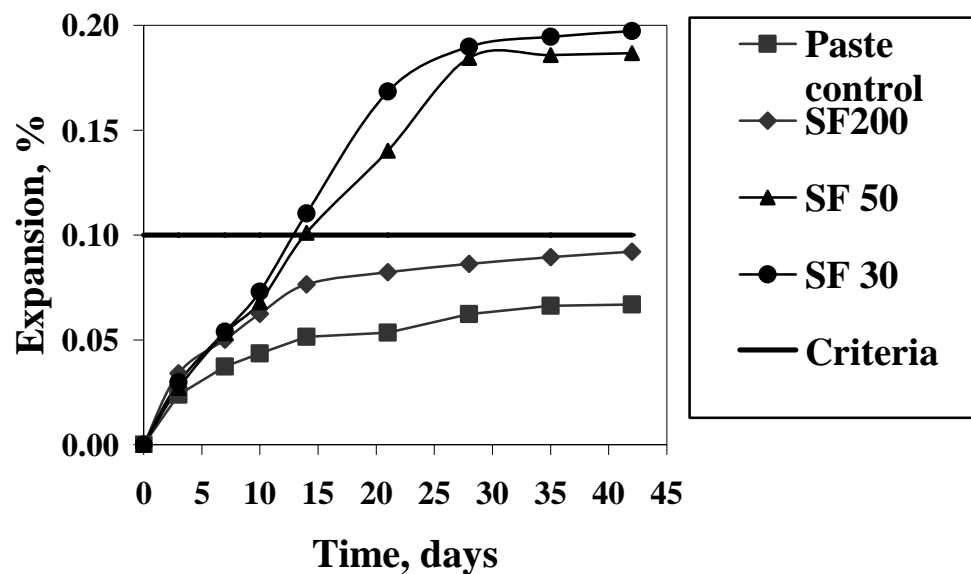


Figure 34. Expansions of paste bars, with/without 5% silica fume cement substitution under ASTM C 1260 condition

fume always increased expansion, with the large particles increasing the expansion more. The expansion differences between paste and those with SF200 are much less significant than those between paste and those with larger particle silica fume. These data suggest that expansion is not problematic for particles smaller than 74 microns. These are consistent with results reported from other researchers (73).

4.4 Glass as a Potential Admixture for ASR Mitigation

It was clear that amorphous silica played an important role in mitigating ASR (74). Waste materials that have fine amorphous silica particles may also have the potential to control ASR. It has been reported that an amorphous silica residual, which is a by-product

in the silica gel making process, acted similar to silica fume and had high pozzolanic reactivity (75, 76). Glass fits in this category since most glasses have silica in their structure. Post consumer glass is abundant in metropolitan areas and its recycling in beneficial uses such as in concrete can be economical and environmentally green.

4.4.1 Glass chemical composition

Glass is defined as “an inorganic product of fusion which has been cooled to a rigid condition without crystallizing” by ASTM C 162 (77). More than 99 percent of the commercial glasses are oxides in composition and a large percentage of these are silica based. Typical commercial glass compositions are presented as in table 33 (78).

Table 33. Typical commercial glass oxide composition by weight percentage

	Plate	Window	Bottle or Container	E Glass	Vycor	Pyrex
SiO ₂	72.7	72	74	52.9	94	81
Al ₂ O ₃	0.5	0.6	1.0	14.5		2.0
Na ₂ O	13.2	14.2	15.3		1.0	4.5
K ₂ O			0.6	1.0		
CaO	13.0	10.0	5.4	17.4		
MgO		2.5	3.7	4.4		
SO ₃	0.5	0.7	Trace			
B ₂ O ₃				9.2	5.0	12.0
As ₂ O ₅	Trace	Trace	Trace			
BaO			Trace			

All the glass has more than 50 percent silica by weight. Pyrex glass has been used as a very reactive aggregate to test the effectiveness of SCMs to control ASR in ASTM C441. Even though glass is a very reactive material, it has been reported that fine particles of glass do not have a detrimental effect on ASR and may even control ASR due

to their pozzolanic reactivity (79, 80, 81). Most post-consumer glasses are bottles and containers. They have high silica content and amorphous structure. They also contain alkalis and calcium as shown in table 33.

Glass cutlets are chemically attacked by pore solution in typical concretes. There are three chemical attack mechanisms:

1. leaching of mobile ions out of glass
2. uniform dissolution of the glass network
3. preferential dissolution of glass.

Because of the high solubility of silica at high pH, the second mechanism dominates in concrete pore solution (78).

4.4.2 Glass powder for ASR mitigation

Three glass powders were tested using the ASTM C 1260 test procedure and they are: E-glass powder, window glass powder and crushed post consumer glass powder.

The E-glass powder used was a by-product of fiber glass manufacturing. The powder is very fine with more than 95 percent passing the #200 sieve. The window glass powder used in the research was a by-product of the glass window industry. The grading is shown in table 34. Waste glass was obtained from Conigliaro Industries in Framingham, Massachusetts as glass gravel. They were further crushed to pass the #100 sieve.

ASTM C 1260 mortar bars were made with different levels of cement substitution with E-glass powder, window glass powder and crushed waste glass powder. Both Blue

Rock and RCA were used as aggregates. The expansions were measured up to 28 days and results were shown in figures 35 through 40.

Table 34. Window glass powder grading

Passing	0.6mm	0.3mm	0.15mm	75 μ m
Retained on	0.3mm	0.15mm	75 μ m	pan
Mass (%)	6	25	39.2	29.8

From figures 35 and 36 it can be seen that, 15 percent E-glass powder substitution did not control the 14 day expansion below 0.1 percent criteria. Substitution of 25 percent controlled the expansion below the 0.1 percent criteria at 28 days. 20 percent E-glass powder substitution did not control the 28 days expansion below 0.1 percent criteria, but controlled 14-day expansion below 0.1 percent.

From the figures 37 and 38 it can be seen that, only 50 percent window glass powder substitution controlled the 28-day expansion below 0.1 percent criteria. Substitution of 15 percent and 30 percent did not control the expansion.

From the figures 39 and 40 it can be seen that, only 50 percent waste glass powder substitution controls the 28-day expansion below 0.1 percent criteria. Substitution of 15 percent and 30 percent did not control the expansion.

As shown in the ASTM C 1260 expansion results, glass powders have ASR mitigation potential, especially the E-glass. Fineness and alkali contribution are two potential factors that need further study. A long term test such as ASTM C 1293 is needed before a definitive conclusion can be reached.

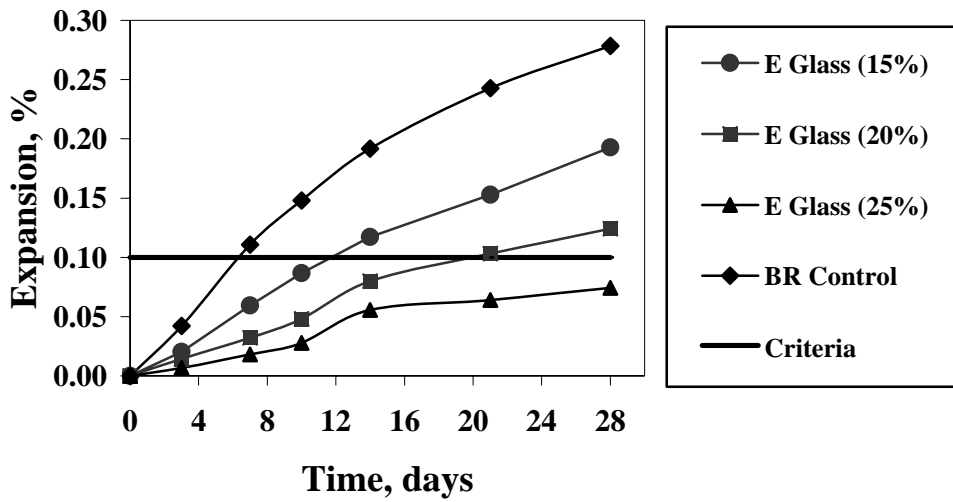


Figure 35. ASTM C 1260 expansions for BR control samples, with/without E-glass powder

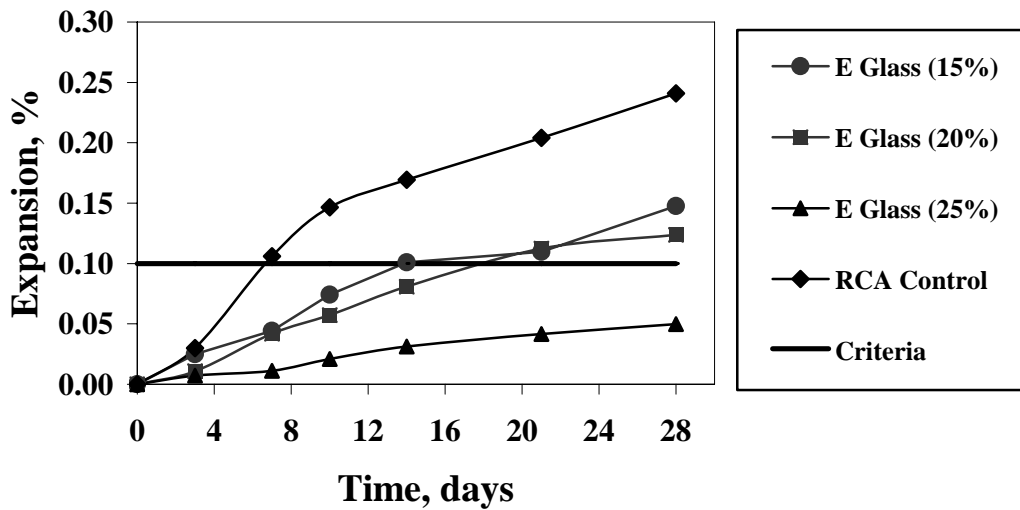


Figure 36. ASTM C 1260 expansions for RCA control samples, with/without E-glass powder

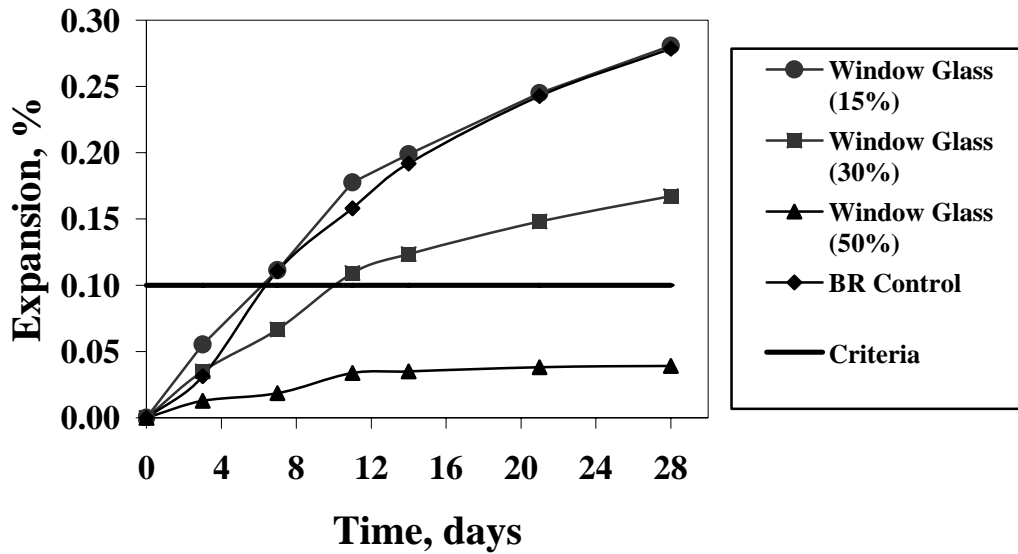


Figure 37. ASTM C 1260 expansions for BR control samples, with/without window glass powder

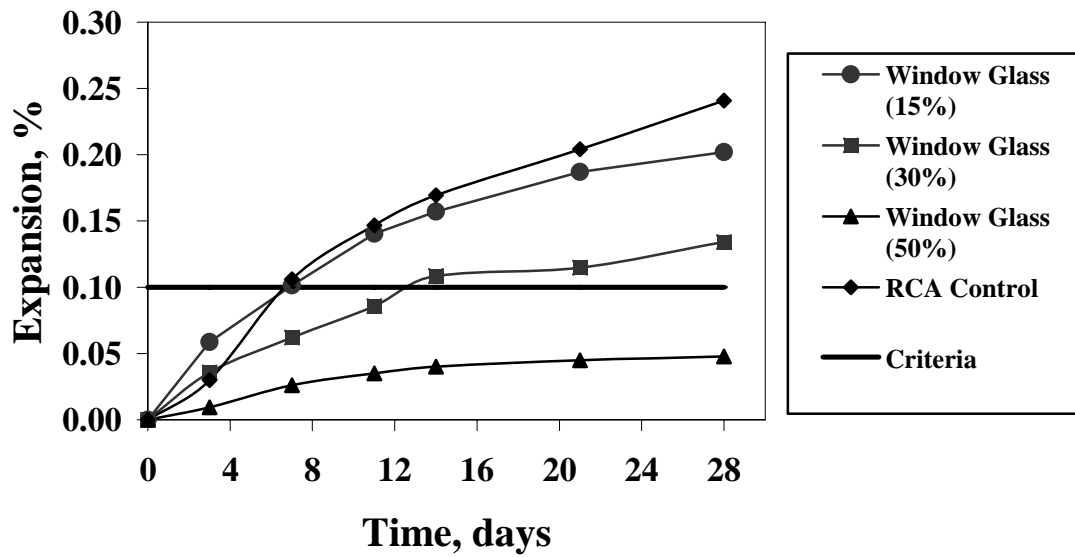


Figure 38. ASTM C 1260 expansions for RCA control samples, with/without window glass powder

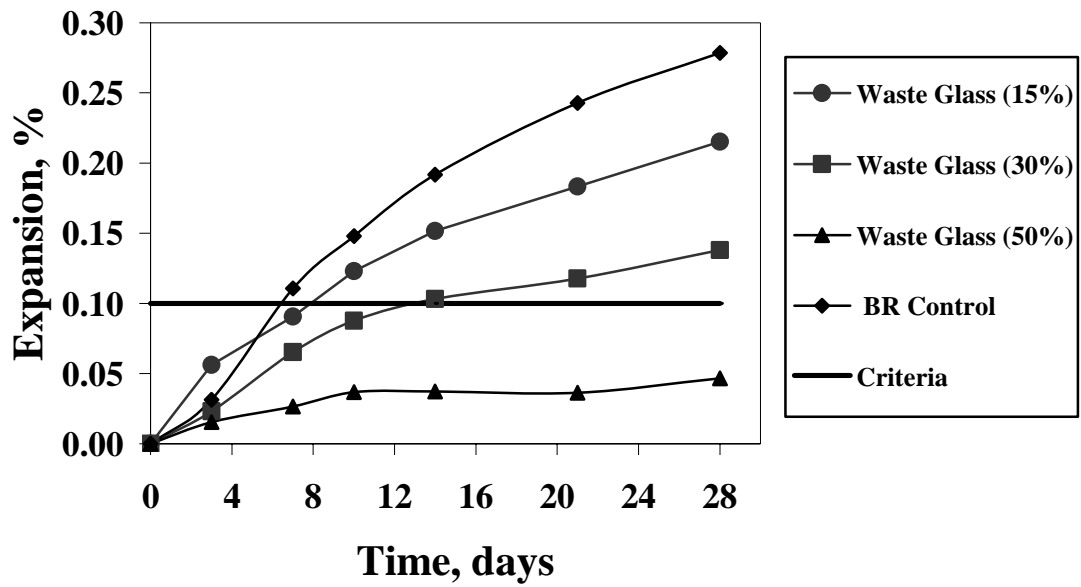


Figure 39. ASTM C 1260 expansions for BR control samples, with/without crushed waste glass powder

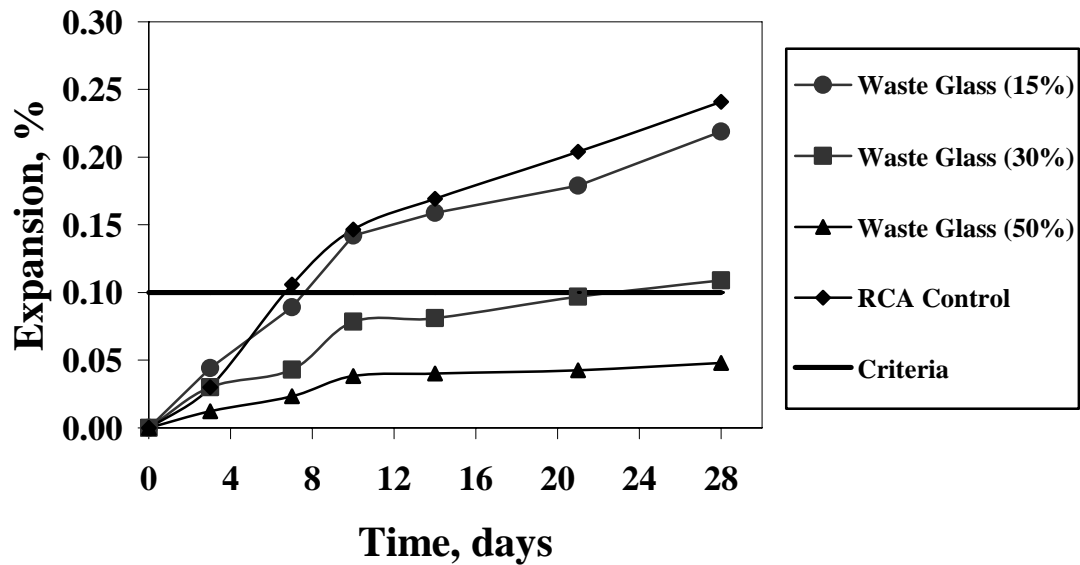


Figure 40. ASTM C 1260 expansions for RCA control samples, with/without crushed waste glass powder

CHAPTER 5

ASR MITIGATION OF RCA CONCRETE AND EXISTING CONCRETE BY LITHIUM

5.1 Lithium as an Admixture for ASR Mitigation

Compared to mineral admixtures, most ASR chemical admixtures are water soluble. Since ASR was observed in late 1940's, many researchers have devoted much effort to search for chemicals that can mitigate the ASR problem in concrete (82).

It was discovered by McCoy and Caldwell in the 1950's that lithium salts mitigate ASR (83). Even though the benefit of using lithium has been known since the 1950's, it did not become popular for almost 40 years. Considerable research has been conducted over the past 10-15 years on ASR mitigation using lithium compounds (84).

5.1.1 Lithium basic chemistry

Lithium (from the Greek word "lithos" meaning stone) is the lightest and smallest of all metals. It is a group IA alkali metal with an electron configuration of $1s^2 2s^1$ (85). The lithium ion is exceptionally small and has, therefore, an exceptionally high charge to

radius ratio. As a result, its properties are considerably different from same group ions such as sodium and potassium. Contrarily, its hydrated radius (size of the ion in water

solution) is large and therefore exhibits very different solution properties such as very low vapor pressure, freezing point depression, and other colligative properties. This large solvation shell around the lithium ion also causes it to have low mobility in solution. The basic ionic characteristics of Li with reference to Na and K are presented in table 35 (86, 87).

Table 35. Basic ionic characteristics of Li, Na and K

	Li	Na	K
Ion radius (nm)	0.09	0.116	0.152
Hydrated ion radius (nm)	0.34	0.276	0.232
Ionic mobility ($10^{-9}m^2/s/V$)*	40.1	51.9	76.2

* at 25°C and indefinite dilution

Lithium does not occur "free" (purified or uncombined) in nature, but is found joined (ionized) as various salts in nearly all igneous rocks and hydrated in many mineral springs and seawater. The natural occurrence of lithium is very low in the lithosphere. In natural seawater, lithium is found hydrated at substantially low levels and usually ranges from 140 to 250 parts per billion. The main lithium-bearing minerals include spodumene, petalite, amblygonite, lepidolite and eucryptite. Lithium carbonate is the most commonly produced mineral and is an important feedstock for downstream lithium products (84). Lithium found its commercial use in the production of ceramics, glass and primarily aluminum. The consumption in lithium batteries, industrial catalyst and more recently in concrete admixture has expanded rapidly (88).

5.1.2 Lithium compounds as concrete admixtures

Theoretically, addition of any soluble salt of lithium should provide lithium ions into concrete pore solution, but the effect of balancing anions also needs to be considered. Many lithium compounds have been used and evaluated for ASR mitigation. These compounds include: LiCl, LiF, LiNO₃, LiNO₂, LiOH·H₂O, Li₂CO₃ and Li₂SO₄ (84).

Lithium chloride is unsuitable because the chloride contributes to rebar corrosion. The addition of lithium sulfate changes the balance between tricalcium aluminate (C₃A) and sulfate, which may be not desirable for concrete. Lithium hydroxide or its monohydrate is a strong soluble base. It has a pessimism effect when used to mitigate ASR, which when added in small amounts, actually aggravates the ASR problem instead of mitigating it (89).

Lithium carbonate and lithium fluoride have low solubility and their calcium counterparts have even lower solubility. The solubility at 25°C of some lithium salts and their calcium counterparts are presented in table 36. The solubility product is defined as the equilibrium constant of the dissolution reaction of electrolytes and is denoted K_{sp} (6, 87).

Table 36. Solubility products of lithium salts and their calcium counterparts.

Compounds	LiF	Li ₂ CO ₃
K _{sp}	3.8x10 ⁻³	2.5x10 ⁻²
Compounds	CaF ₂	CaCO ₃
K _{sp}	5.3x10 ⁻⁹	2.8x10 ⁻⁹

Addition of lithium fluoride or lithium carbonate promotes the precipitation of calcium salts. More calcium hydroxide goes into solution because of less ionic calcium in

the pore solution and then pH increases. Laboratory testing has shown the addition of insoluble lithium salts increases pore solution pH (90). A pessimism effect was also reported in some cases for lithium carbonate (89).

Lithium nitrate and lithium nitrite are the two favorable salts. They are soluble and have no known detrimental effects on concrete (90). Lithium nitrite is not very stable and not widely commercially available. On the other hand, lithium nitrate is the most widely used lithium salt in combating ASR in concrete.

The lithium compound used in this research was Renew from FMC Corp. in North Carolina, and the main component is 30 percent lithium nitrate solution which contains a surfactant. Lithium hydroxide monohydrate from the same source was used for soaking solution modification.

5.1.3 Mechanisms of lithium ASR mitigation

Although lithium has been known to mitigate ASR for over a half century, the mechanism is still not well understood. Several mechanisms have been proposed for lithium mitigation and they are as follows:

1. lithium may alter the gel composition, resulting in a less or non-expansive product
2. lithium may decrease silica dissolution
3. lithium may halt the re-polymerization process of silicate
4. lithium may reduce the repulsive force in the double layer theory

5.1.3.1 Proposed mechanism: less expansive product or less repulsive force

In this theory, gel continues to form even with lithium addition. But gel with lithium has less expansion potential (*See references 89, 91, 92 and 93*). Why there is less expansion is not completely understood. No clear correlation between gel composition and expansion is known (*94*). A double layer theory has been proposed which states the reason for less expansion is reduced electrical repulsive forces in the gel (*19, 21*). A decrease of electrical repulsive forces generated by swelling of the gel has been reported with LiCl (*95, 96*). Another proposed theory suggests there is a protective barrier formed on the aggregate surface when lithium is added which slows down ionic diffusion (*97*).

5.1.3.2 Proposed mechanism: suppression of silica dissolution

It was reported that the dissolution rate of the silica is in the following order: $\text{LiOH} < \text{NaOH} < \text{KOH}$. Depending on the lithium to alkali ratio, the solubility may remain the same or decrease. The larger hydrated ion radius of lithium may play a role here (*98, 99, 100*). ASR was mitigated by slowing the dissolution, the first step of the whole ASR process.

5.1.3.3 Proposed mechanism: slower re-polymerization process

Dissolution of the silica is only the first step of the ASR. The gel formation or re-polymerization process may also be decreased due to the presence of lithium. It has been reported the gel formation decreases with LiCl addition as compared to alkali hydroxide solution only (*101*). But other researchers' results suggest that lithium may enhance polymerization (*102, 103*).

5.1.3.4 Silica gel slurry test

The effect of lithium ion on the ASR gel formation was evaluated by a volume measurement of gel as produced. Chromatograph grade silica gel (230-450mesh) from Sorbent Technologies in Atlanta GA was chosen as the reactive silica. The alkali concentration level was chosen at 0.6 mol/l, with reference to the pore solution results in chapter 3 and other researchers' methodologies (98). The potassium to sodium molar ratio was set at 2. The silica to alkali ratio was set at a pessimism level of 4.8 as reported by other researchers (10).

In experiments with calcium, the silica gel was mixed with distilled water before alkali hydroxide and lithium nitrate solution was added. In experiments with calcium, the silica gel was thoroughly blended with dry calcium hydroxide before alkali hydroxide and lithium nitrate solution was added. Calcium hydroxide was added in the amount that is 50 times the saturated value. Lithium to sodium plus potassium ratio was chosen at 0.5, 0.74 and 1.0.

The containers were 250ml PETE bottles with rubber stoppers and 1 ml or 5 ml syringes with out their pistons attached. The syringes were graduated with 0.02 ml marks as shown in figure 41. A drop of vegetable oil was added at the top of the syringe to avoid solution evaporation. Volume readings were taken at the oil-solution interface. All bottles were put in 38°C oven. The volume changes were measured as a function of time up to 28 days. The results are presented in table 37.



Figure 41. Container for measuring silica gel slurry volume change

Table 37 Volume changes for silica gel slurries (ml)

	7 days, with/without calcium	14 days, with/without calcium	28 days, with/without calcium
$\text{Li}_2\text{O}/\text{A}_2\text{O}^*=0$ (control)	0.09/0.02	0.26/0.01	0.44/-0.01
$\text{Li}_2\text{O}/\text{A}_2\text{O}=0.5$	0.05/0.03	0.18/-0.02	0.21/-0.04
$\text{Li}_2\text{O}/\text{A}_2\text{O}=0.74$	0.04/-0.04	0.05/0.01	0.06/0.03
$\text{Li}_2\text{O}/\text{A}_2\text{O}=1.0$	0.02/0.02	0.05/0.04	0.04/-0.03

* A_2O is the sum of Na_2O and K_2O

As shown in table 37, there are no obvious differences among the volumes when calcium is not present. This indirectly shows calcium is an indispensable element in gel formation and expansion. For the slurry samples with calcium, the presence of lithium had a significant effect on the volume change. This suggests that lithium reduces the volume increase. The results of this preliminary test reaffirm the hypothesis of less

expansive gel when using Lithium as a form of mitigation.

5.2 Lithium Effectiveness Evaluation

To show the effect of different alkali metal ions on ASR expansion, three groups of ASTM C 1260 Blue Rock mortar bars were made. After the 1 day water soaking period, they were put in 1N NaOH, KOH, and LiOH solution. All other environmental parameters were the same as standard ASTM C 1260. The soaking solutions had equal hydroxyl's concentration and the only difference was the alkali cation. The expansions up to 28 days are shown as in figure 42. It is clear the expansion in potassium or sodium hydroxide solution is much higher than that in lithium hydroxide solution. This is consistent with results reported by other researchers (99). The exception is that sodium and potassium act similar in promoting ASR. The expansion differences between potassium and sodium hydroxide are all within 1.5 standard deviations. Lithium is a very unique group IA metal relative to its mitigation effect on ASR.

As regards to dosage, there is agreement among researchers that it should be based on the lithium to alkali ratio. Many researchers proposed that a lithium to alkali molar ratio of 0.74 is the threshold, although it most likely depends on aggregate reactivity (84). In this research, ratios of 0.74 and 1.0 were evaluated.

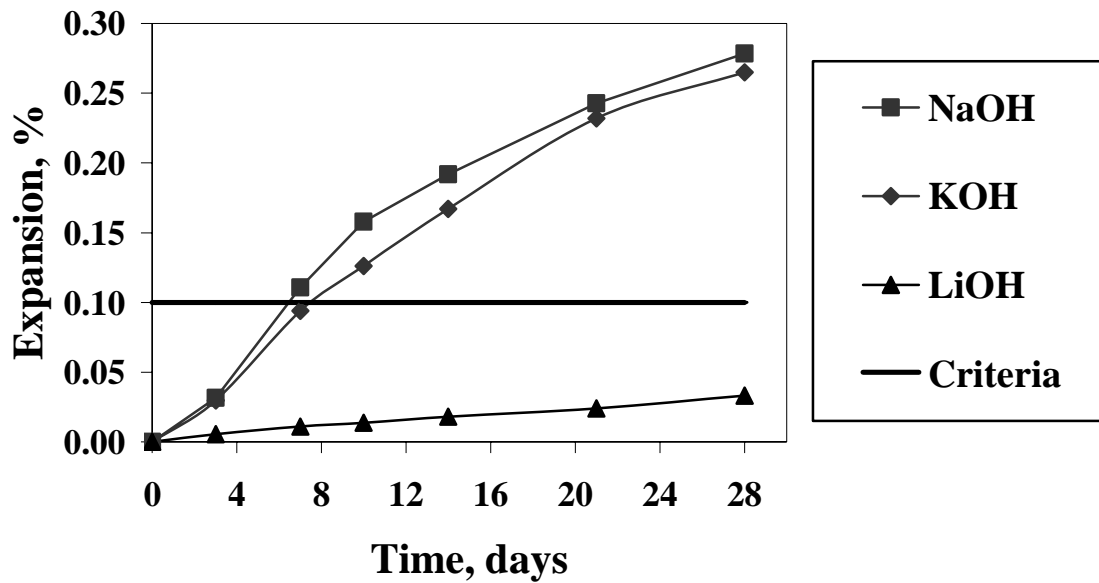


Figure 42. BR mortar bar expansions in 1N different alkali hydroxide solutions

5.2.1 ASTM C 1293 results and analysis

Lithium effectiveness has been evaluated using ASTM C 1260 and ASTM C1293. ASTM C 1293 test is reliable and correlates with field performance well, although the proposed two-year test period is too long. ASTM C 1293 concrete prisms were made with Blue Rock and RCA with the mix proportions shown in table 30 in Chapter 4 and the exception is that the lithium mitigation dosage was chosen at 0.74 and 1.0. All RCA was vacuum- saturated before batched to alleviate early moisture expansion. Sodium hydroxide was added to boost the alkali content of the cement to 1.25 percent $\text{Na}_2\text{O}_{\text{eq}}$. Fine aggregate was glacial sand from Ossipee NH. Every batch had 3 samples and the expansions were measured up to 2 years. The expansion results are as shown in figures 43 and 44. From figure 43, it can be seen that both 0.74 and 1.0 dosages controlled the 1

year expansion below 0.04 percent for Blue Rock concrete, but only the higher dosage controlled 2-year expansion below 0.04 percent.

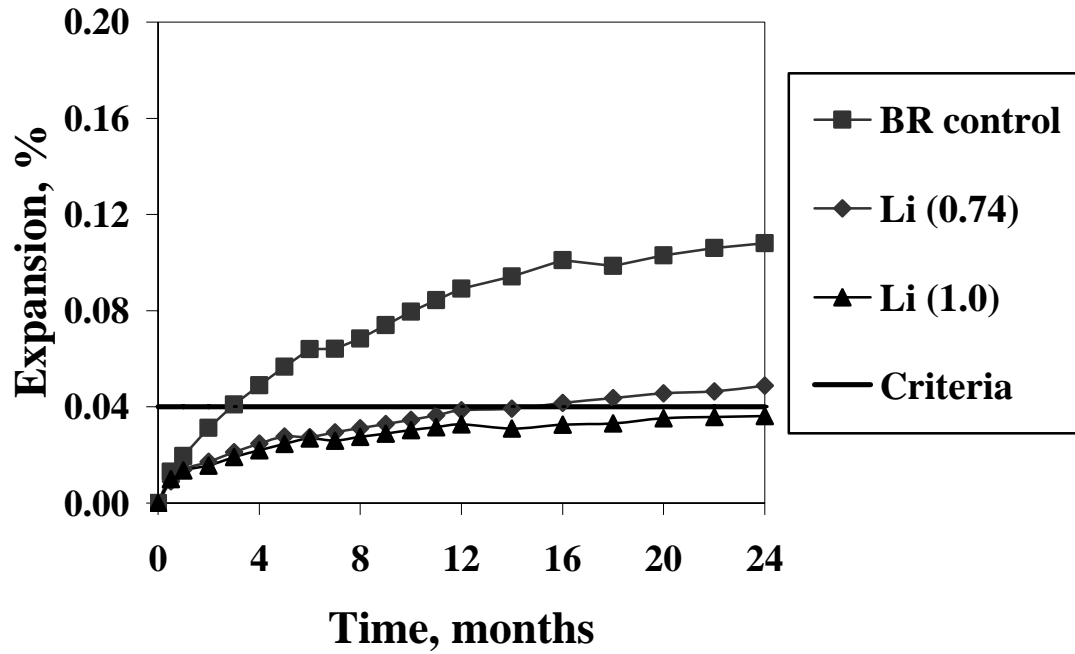
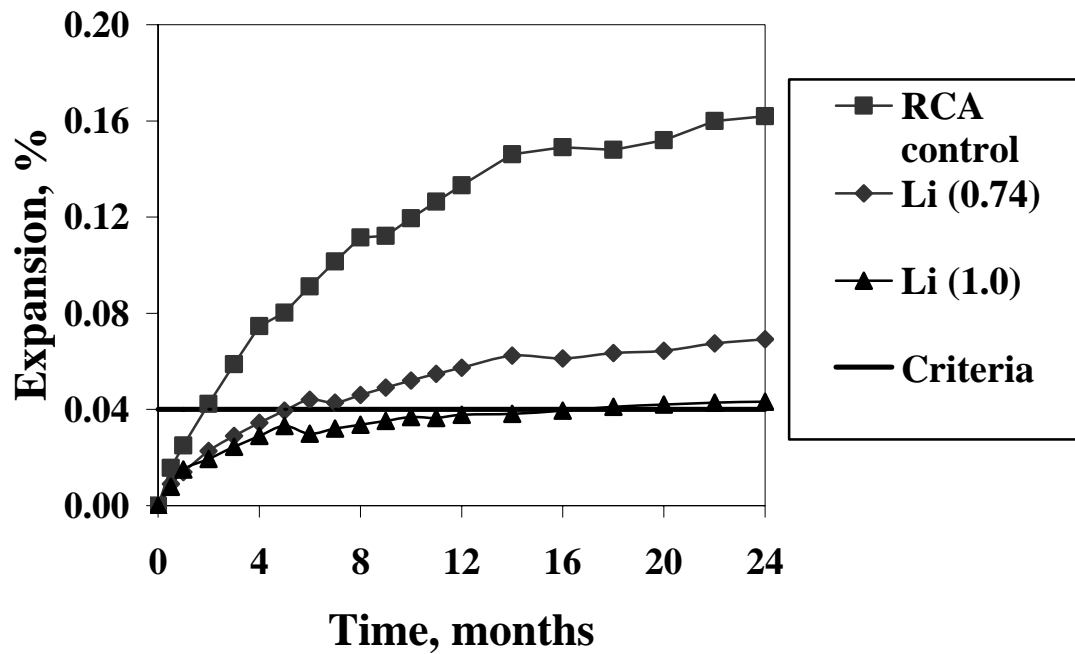


Figure 43. ASTM C 1293 expansion of BR control concrete prisms, with/without lithium

From figure 44, it can be seen that neither 0.74 nor 1.0 dosage controlled the 2 year expansion below 0.04 percent for RCA concrete, but the higher dosage is very close (0.0433%). For the 1 year expansion the 1.0 dosage controlled it under 0.04 percent, whereas the lower dosage did not.



F

Figure 44. ASTM C 1293 expansion of RCA concrete prisms, with/without lithium

5.2.2 ASTM C 1260 modification, results and analysis

Compared with ASTM C 1293, the ASTM C1260 test is much faster, but it needs to be modified for lithium mitigation evaluation. If the exact ASTM C1260 test procedure is followed, lithium leaches out during the 1-day water bath and 14-day 1N NaOH expansion solution bath due to the concentration gradient. The true mitigation effect can not be accurately evaluated. To clearly show this, two batches of Blue Rock mortar bar samples with lithium to alkali ratio of 0.74 and 1.0 were made and tested under standard ASTM C 1260 conditions. As shown in figure 45, standard ASTM C 1260 yields expansions higher than 0.10 percent for lithium mitigation of 0.74 and 1.0. The mitigation effect was underestimated by standard ASTM C 1260 method due to lithium leaching into the

soaking solution. The measured lithium concentrations in the soaking solutions at 28 days were 0.13 and 0.179 g/l for dosages of 0.74 and 1.0 respectively. This suggests that approximately 20 percent of the lithium dosage leached out during the 28 days of testing.

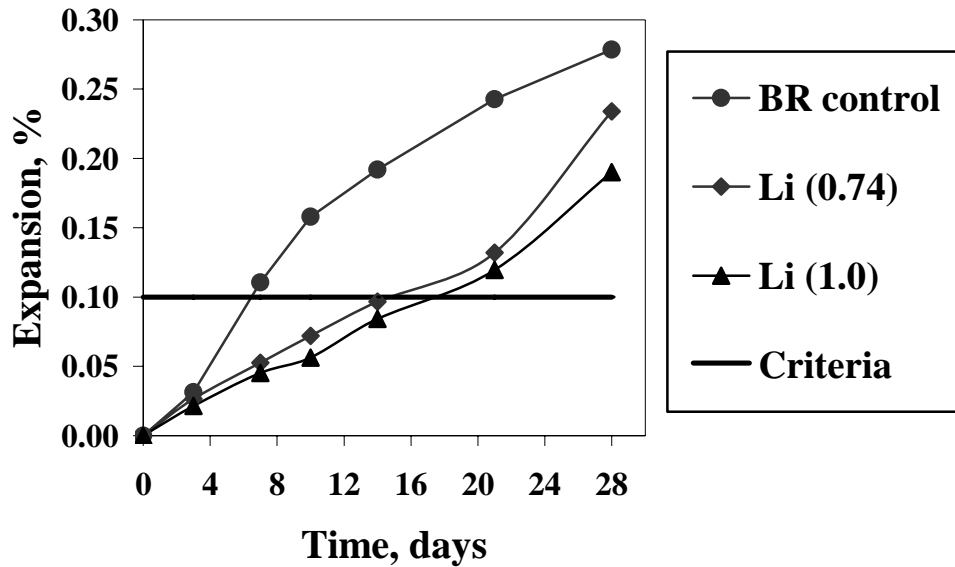


Figure 45. Standard ASTM C 1260 expansions for BR control mortar samples, with/without lithium

A soaking solution adjustment was needed to balance the lithium ion when in the soaking solution to prevent leaching. One approach proposed by other researchers is to add lithium into the NaOH solution so that the lithium to alkali ratio is the same for both the mortar sample and the soaking solution (84, 104). There are two possible solutions. One is to maintain the lithium to alkali ratio of the solution the same as that of the mortar bar samples by adding lithium hydroxide, so that the unit normality of hydroxyl remains unchanged. This is referred to as lithium hydroxide modification (LH). The second one is to maintain the lithium to alkali ratio of the solution the same as that of the mortar bar

samples by adding lithium nitrate, so that the unit normality of hydroxyl remains unchanged. This is referred as lithium nitrate modification (LN). The pH of soak solutions was the same, but the sodium concentration was higher in the LN method to match the pH. Both methods were evaluated in this research.

The modified soaking solutions are presented in tables 38 and 39. The expansions were measured up to 28 days and presented in figures 46 through 49. It should be noted that the lithium samples were not soaked in standard 1N NaOH solution as was the control because the lithium would have leached from the samples.

Table 38. Lithium nitrate modification of soaking solution (LN)

Dosage	NaOH (g)	Renew [®] solution (30 % LiNO ₃) (g)	Total solution volume (ml)
0.74	80	340.4	2000
1	80	460	2000

Table 39. Lithium hydroxide modification of soaking solution (LH)

Dosage	NaOH (g)	LiOH • H ₂ O (g)	Total solution volume (ml)
0.74	46	35.72	2000
1	40	42	2000

From figures 46 to 49, it can be seen that both 0.74 and 1.0 dosage controlled the 14 days and 28 days expansion below 0.10 percent for Blue Rock and RCA mortar bars.

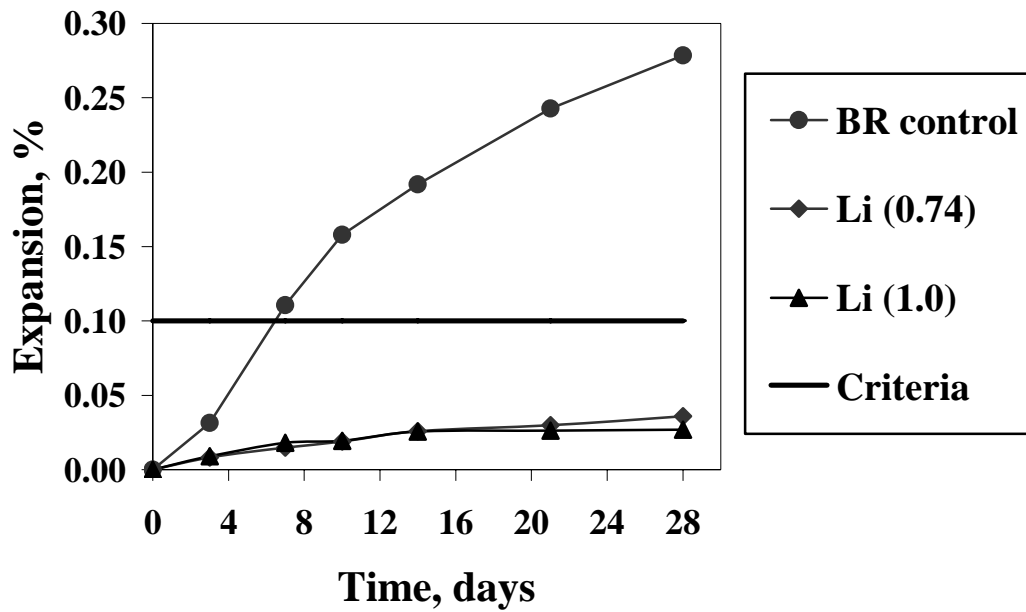


Figure 46. LN Modified ASTM C 1260 expansions for BR control mortar samples, with/without lithium

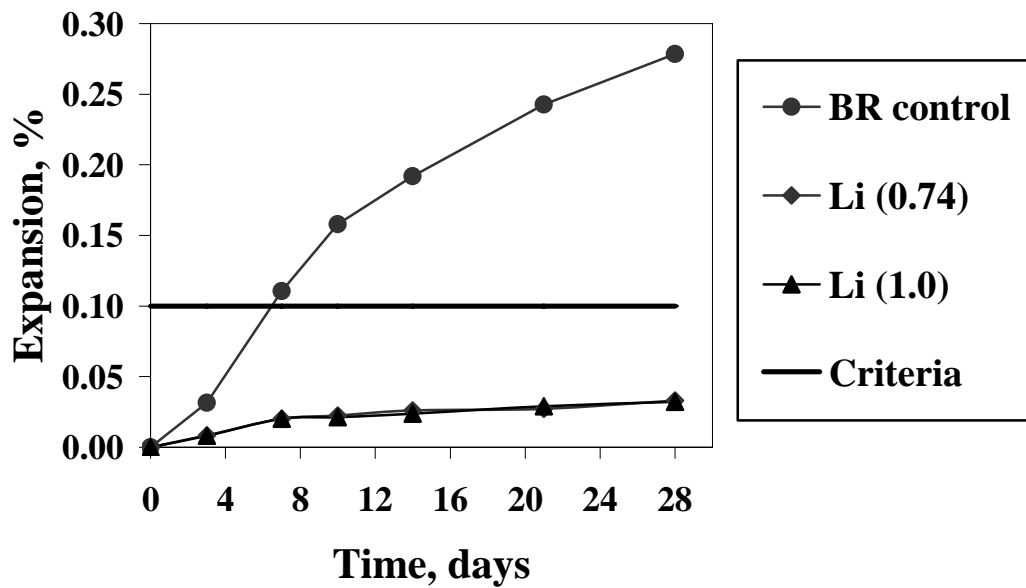


Figure 47. LH Modified ASTM C 1260 expansions for BR control mortar samples, with/without lithium

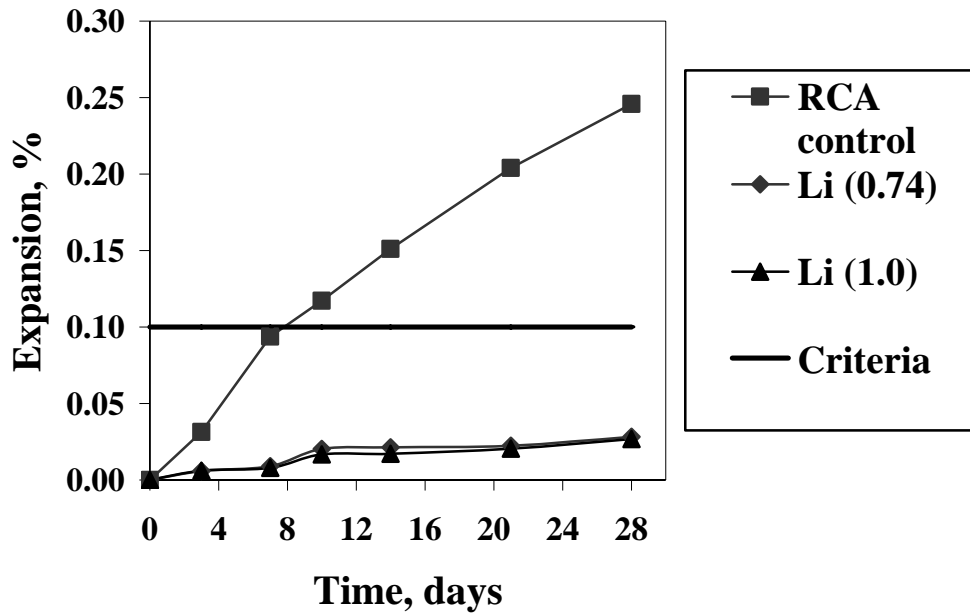


Figure 48. LN Modified ASTM C 1260 expansions for RCA control mortar samples, with/without lithium

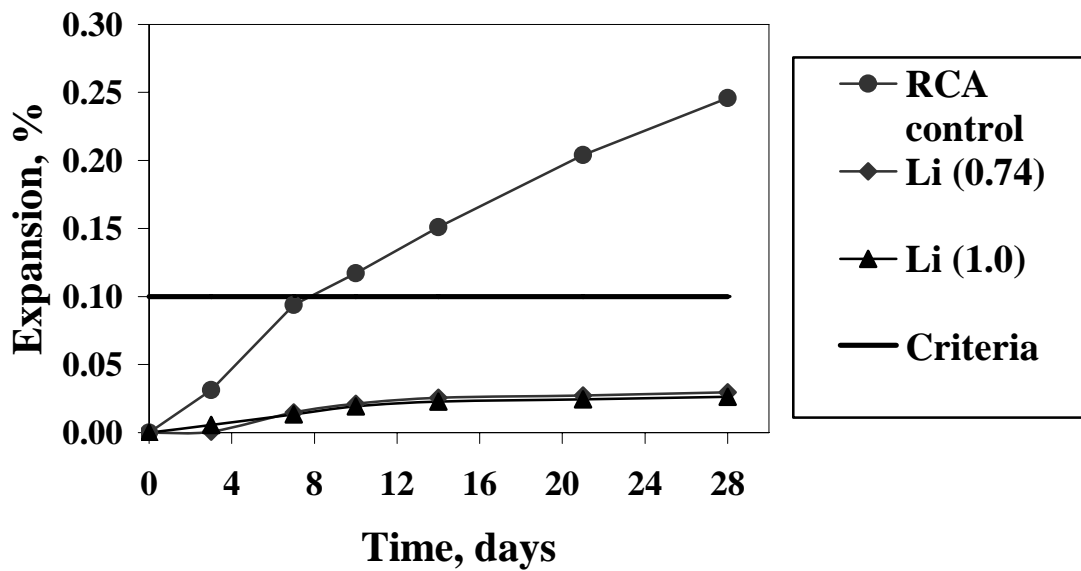


Figure 49. LH Modified ASTM C 1260 expansions for RCA control mortar samples, with/without lithium

There are no statistically differences between the two dosages since the expansion differences are all within 0.5 times standard deviation. The comparison with ASTM C 1293 test results is presented in table 40. From the table 40 it can be seen, the ASTM C 1260 test results by modifying soaking solution are not in agreement with the ASTM C 1293 results.

Using modified soaking solution seems to overestimate the lithium mitigation effect when compared to the ASTM C 1293 results. The mitigation effect may include contributions from lithium in the soaking solution. To illustrate this, three sets of regular Blue Rock mortar bars were cast without lithium mitigation. After demolding and 1 day water soaking, they were put in 1N NaOH, lithium hydroxide modified soaking solution with a ratio of 0.74 (LH), and lithium nitrate modified soaking solution with a ratio of 0.74 (LN). All other environment parameters were the same as ASTM C 1260. The expansions were measured up to 28 days and are shown in figure 50. It is clearly shown in figure 50 that the lithium in the soaking solutions contributed to the mitigation effect.

Table 40. Comparison of ASTM C 1260 and ASTM C 1293 for lithium

Mitigation methods	ASTM C 1260 14 days	ASTM C 1293 1 year	ASTM C 1260 28 days	ASTM C 1293 2 years
Blue Rock (lithium 0.74)	Pass	Pass	Pass	Fail
Blue Rock (lithium 1.0)	Pass	Pass	Pass	Pass
RCA (lithium 0.74)	Pass	Fail	Pass	Fail
RCA (lithium 1.0)	Pass	Pass	Pass	Fail (0.043 %).

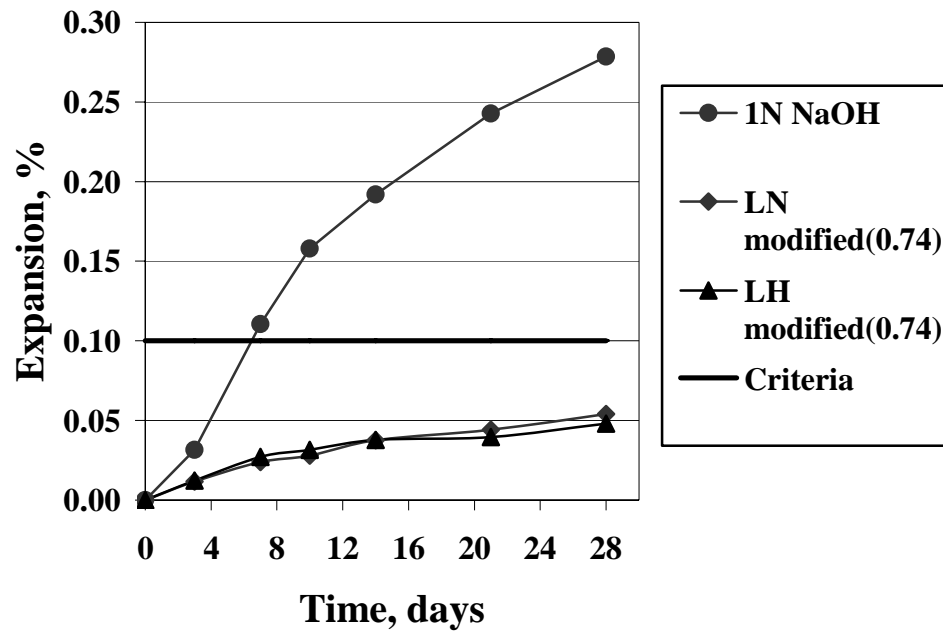


Figure 50. Soaking solution effects on Blue Rock mortar samples ASTM C 1260 expansion

5.3 Pore Solution Analysis

To understand the evolution of lithium with respect to sodium and potassium, pore solution mortar samples were made using ASR non-reactive Ottawa sand with varying amounts of lithium mitigation. All pore solution samples were vacuumed bagged with 5ml water and stored at 38°C.

For comparison with ASTM C 1260 mortar bars discussed in the preceding section, some Blue Rock and RCA mortar bars were made and put in ASTM C 227 conditions 38°C and 95 percent RH. Pore solution was extracted from mortar bar samples in ASTM C 227 and ASTM C 1260 conditions and pore solution samples at different age. Lithium, sodium and potassium concentrations were analyzed by ICP-OES. The results

are presented in tables 41 through 43 and figures 51 through 56.

From figure 51 it can be seen, the lithium to alkali ratio is substantially lower than the nominal value (original load), either 0.74 or 1. These are consistent with results reported by other researchers (98, 105). Since Ottawa sand is ASR non-reactive, the results should not be caused by ASR. It is well known that not all alkalis end up in pore solution, some are absorbed (44, 45, 46). These data suggest that lithium was also absorbed by the solid phase. It appears lithium was preferably absorbed to sodium and/or potassium based on a smaller ratio of lithium to alkali in the pore solution.

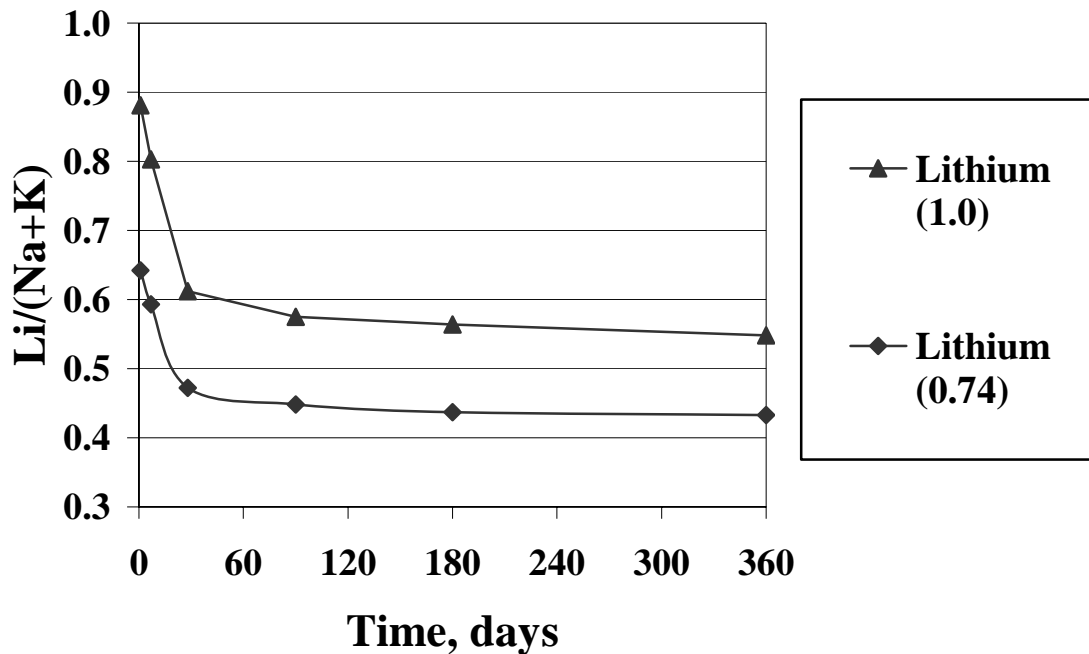


Figure 51. Lithium to alkali ratio evolution for Ottawa sand mortar samples with lithium

Compared with non-soaked samples under ASTM C 227 conditions, the soaked ASTM C 1260 sample pore solution have higher lithium concentration as shown in tables

42 and 42, with only one exception. The lithium to alkali ratio is much higher than non-soaked samples as shown in figures 52 to 55. Apparently, lithium migrated more into the samples from soaking solution than sodium or potassium. These obviously led to overestimate the mitigation effect, which was apparent in the expansion results. The

Table 41. Alkali evolution for Ottawa sand samples with lithium

Lithium dosage	Li (mmol/l) at different ages (days)						Na+K (mmol/l) at different ages (days)					
	1	7	28	90	180	360	1	7	28	90	180	360
0.74	508	524	402	224	184	173	792	884	852	499	421	400
1.0	683	714	528	294	245	224	775	889	863	512	435	409

Table 42. Alkali evolution for BR mortar bars with lithium

Lithium dosage	Environment	Li (mmol/l) at different ages (days)					Na+K (mmol/l) at different ages (days)				
		1	7	14	21	28	1	7	14	21	28
0.74	ASTM C227	502	485	460	412	378	784	826	845	867	860
	LN modified	502	538	564	592	609	784	815	827	846	864
	LH modified	502	488	481	486	488	784	745	718	702	694
1.0	ASTM C227	670	648	611	552	504	766	817	844	882	854
	LN modified	670	699	725	753	773	766	789	808	826	844
	LH modified	670	638	631	623	615	766	726	710	691	678

Table 43. Alkali evolution for RCA mortar bars with lithium

Lithium dosage	Environment	Li (mmol/l) at different ages (days)					Na+K (mmol/l) at different ages (days)				
		1	7	14	21	28	1	7	14	21	28
0.74	ASTM C227	482	465	426	390	338	781	814	840	862	870
	LN modified	482	534	551	589	591	781	820	827	843	835
	LH modified	482	481	484	486	488	781	758	742	730	711
1.0	ASTM C227	640	624	584	524	475	774	824	836	874	868
	LN modified	640	697	726	751	774	774	811	825	839	858
	LH modified	640	636	632	621	617	774	744	731	706	693

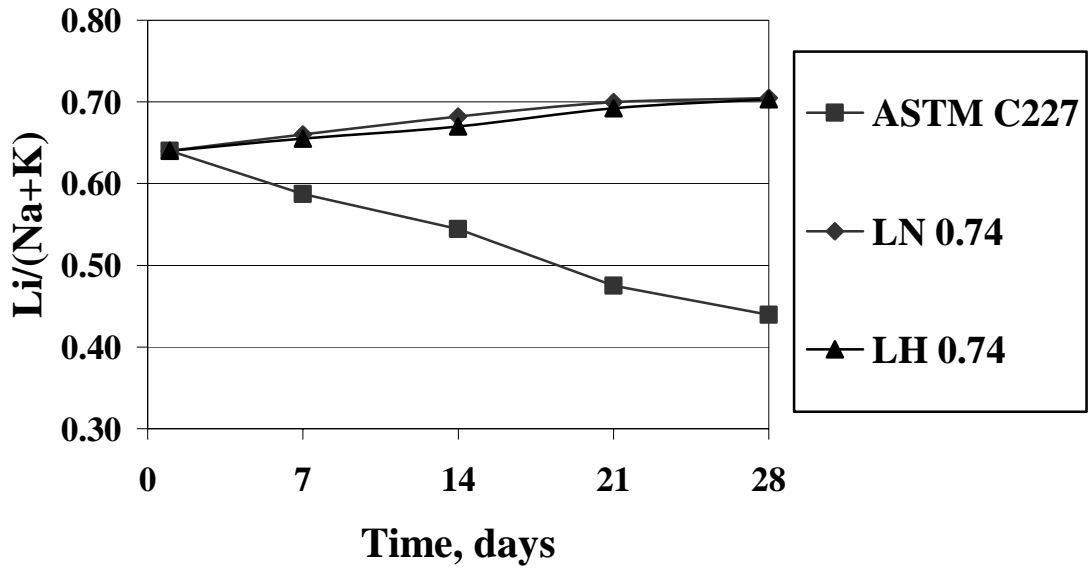


Figure 52. Lithium to alkali ratio evolution for BR mortar samples with lithium dosage 0.74

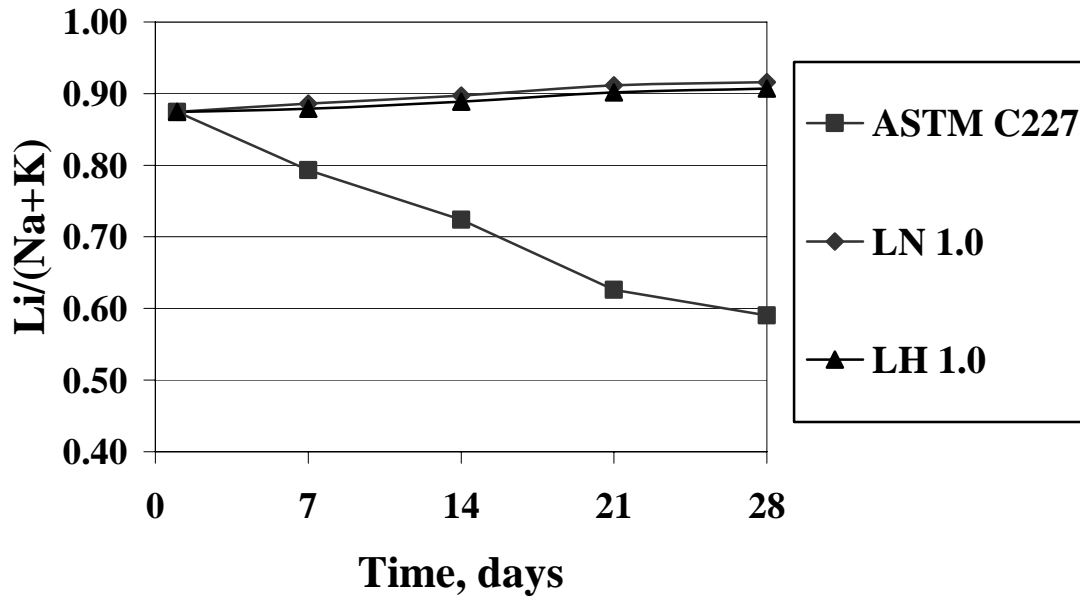


Figure 53. Lithium to alkali ratio evolution for BR mortar samples with lithium dosage 1.0

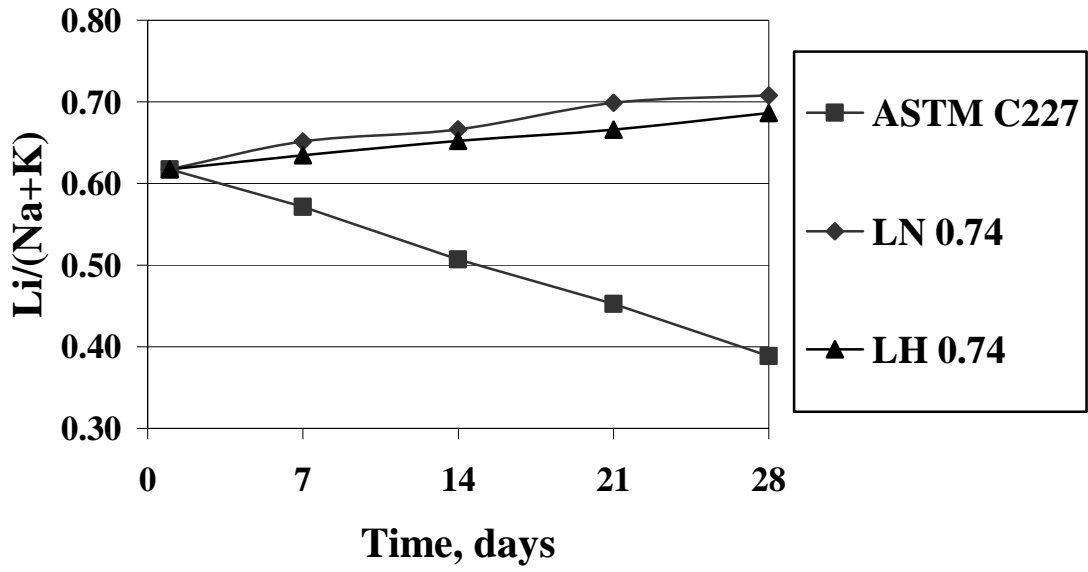


Figure 54. Lithium to alkali ratio evolution for RCA mortar samples with lithium dosage 0.74

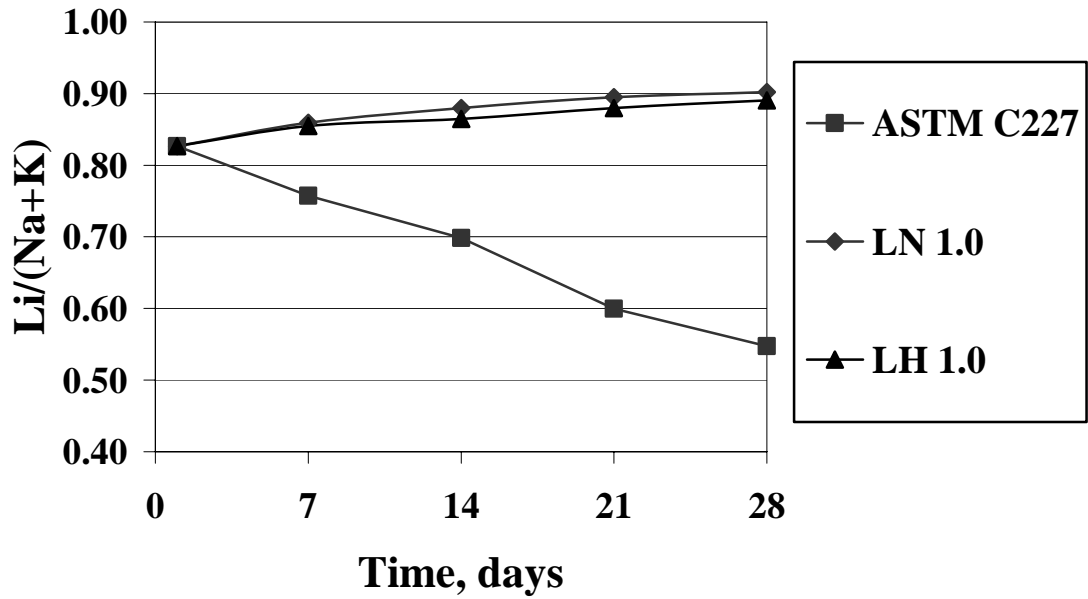


Figure 55. Lithium to alkali ratio evolution for RCA mortar samples with lithium dosage 1.0

mitigation effect is not solely from the internal lithium and the lithium in the soaking solution also contributed. ASTM C 1260 testing for lithium evaluation with the lithium to alkali ratio match modification does not work as intended. The mitigation effect is a combination of lithium in the soaking solution and internal lithium. It is not easy to decouple these two effects to get a clear representation of the sampled internal lithium effect. Exact matching of the soaking solution and samples in lithium to alkali ratio is a tough challenge since the pore solution is evolving during the test period.

Also shown in figure 56 the pore solution results of the ASTM C 227 samples, the lithium to alkali ratio in pore solution for RCA mortar is lower than those for Blue Rock at a similar age. It suggests that in RCA concrete, more lithium was absorbed into the

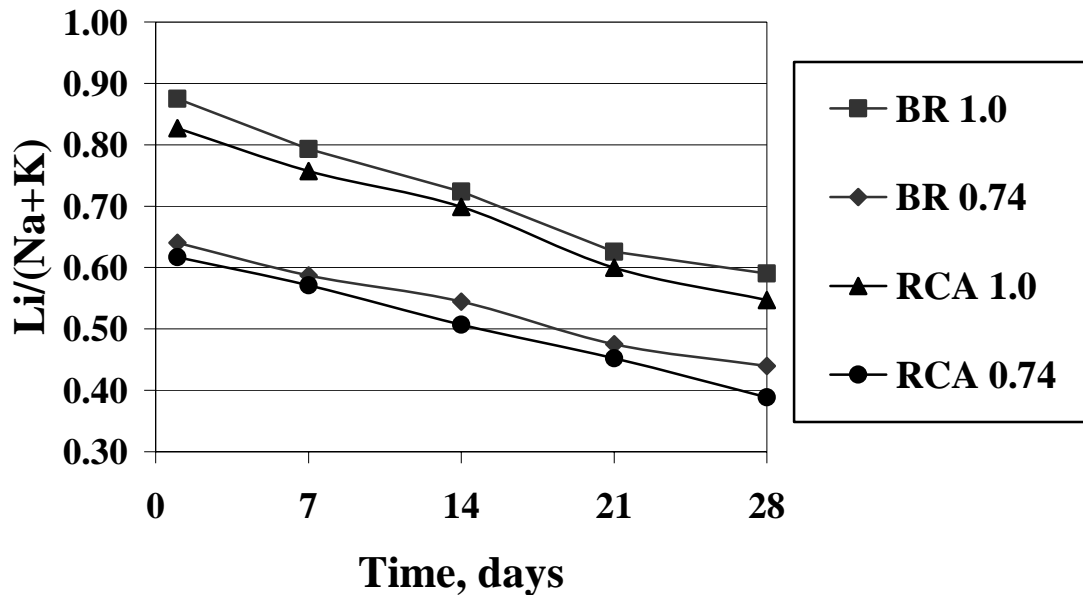


Figure 56. Comparison of lithium to alkali ratio evolution for RCA and BR mortar

solid phase. These results also give some explanation for the higher dosage need for RCA concrete than Blue Rock as showed in the ASTM C 1293 expansion results. It is presumably the old paste absorbed more lithium than potassium or sodium. To clarify this, ASTM C 1260 graded RCA was immersed in simulated pore solution with lithium mitigation (0.1N NaOH+0.2NKOH+0.3NLiOH) for 72 hours. Both pre-soak and post-soak solutions are measured by ICP-OES for Li, Na and K concentration. As expected, it did show in table 44 that lithium decrease substantially. The sodium and potassium concentration change is negligible and within the ICP-OES measurement error.

Table 44. Comparison on alkali and lithium concentration, before/after RCA soaking

	Na	K	Li
Before soaking (mg/l)	2310	7749	2170
After soaking (mg/l)	2328	7738	1940
Change (%)	0.8	-0.14	-10.6

5.4 Mitigation of Existing Concrete with ASR

When used in new concrete, admixtures either in solution form or powder form can be easily proportioned into concrete mixtures. On the other hand, for existing concrete affected by ASR, only liquid chemical admixtures are a viable option. Applying a topical spray is the most common procedure. Other methods of controlling ASR in existing concrete include electrochemical migration and vacuum impregnation (84, 106).

Mitigation of new concrete using lithium as a admixture serves as both prevention and possible treatment if the external alkalis enter the concrete in the future. For existing concrete, ASR has initiated and has been recognized before application of the admixture.

Whether applying a treatment can preserve the concrete's functionality and prevent further deterioration is the main concern. For existing concrete, how to get sufficient dosage into the concrete is the pivotal issue since the permeability of concrete is relatively low. Also when to apply and at what dosage/rate are challenges for external application. Lab testing was done to shed more light on the preceding questions.

5.4.1 Concrete prism test

Prisms about 304mm x38mm x25mm (12inch x1.5inch x1inch)., which are similar to ASTM C 1260 bars, were cut from the pavement slabs described in Chapter 2.

The size of the prisms was chosen to accelerate ASR and be able to evaluate migration of lithium. Small studs with a cone shaped hole on top as shown in figure 57 were mounted on the prism samples to measure the expansion between two specified points. All samples were divided into 4 sets with 5 samples per set, all 4 sets were vacuum bagged with 5ml of water for 7 days before treatment to eliminate the expansion due to moisture gain.

One set, the control, was vacuum-bagged with 3 percent water by weight of the sample and stored at 38°C. The second set was vacuum-bagged with 3 percent Renew[®] solution by weight of the sample and stored at 38°C. The third set was vacuum-bagged with 3 percent 1 N NaCl solution by weight of the sample and stored at 38°C to simulate the deicing salt situation. The fourth set was put in the ASTM C1260 condition for comparison. The objective is to test the effectiveness of lithium on mitigating ongoing ASR given the assumption that enough lithium migrated completely into the concrete.

The validity of the assumption was checked using pore solution chemistry. The expansions are shown in figures 58 and 59. All expansion data are the average of a minimum of five samples.

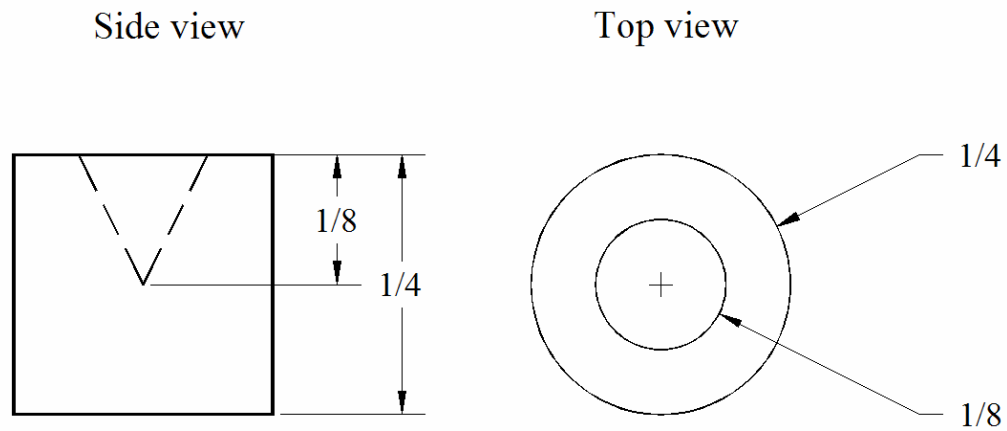


Figure 57. Sketch of the 1/4 inch studs

Figure 58 shows that the samples still have much reaction potential given external alkali supply as in ASTM C1260 condition. The NaCl treatment, simulating deicing salt, has no significant detrimental effect on ASR expansion as shown in figure 59. Although at later ages the expansions are slightly greater than the control, they are statistically insignificant. The expansion of the control and NaCl treatments are all within 1.5 standard deviations, suggesting using NaCl has no effect on ASR expansion. It also shows that after the lithium treatment the sample expansions are significantly lower than control samples at all ages. The external application of lithium controlled the continuing expansion below 0.02 percent at 14 months.

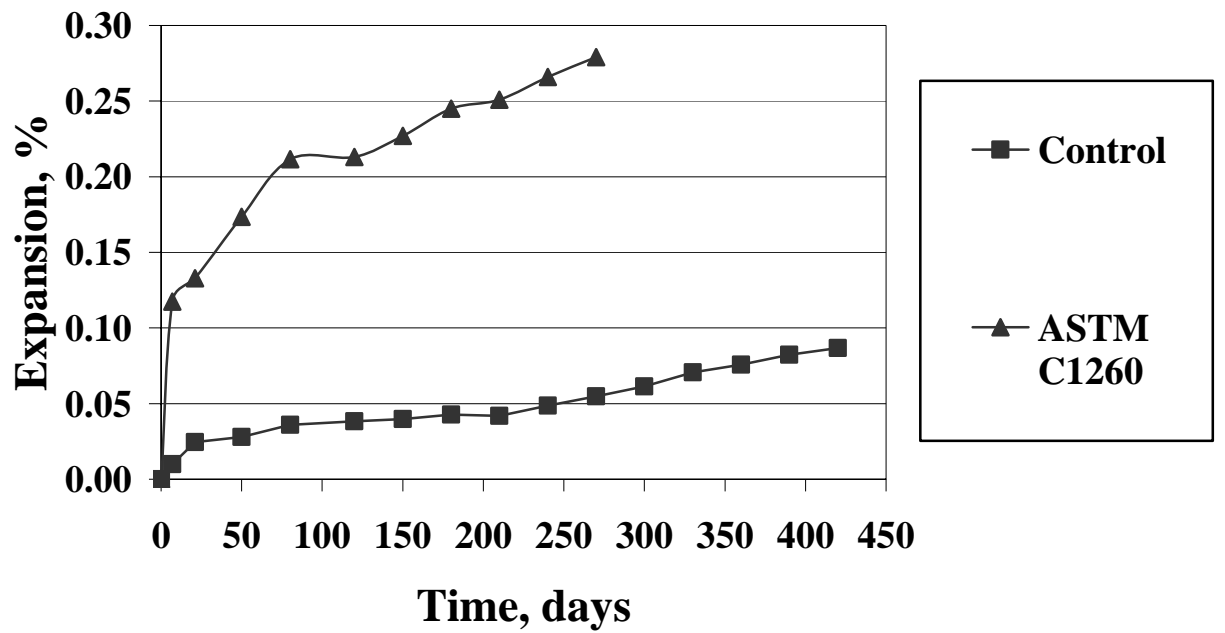


Figure 58. Expansion of existing concrete prisms, control versus ASTM C 1260

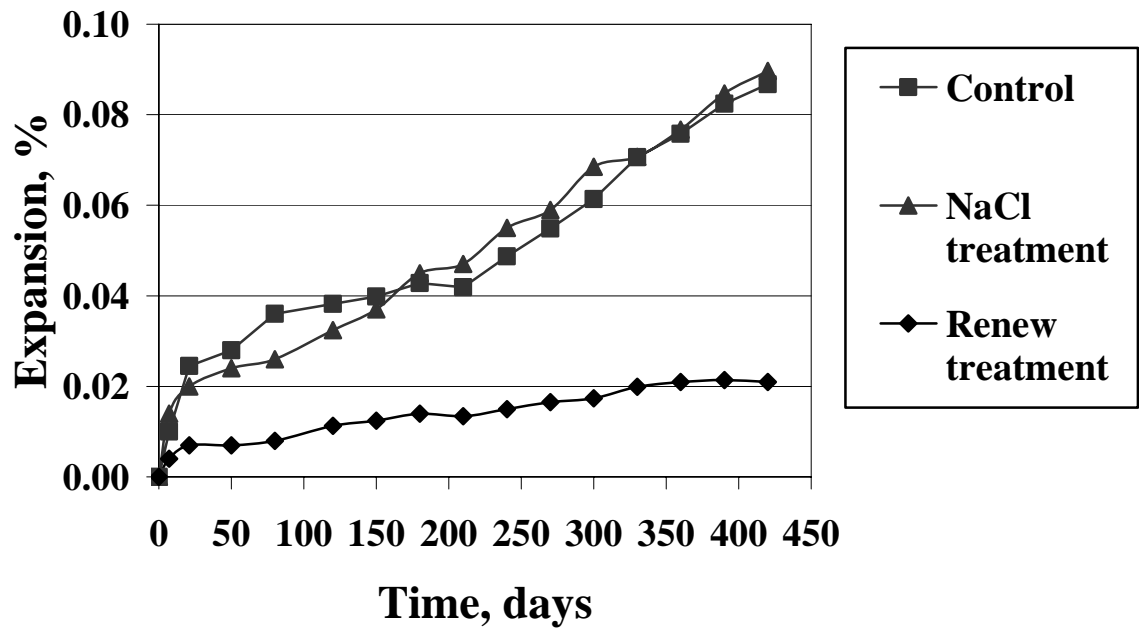


Figure 59. Expansion of existing concrete prisms, control versus NaCl, lithium treatment

One sample of the control and lithium treatment were crushed and pore solution was extracted at the end of expansion test. Lithium, sodium and potassium concentration was analyzed by ICP-OES. Pore solution testing showed the lithium to alkali ratio to be 1.27, apparently enough to mitigate ASR. This also validated the assumption of complete migration. Due to the small lateral dimension of the sample and long time contact with lithium solution, the lithium migrated into concrete well as the pore solution test showed. These results suggest that ongoing ASR expansion is mitigated given enough lithium migration into the concrete.

5.4.2 Simulated mortar bar test

To test the mitigation effect of external lithium on different ASR stages, batches of ASTM C1260 mortar bars with Blue Rock and RCA aggregate were made. After demolding and initial measurement, they were placed under ASTM C1260 conditions to accelerate the ASR expansion and to simulate different ASR stages in real field. The expansions were periodically checked for expansion and cracks. When about half of the samples cracked, the samples without cracks were taken out, washed and cooled down to room temperature and they served as ASR pre-crack samples. The cracked samples remained in the solution for 2 more weeks to develop cracking. They were taken out then, washed and cooled down to room temperature and they serve as ASR post-crack samples.

For pre-crack samples, they were divided to two sets. One set, the control, was vacuum-bagged with 3 percent water by weight of the sample and stored at 38°C. The second set was sprayed with Renew[®] solution, then bagged with 3 percent water by

weight of the sample and stored at 38°C. The continuing expansion was measured monthly and the second set was sprayed every three months with Renew[®] solution. This treatment plan was chosen to simulate topical application in the field practice.

The average expansion of the pre-crack samples when treated was 0.22 percent. The continuing expansions of pre-crack samples after treatment are presented in figure 60 and the expansion data are the average. The lithium treatment had little effect on the continuing expansion as shown. The expansion differences are all within 0.5 times standard deviation. Pore solution squeezed out of the sample was tested and lithium to alkali ratio was 0.12 at 90 days and 0.19 at 180 days. Little lithium migrated into the sample presumably due to the low permeability of the mortar bar.

The post-crack samples were divided to three sets. One set, the control, was vacuum-bagged with 3 percent water by weight of the sample and stored at 38°C. The second set was vacuum-bagged with 3 percent Renew[®] solution by weight of the sample and stored at 38°C. The third set was vacuum-bagged with 1 N NaCl solution in the amount of 3 percent weight of the sample and stored at 38°C. With extensive cracks, the average expansion of the post-crack samples when treated was 0.5 percent. The continuing expansion averages of post-crack samples after treatment are presented in figure 61.

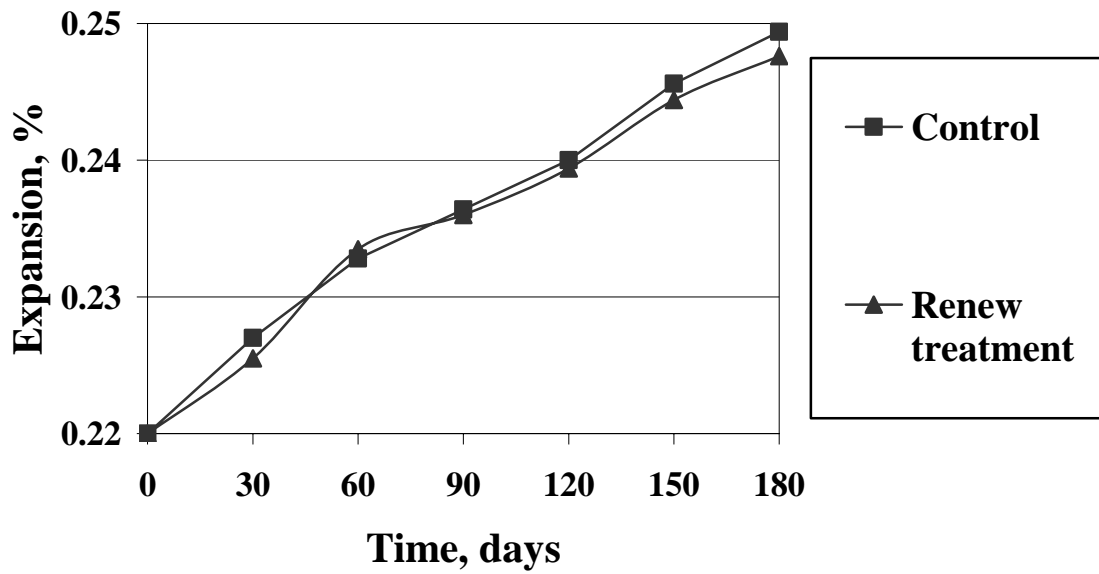


Figure 60. Continuing expansion of pre-crack mortar samples, with/without treatment

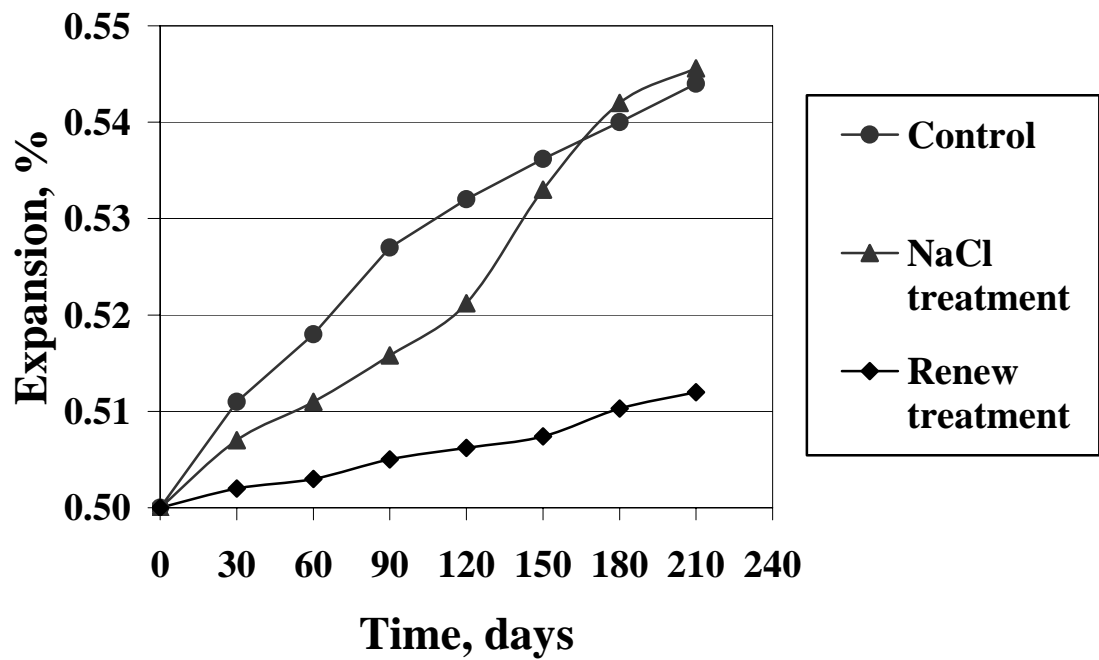


Figure 61. Continuing expansion of post-crack mortar samples, with/without treatment

The lithium treatment has almost prevented the continuing expansion. Pore solution squeezed out of the sample was tested and lithium to alkali ratio was 0.45 at 90 days and 0.76 at 150 days. The lithium penetration is much higher than pre-crack samples due to higher permeability.

The results showed post crack age is probably a starting point for treatment. The cracks should be allowed to fully progress to facilitate lithium migration as long as functionality is still acceptable. As long as enough lithium migrates into the concrete, ASR will be arrested. The treatment condition used herein is ideal but impractical in the field because it is impossible to assure lithium migration unless the concrete is extensively cracked and lithium is available long term. The pivotal issue then lies in how to effectively migrate lithium into the concrete system, which will be presented in the next section.

5.4.3 Pavement block test

5.4.3.1 Sample preparation

Blocks approximately 457mm x305mm x229mm (18 inch x 12 inch x 9 inch) were cut from the slabs obtained from the pavement near Gardener, Maine. In order to measure the overall expansion, four-inch long stainless steel inserts (studs) with a quarter inch diameter were machined similar to the normal studs used in ASTM 1260 and 1293 except for the cone shaped hole on top (see figure 62 for sketches). The procedure for mounting the long studs was to drill quarter-inch holes to a four-inch depth and then each hole was oversized to 3/8 inch to a depth of three and a half inches. This allowed the stud

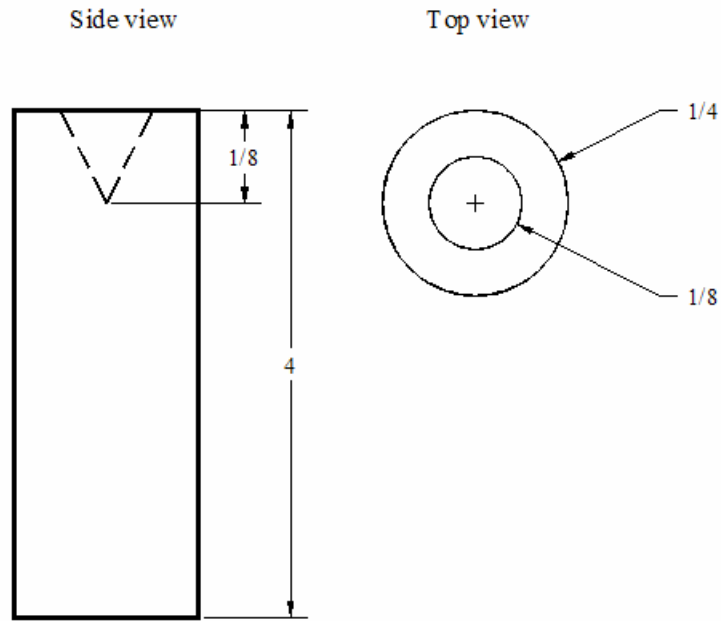


Figure 62. Sketch of the 4-inch studs (not to scale)

to seat into the a half inch deep hole at the bottom of the original drilled hole but still have ample clearance from touching the side walls. The studs were secured to the bottom of the holes at the lower end using epoxy. The gaps were filled and sealed using 3M Marine Adhesive Sealant 5200. Surface expansion 1/8 inch long studs with a cone-shaped hole on top (see figure 57) were mounted on the top surface on similar positions to the long studs as shown by figure 63.

An accelerated laboratory test was designed to subject the large blocks to ASTM 1293 environmental conditions, 38°C and 85 to 100 percent RH. The practicality of using conventional laboratory ovens was out of the question when contending with blocks that weigh almost 80 Kg (176lbs) each so it was decided to convert an existing room to

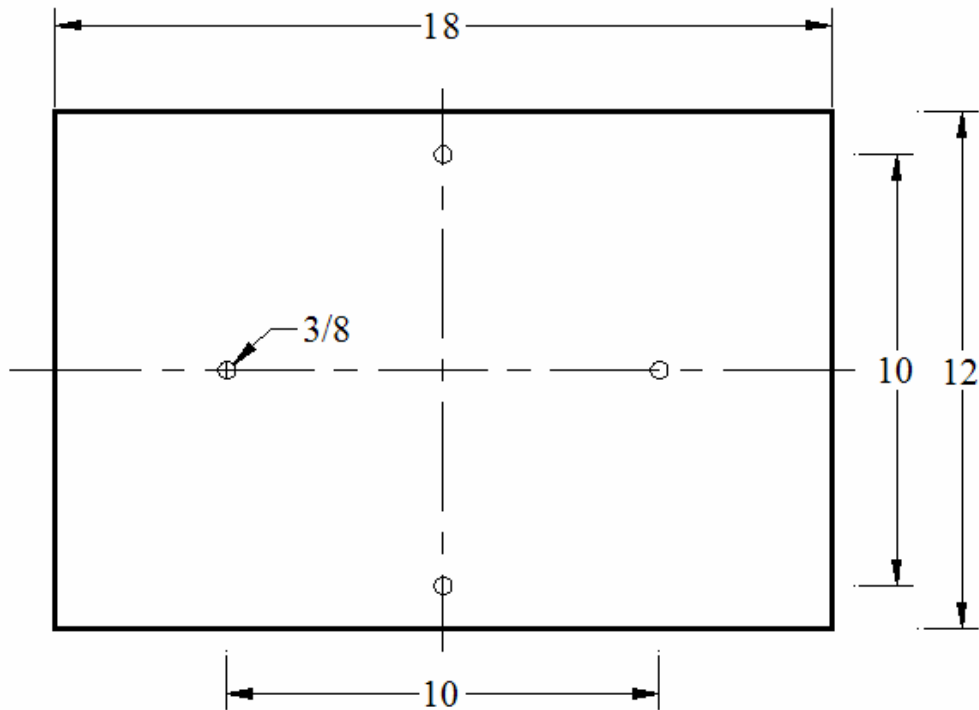


Figure 63. Positioning of the studs

maintain the 38°C temperature. The room was modified for this purpose by utilizing thick insulating foam on the walls and ceiling and several portable electric heaters were installed. A fan was used to assure uniform heating of the area. The temperature was measured, and typically fluctuated between 35 to 38°C. A 2438mm x609mm x406mm (96 inch x24 inch x16 inch) wood box was built that held seven to eight blocks. Large plastic sheets were used to line the boxes so they may envelope the samples on all sides. Wicking material was put between the plastic envelope and the samples. The two layers were separated from the blocks by a PVC frame. Wet sand was placed on the bottom of the envelopes to simulate a field base material. A schematic sketch and picture are shown in figures 64 and 65. The intent was to replicate the environment required in ASTM C 1293.

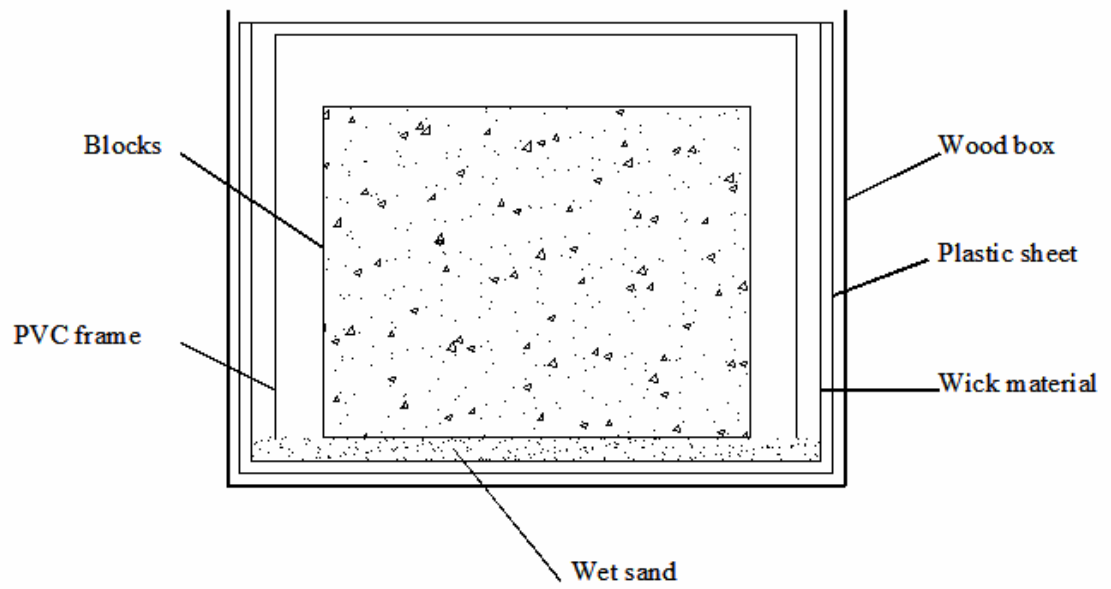


Figure 64. Schematic sketch of wood box holding blocks



Figure 65. Picture of wood box holding blocks

When the blocks are finally placed in the field or in Laboratory under ASTM C 1293 conditions the internal moisture content increases until it comes to equilibrium. As the moisture content increases in any concrete that has undergone shrinkage, expansion occurs as in a normal wetting and drying cycle. From a research point of view it is essential to differentiate the moisture gain expansion from that induced by ASR.

Obviously, moisture equilibrium is needed to address this issue. It is also essential not to loose any of the soluble alkali because this would lower the expansion due to ASR and possibly even suggest that future ASR was not problematic.

5.4.3.2 Moisture equilibrium procedure

It is difficult in the laboratory to increase concrete's moisture content to equilibrium because it cannot be submerged in water for saturation without leaching out the highly soluble alkali. To prevent alkali from leaching out during the saturation process, a sand pressure method was used as follows:

A block was first lifted by an overhead crane using a cotton lift belt. It was then lowered slowly into a plastic bag, which sat in a wood container partially filled with fine sand. The gap between container walls and plastic bags was then filled with fine sand. Water was added into the bags progressively, but in small and controlled increments. The outside sand applied a passive pressure on the plastic bags and assured a thin water film formed around the block perimeters. The intent was to minimize the amount of water added to that which would permeate into the concrete therefore minimizing the leaching of alkali. To avoid breaking the plastic bags, sharp edges and surfaces of blocks were

covered by thin packing foam. It took roughly 4 months to complete the moisture equilibrium process. The water addition was stopped when no significant water reduction in the bag was observed.

After the saturation process, the sides of the blocks were wax sealed so that only the bottom and top of the block have access to moisture in an effort to simulate field conditions. The assumption was that in the field, the moisture comes either from the air or subbase. They then were placed in the aforementioned wood box, which simulates the ASTM C 1293 condition.

5.4.3.3 Treatment procedure and results

Two lithium treatment schemes were used with the application rate of 0.2 liter/m². Treatment 1 is one application every three months, whereas treatment 2 is one every half year. The first treatment was initiated 1 month after samples were put in ASTM C 1293 conditions. The surface expansion and inside expansion were monitored for up to 16 months and the results are shown in figures 66 and 67. The expansion differences, which were calculated by subtracting the inside expansion from the surface expansion, are presented in figure 68. All expansion data are the average of a minimum of five samples.

From figures 66 and 67, it can be seen that both treatments affected the surface expansions measured. But the difference between the two treatments is insignificant since the expansion differences are within 1.5 standard deviations. The inside expansion, on the other hand, was not affected by the treatments. These surface results are consistent with results reported in a field treatment case (107).

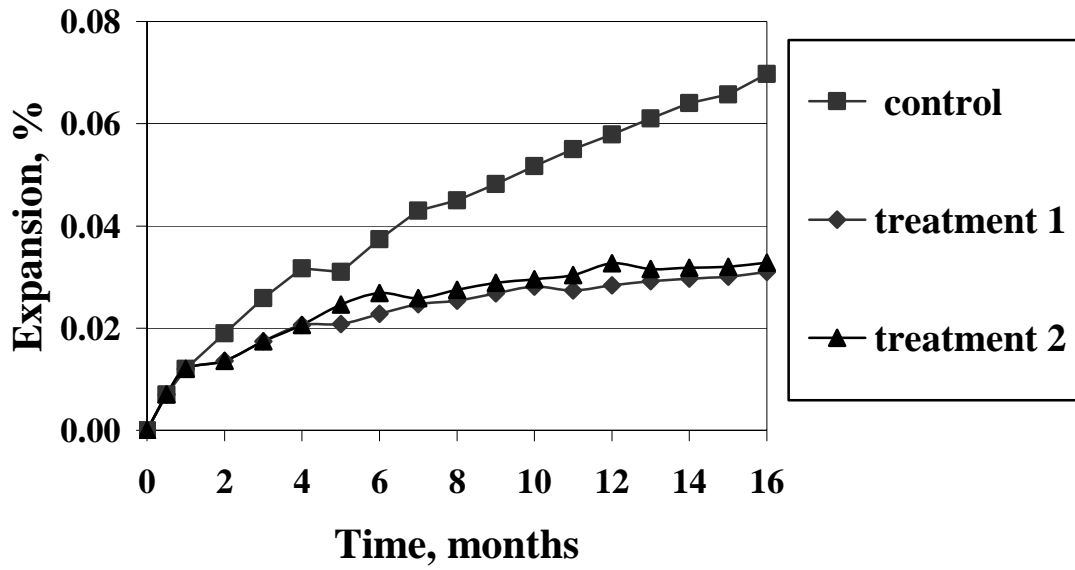


Figure 66. Surface expansion comparison of concrete pavement blocks, with/without treatments

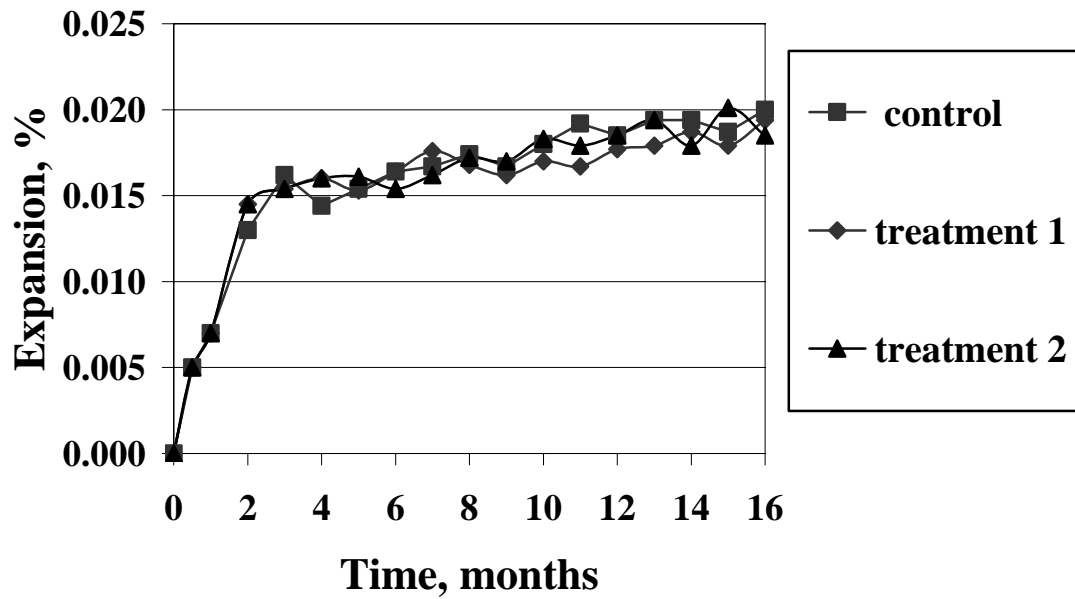


Figure 67. Inside expansion comparison of concrete pavement blocks, with/without treatments

F

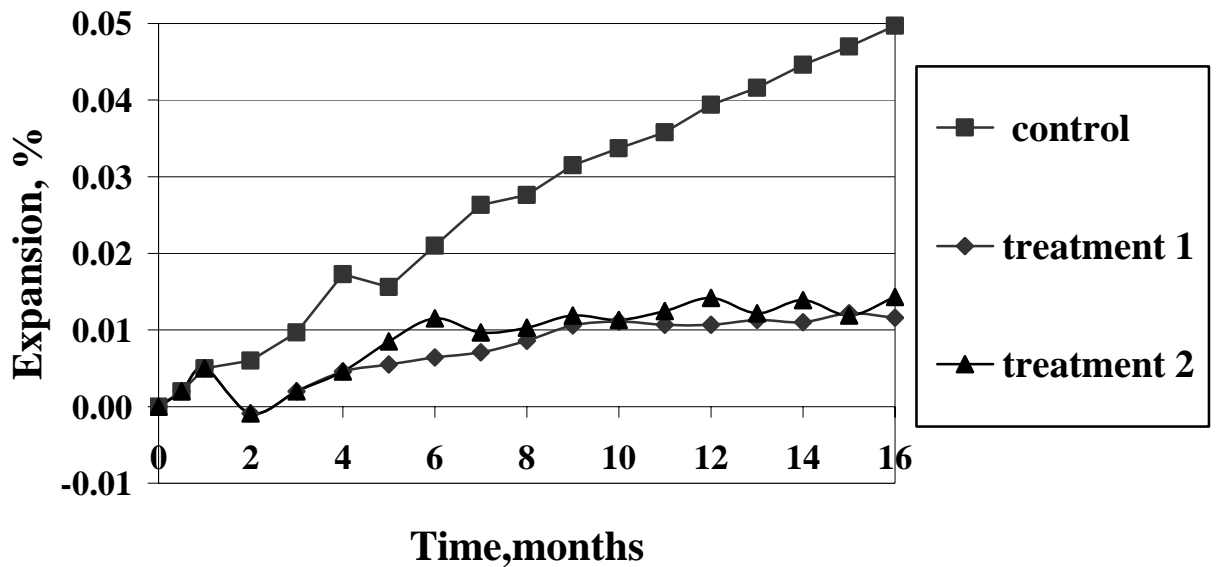


Figure 68. Expansion difference between inside and surface of concrete pavement blocks, with/without treatments

It is possible that the expansion spike in the first two months, as shown in figure 67, even though the blocks were moisture stabilized for more than four months, may be the result of moisture increase only, not ASR. The data fluctuation at later time is most likely statistically insignificant random error, since the differences are all within 1 standard deviation.

The depth of the measured point is a little less than four inches and the blocks are nine to ten inches in thickness, so the inside expansion plane is still on the upper side of the neutral axis. Figure 68 shows that the expansion patterns of the blocks are very complex. It could be a combination of bending and isotropic expansion.

It should be noted that the relative humidity, as measured by a RH meter inside the box, was a little lower (around 89 to 95 percent) than ASTM C 1293 criteria.

To test the penetration of lithium into concrete blocks, holes were drilled and powder was collected at different depths up to 30mm deep at the end of the 16 months. The powder was dissolved by nitric acid and the lithium, potassium and sodium concentration was analyzed. The lithium penetration profile is presented in figure 69.

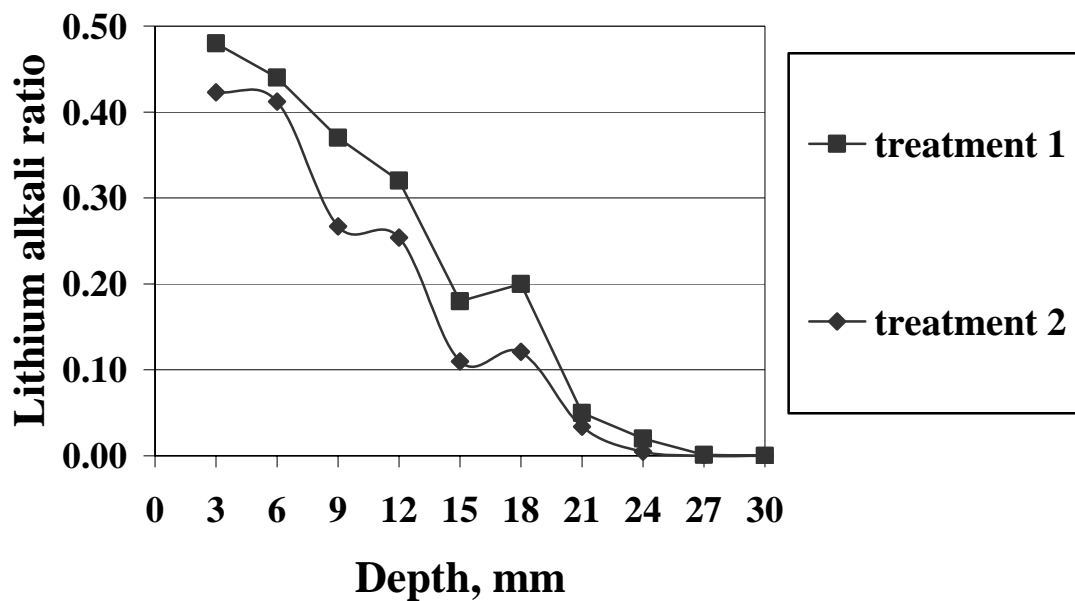


Figure 69. Lithium alkali ratio profile of concrete pavement blocks, with/without treatments

From figure 69, it can be seen that there is hardly any detectable lithium beyond 24 mm depth. These results suggest the inside expansion change could not be the effect of lithium because it only penetrated 24 mm. Although the lithium alkali ratio for treatment one is higher than that in treatment two at the same depth, the penetration depth is only marginally deeper. It should be noted the results fluctuate since the powder

collected are hardly homogeneous. They may contain aggregates as well as paste, although effort was made to avoid aggregate.

CHAPTER 6

SUMMARY AND CONCLUSIONS

In this research, different methods were studied to mitigate ASR in Blue Rock and RCA concrete. Pore solution analysis and TGA were used to physically and chemically analyze mitigation strategies. Different lithium treatments were evaluated on existing concrete which showed ASR distress. Major findings and conclusions are as follows:

1. As expected, RCA was shown to be susceptible to ASR in new concrete. Using RCA as aggregate in new concrete a viable option when mitigated. The Class F fly ash used in this research, at 25 percent cement substitution, mitigated ASR for both RCA and Blue Rock concrete. The silica fume used in this research, at cement substitution level of 12 percent, mitigated ASR for both RCA and Blue Rock concrete. Larger silica fume lumps reduced mitigation efficiency. Substituting 55 percent GGFGS mitigated ASR for both RCA and Blue Rock concrete. Two year RCA concrete ASTM C 1293 expansion was marginally over the limit of 0.04 percent. The ASTM C 1260 test results correlated well with ASTM C 1293 results when SCMs were used for mitigation, with few exceptions. The ASTM C 1260 criteria of 0.10 percent at 14 days correlated well with ASTM

C 1293 criteria of 0.04 percent at 1 year. The ASTM C 1260 criteria of 0.10 percent at 28 days for also correlated well with the ASTM C 1293 0.04 percent at 2 years.

2. SCMs reduced alkali concentration and pH of pore solution significantly. TGA revealed that at practical substitution levels, SCMs do not deplete the calcium hydroxide in a concrete system, even though calcium depletion alone warrants ASR mitigation. Blue Rock RCA contributes alkali to the concrete system however the pore solution alkali concentration does not increase. For the particular cement used in this research it appears the RCA alkali is in balance with the pore solution.
3. RCA concrete calls for higher lithium dosage compared to Blue Rock concrete. ASTM C 1260 test was modified to evaluate mortar bars that contained lithium nitrate by adding lithium hydroxide or lithium nitrate into the soaking solution. The alkali to lithium ratio was held constant in the mortar sample and soaking solution. This modified ASTM C 1260 test procedure was in disagreement with ASTM C 1293. Pore solution results showed the lithium to alkali ratio in ASTM C 1260 mortar bars were higher than in ASTM C 227 mortar bars. The alkali to lithium ratio in both RCA and Blue Rock concrete was significantly lower than the amount dosed. This suggested that lithium was preferably absorbed into the solid phase over sodium or potassium. The RCA concrete showed lower lithium to alkali ratio than Blue Rock concrete at equal dosages and ages. This suggested

that more lithium was bound to solid phase in RCA concrete than in Blue Rock concrete. The RCA soaked in simulated pore solution with lithium reduced the lithium concentration significantly, confirming the preceding hypothesis. This gave some explanation of why a higher dosage is required for RCA concrete.

4. For existing concrete, lithium treatment is the only option currently available. Lithium was shown to be effective in reducing surface expansion, which could extend the service life of a structure by slowing surface deterioration. Lithium nitrate topologically applied migrated into the concrete surface about 25mm. Simulated mortar bar test results suggested that lithium application should start after visible cracking is apparent.

REFERENCES:

- 1 Mindess, S., Young, J. F. and Darwin, D. *Concrete Second Edition*, Prentice Hall 2003
- 2 Stanton, T. E. Expansion of Concrete through Reaction between Cement and Aggregate. *Proceedings of American Society of Civil Engineers*, V66 No. 10 pp. 1781-1811
- 3 AASHTO Innovative Highway Technologies web resources:
<http://leadstates.transportation.org/asr/transition/>
- 4 Berube, M-A., Dorion, J.F., Duchesne, J. and Rivest, M. Laboratory Assessment of Alkali Contribution by Aggregates to Concrete and Application to Concrete Structures Affected by Alkali-Silica Reactivity. *Cement and Concrete Research*, V32 2002 pp. 1215-1227
- 5 Constantiner D. and Diamond S. Alkali Release from Feldspar into Pore Solutions. *Cement and Concrete Research*, V33 2003 pp. 549-554
- 6 Dean, John A. *Lange's Handbook of Chemistry 13th Edition*, McGraw-Hill Professional 1985
- 7 ASTM C 150-04 Specification for Portland Cement. *American Society for Testing and Materials*, West Conshohocken, PA 2005
- 8 Malvar, L. J., Cline, G. D., Burke, D. F., Rollings, R., Sherman, T. W and Greene J. L. Alkali-Silica Reaction Mitigation: State of the Art and Recommendations. *ACI Materials Journal*, V 99 No 5 2002 pp. 480-489
- 9 Berra, M., Mangialardri T., and Paolini, E. Rapid Evaluation of the Threshold Alkali Level for Alkali-Reactive Siliceous Aggregates in Concrete. *Cement and Concrete Composite*, V21 1999 pp. 325-333
- 10 Glasser, L. S. D. and Kataoka N. The Chemistry of 'Alkali-Aggregate' Reaction. *Cement and Concrete Research*, V11 1981 pp. 1-9
- 11 Helmuth, R., Stark, D., Diamond, S. and Moranville-Regourd, M. Alkali-Silica Reactivity: An Overview of Research, SHRP-C-342. *Strategic Highway Research Program*, National Research Council Washington DC 1993

- 12 Bensted, J. and Barnes, P. *Structure and Performance of Cements 2nd Edition*, Spon Press, NY 2002
- 13 Stark, D., Morgan, B., Okamoto, P. and Diamond, S. Eliminating or Minimizing Alkali-Silica Reactivity, SHRP-C-343. *Strategic Highway Research Program*, National Research Council Washington DC 1993
- 14 Chaumont, D., Gaboriaud, F., Nonat, A. and Craievich, A. The Structural Properties of Soda-Silicate Sols and of the Lime-Soda-Silicate Gel Formation. *Journal of Non-Crystalline*, V247 May 1999 pp. 254-261
- 15 Hansen, W.C. Studies Relating to the Mechanism by Which the Alkali-Aggregate Reaction Proceeds in Concrete. *Journal of American Concrete Institute*, V 15 No 3 1944 pp. 213-227
- 16 McGowan, J.K and Vivian, H.E. Studies in Cement-Aggregate Reaction: Correlation between Crack Development and Expansion of Mortars. *Australian Journal of applied science*, V3 1952 pp. 228-232
- 17 Tang, M. Some Remarks about Alkali-Silica Reactions. *Cement and Concrete Research*, V11 1981 pp. 477-478
- 18 Powers, T.C. and Steinour, H. An Investigation of Some Published Researches on Alkali-Silica Reaction: I The Chemical Reactions and Mechanism of Expansion. *Journal of American Concrete Institute*, V 26 No 6 1955 pp. 497-516
- 19 Prezzi, M., Monteiro, P.J.M. and Sposito, G. The Alkali-Silica Reaction, Part I Use of the Double-Layer Theory to Explain the Behavior of Reaction-Product Gels. *ACI Materials Journal*, V94 1997 No. 1 pp. 10-17
- 20 [Monteiro, P.J.M.](#), [Wang, K.](#), [Sposito, G.](#), [Santos, M.C.](#), and [Andrade, W.P.](#) Influence of Mineral Admixtures on the Alkali-Aggregate Reaction. *Cement and Concrete Research*, V27 1997 pp. 1899-1909
- 21 Prezzi, M., Monteiro, P.J.M. and Sposito, G. Alkali-Silica Reaction, Part II The Effect of Chemical Admixtures. *ACI Materials Journal*, V95 1998 No. 1 pp. 3-10
- 22 Diamond, S. Another Look at Mechanisms. *8th International Conference on Alkali-Aggregate Reaction*, Kyoto, Japan 1988
- 23 Hou X., Struble, L.J. and Kirkpatrick R.J. Formation of ASR Gel and the Roles of C-S-H and Portlandite. *Cement and Concrete Research*, V34 2004 pp. 1683-1696
- 24 ASTM C 227-03 Test Method for Potential Alkali Reactivity of Cement-Aggregate Combinations (Mortar-Bar Method). *American Society for Testing and Materials*, West Conshohocken, PA 2005

25 ASTM C 441-05 Test Method for Effectiveness of Pozzolans or Ground Blast-Furnace Slag in Preventing Excessive Expansion of Concrete Due to the Alkali-Silica Reaction. *American Society for Testing and Materials*, West Conshohocken, PA 2005

26 ASTM C 1260-05 Test Method for Potential Alkali Reactivity of Aggregates (Mortar-Bar Method). *American Society for Testing and Materials*, West Conshohocken, PA 2005

27 ASTM C 1293-05 Test Method for Determination of Length Change of Concrete Due to Alkali-Silica Reaction. *American Society for Testing and Materials*, West Conshohocken, PA 2005

28 ASTM C 1567-04 Test Method for Determining the Potential Alkali-Silica Reactivity of Combinations of Cementitious Materials and Aggregate (Accelerated Mortar-Bar Method). *American Society for Testing and Materials*, West Conshohocken, PA 2005

29 USGS (US Geological Survey), Recycled aggregates: profitable resource conservation. Feb 2000 <http://pubs.usgs.gov/fs/fs-0181-99/fs-0181-99po.pdf>

30 Federal Highway Administration, Transportation Applications of Recycled Concrete Aggregate. *FHWA State of the Practice National Review*, September 2004

31 Levy, S. M. and Helene P. Durability of Recycled Aggregates Concrete: A Safe Way to Sustainable Development. *Cement and Concrete Research*, V34 2004 pp. 1975-1980

32 Lauritzen, E. K. Recycling Concrete—an Overview of Challenges and Opportunities. ACI SP-219 American Concrete Institute Michigan 2004

33 Eighmy, T. T. and Magee B. The Road to Reuse. *Civil Engineering*, V15 No.5 Sep 2001 pp. 66-81

34 Liu, T. C. and Meyer, C. Recycling Concrete and Other Materials for Sustainable Development ACI SP-219 American Concrete Institute Michigan 2004

35 Otsuki, N., Miyazato, S. and Yodsudjai, W. Influence of Recycled Aggregate on Interfacial Transition Zone, Strength, Chloride Penetration and Carbonation of Concrete. *Journal of materials in Civil Engineering*, V15 No.5 2003 pp. 443-451

36 Shayan, A. and Xu, A., Performance and Properties of Structural Concrete Made With Recycle Concrete Aggregate. *ACI Materials Journal*, V100 No 5 2003 pp. 371-380

37 Recycled Materials Resource Center web resources: <http://www.rmrc.unh.edu>

38 Cuttell, G.D., Snyder, M.B., Vandenbossche, J.M. and Wade M. J. Performance of Rigid Pavements Containing Recycled Concrete Aggregates. *Transportation Research Record*, No. 1574 pp. 89-98

- 39 ASTM C 127-04 Test Method for Density, Relative Density (Specific Gravity), and Absorption of Coarse Aggregate. *American Society for Testing and Materials*, West Conshohocken, PA 2005
- 40 Salem, R. M., Burdette, E. G. and Jackson, N. M. Resistance to Freezing and Thawing of Recycled Aggregate Concrete. *ACI Materials Journal*, V100 No 3 2003 pp. 216-221
- 41 Taylor H. F. W. *Cement Chemistry 2nd Edition*, Thomas Telford Services Ltd., NY 1997
- 42 Brouwers, H.J.H. and Eijk R.J. van Alkali Concentrations of Pore Solution in Hydrating OPC. *Cement and Concrete Research*, V33 2003 pp. 191-196
- 43 ASTM C 114-05 Standard Test Methods for Chemical Analysis of Hydraulic Cement. *American Society for Testing and Materials*, West Conshohocken, PA 2005
- 44 Taylor H. F. W. A Method for Predicting Alkali Ion Concentrations in Cement Pore Solution. *Advance in Cement Research*, V1 No 1 October 1987 pp. 5-16
- 45 Hong, S-Y. and Glasser, F.P. Alkali Binding in Cement Paste Part I. The C-S-H Phase. *Cement and Concrete Research*, V29 1999 pp. 1893-1903
- 46 Hong, S-Y. and Glasser, F.P. Alkali Sorption by C-S-H And C-A-S-H Gels Part II. Role of Alumina. *Cement and Concrete Research*, V29 1999 pp. 1893-1903
- 47 Reardon, E.J. Problems and Approaches to the Prediction of Chemical Composition in Cement/Water System. *Waste Management*, V12 1992 pp. 221-239
- 48 Nolte J. *ICP Emission Spectrometry*, Wiley-VCH Weinheim Germany 2003
- 49 Westcott C.C. *pH Measurements*, Academic Press Inc. 1978
- 50 Raff, L.M. *Principles of Physical Chemistry 1st Edition*, Prentice-Hall Inc., NJ 2001
- 51 Shehata, M.H. ,Thomas, M.D.A. and Bleszynski, R. F. The Effect of Fly Ash Composition on the Chemistry of Pore Solution in Hydrated Cement Pastes. *Cement and Concrete Research*, V29 1999 pp. 1915-1920
- 52 Scott, H. C., and Gress, D. L. Mitigating Alkali Silica Reaction in Recycled Concrete. *Recycling Concrete and Other Materials for Sustainable development*, ACI SP-219, American Concrete Institute, Michigan 2004, pp. 61-76.
- 53 ASTM C 618-03 Specification for Coal Fly Ash and Raw or Calcined Natural Pozzolan for Use in Concrete. *American Society for Testing and Materials*, West Conshohocken, PA 2005

- 54 American Coal Ash Association, Inc Web resource <http://www.ACAA-USA.org>
- 55 Federal Highway Administration, *Fly Ash Facts for Engineers*, FHWA-IF-03-019, June 2003
- 56 Wang, A., Zhang, C. and Sun, W. Fly Ash Effects: I. The Morphological Effect of Fly Ash. *Cement and Concrete Research*, V33 2003 pp. 2023-2029
- 57 Wang, A., Zhang, C. and Sun, W. Fly Ash Effects: II. The Active Effect of Fly Ash. *Cement and Concrete Research*, V34 2004 pp. 2057-2060
- 58 Wang, A., Zhang, C. and Sun, W. Fly Ash Effects: III. The Microaggregate Effect of Fly Ash. *Cement and Concrete Research*, V34 2004 pp. 2061-2066
- 59 Shehata, M.H. and Thomas, M.D.A. The Effect of Fly Ash Composition on the Expansion of Concrete Due to Alkali-Silica Reaction. *Cement and Concrete Research*, V30 2000 pp. 1063-1074
- 60 Biernacki, J. J., Williams, P. J. and Stutzman, P.E. Kinetics of Reaction of Calcium Hydroxide and Fly Ash. *ACI Materials Journal*, V98 No.4 2001 pp. 340-349
- 61 Milton, J.S. and Arnold J.C. *Introduction to probability and statistics 2nd Edition*. McGraw-Hill 1990
- 62 Duchesne, J. and Berube, M-A. Effectiveness of Supplementary Cementing Materials in Suppressing Expansion Due to ASR: Another Look at The Reaction Mechanisms. Part I: Concrete Expansion and Portlandite Depletion. *Cement and Concrete Research*, V24 1994 pp. 73-82
- 63 Duchesne, J. and Berube, M-A. Effectiveness of Supplementary Cementing Materials in Suppressing Expansion Due to ASR: Another Look at The Reaction Mechanisms. Part 2: Pore Solution Chemistry. *Cement and Concrete Research*, V24 1994 pp.221-230
- 64 Bleszynski R.F. and Thomas, M.D.A. Microstructural Studies of Alkali-Silica Reaction in Fly Ash Concrete Immersed in Alkaline Solution. *Advanced Cement Based Materials*, V7 1998 pp. 66-78
- 65 American Iron and Steel Institute Web resource <http://www.steel.org>
- 66 Hooton, D., Donnelly, C. R., Clarida, B. and Rogers, C. A. An Assessment of the Effectiveness of Blast-Furnace Slag in Counteracting the Effects of Alkali-Silica Reaction. *11th International Conference on Alkali-Aggregate Reaction*, Quebec, Canada 2000
- 67 Thomas, M. D. A. and Innis, F. A. Effect of Slag on Expansion Due to Alkali-Aggregate Reaction in Concrete. *ACI Materials Journal*, V95 No.6 December 1998 pp.

716-744

68 ASTM C 1073-97a (2003) Standard Test Method for Hydraulic Activity of Ground Slag by Reaction with Alkali. *American Society for Testing and Materials*, West Conshohocken, PA 2005

69 Rasheeduzzafar and Hussain S.E. Effect of Microsilica and Blast Furnace Slag on Pore Solution Composition and Alkali-Silica Reaction. *Cement and Concrete Composite*, V13 1991 pp. 219-225

70 Bhanja, S. and Sengupta B. Optimum Silica Fume Content and Its Mode of Action on Concrete. *ACI Materials Journal*, V100 No.5 2003 pp. 407-412

71 Diamond, S., Sahu, S. and Thaulow N. Reaction Products of Densified Silica Fume Agglomerates in Concrete. *Cement and Concrete Research*, V34 2003 pp. 1625-1632

72 Rangaraju, P. R. and Olek, J. Evaluation of the Potential of Densified Silica Fume to Cause Alkali-Silica Reaction in Cementitious Matrices Using A Modified ASTM C 1260 Test Procedure *Cement, Concrete and Aggregates*, V22, n 2, December, 2000, pp. 150-159

73 Juenger, M.C.G. and Ostertag C.P. Alkali-Silica Reactivity of Large Silica Fume-Derived Particles. *Cement and Concrete Research*, V34 2003 pp. 1389-1402

74 Boddy, A.M., Hooton, R.D. and Thomas M.D.A. The Effect of the Silica Content of Silica Fume on its Ability to Control Alkali-Silica Reaction. *Cement and Concrete Research*, V33 2003 pp. 1263-1268

75 Wang, L, Seals, R.K. and Roy A. Investigation of Utilization of Amorphous Silica Residues as Supplementary Cementing Materials. *Advance in Cement Research*, V13 No 2 2001 pp. 85-89

76 Anderson, D., Roy, A., Seals, R.K., Cartledge, F.K., Akhter, H. and Jones, S.C. A Preliminary Assessment of the Use of an Amorphous Silica Residual as a Supplementary Cementing Material. *Cement and Concrete Research*, V30 2000 pp. 437-455

77 ASTM C162-99 Standard Terminology of Glass and Glass Products. *American Society for Testing and Materials*, West Conshohocken, PA 2002

78 Varshneya A.K. *Fundamentals of Inorganic Glasses*, Academic Press Inc. 1994

79 Jin, W. Alkali-Silica Reaction in Concrete with Glass Aggregate- A Chemo-Physico-Mechanical Approach. *PhD Dissertation*, Columbia University 1998

80 Shao, Y., Lefort, T., Moras, S. and Rodriguez, D. Studies on Concrete Containing Ground Waste. *Cement and Concrete Research*, V30 2000 pp. 91-100

- 81 Shi, C., Wu, Y., Riefler, C. and Wang, H. Characteristics and Pozzolanic Reactivity of Glass Powders. *Cement and Concrete Research*, V35 2005 pp. 987-993
- 82 Ramachandran, V.S. Alkali-Aggregate Expansion Inhibiting Admixtures. *Cement and Concrete Composite*, V20 1998 pp. 149-161
- 83 McCoy, W.J. and Caldwell, A.G. A New Approach to Inhibiting Alkali-Aggregate Expansion. *Journal of ACI*, V 47 1951 pp. 693-706
- 84 Folliard, K. J., Thomas, M.D.A and Kurtis, K. E. Guideline for the Use Of Lithium to Mitigate or Prevent Alkali-Silica Reaction (ASR). U.S. Department of Transportation, Federal Highway Administration FHWA-RD-03-047
- 85 Web resources <http://www.webelements.com/webelements/elements/text/Li/key.html>
- 86 Cotton, F.A., Wilkinson, G. and Gaus, P.L. *Basic Inorganic Chemistry 3rd Edition*, John Wiley & Sons, Inc, NY 1995
- 87 Oldham, K. B. and Myland, J. C. *Fundamentals of Electrochemical Science*, Academic Press Inc, 1994
- 88 USGS (US Geological Survey), Mineral yearbook, Lithium (2003). <http://minerals.usgs.gov/minerals/pubs/commodity/lithium/lithimyb03.pdf>
- 89 Kawamura M. and Fuwa H. Effects of Lithium Salts on ASR Gel Composition and Expansion of Mortars. *Cement and Concrete Research*, V33 2003 pp.913-919
- 90 Diamond, S. Unique Response of LiNO_3 as an Alkali Silica Reaction Preventive Admixture. *Cement and Concrete Research*, V29 1999 pp. 1271-1275
- 91 Stark D. Lithium Salt Admixtures-an Alternative Method to Prevent Expansive Alkali-Silica Reactivity. 9th *International Conference on Alkali-Aggregate Reaction*, London, UK 1992
- 92 Mo X, Yu, C. and Xu Z. Long-Term Effectiveness and Mechanism of LiOH in Inhibiting Alkali-Silica Reaction. *Cement and Concrete Research*, V33 2003 pp.115-119
- 93 Thomas, M.D.A, Hooper, R. and Stokes, D. Use of Lithium-Containing Compounds to Control Expansion in Concrete Alkali-Silica Reaction. 11th *International Conference on Alkali-Aggregate Reaction*, Quebec Canada 2000
- 94 Ramyar, K., Copuroglu, O., Andic, O. and Fraaij, A.L.A. Comparison of Alkali-Silica Reaction Products of Fly Ash or Lithium-Salt-Bearing Mortar under Long Term Accelerated Curing. *Cement and Concrete Research*, V34 2004 pp. 1179-1183
- 95 Rodrigues, F. A., Monteiro, P.J.M and Sposito, G. The Alkali Silica Reaction: The

Surface Charge Density of Silica and its Effect on Expansive Pressure. *Cement and Concrete Research*, V29 1999 pp. 527-530

96 Rodrigues, F. A., Monteiro, P.J.M and Sposito, G. The Alkali Silica Reaction: The Effect of Monovalent and Bivalent Cations on the Surface Charge of Opal. *Cement and Concrete Research*, V31 2001 pp. 1549-1552

97 Mitchell L. D., Beaudoin J. J. and Grattan-Bellew P. The Effects of Lithium Hydroxide on Alkali Silica Reaction Gels Created With Opal. *Cement and Concrete Research*, V34 2004 pp. 641-649

98 Collins, C.L., Ideker, J.H., Willis, G.S. and Kurtis, K.E. Examination of Effects of LiOH, LiCl, and LiNO₃ on Alkali-Silica Reaction. *Cement and Concrete Research*, V34 2004 pp. 1403-1415

99 Wijnen, P.W.J.G, Beelen, T.P.M. [de Haan, J.W.](#); [Rummens, C.P.J.](#); [van de Ven, L.J.M.](#); and [Van Santen, R.A.](#) Silica Gel Dissolution in Aqueous Alkali Metal Hydroxides Studied By ²⁹Si-NMR. *Journal of Non-Crystalline Solids*, V109, n 1, May, 1989, pp. 85-94

100 Chatterji S., Thalow, N. and Jensen, A.D. Studies of the Alkali-Silica Reaction. Part 4: Effect of Different Alkali Salt Solutions on Expansion. *Cement and Concrete Research*, V17 1987 pp. 777-783

101 Kurtis, K.E. and Monteiro, P.J.M. Chemical Additives to Control Expansion of Alkali-Silica Reaction Gel: Proposed Mechanisms of Control. *Journal of Materials Science*, V38, 2003, pp. 2027-2036

102 Gaboriaud, F., Nonat, A., Chaumont, D., Craievich, A. and Hanquet, B. Study of the Influence of Alkaline Ions(Li, Na And K) on the Structure of the Silicate Entities in Silico Alkaline Sol and the Formation of Silico-Calco-Alkaline Gel. *Journal of Sol-gel Science and Technology*, V13 1998 pp. 353-358

103 Gaboriaud, F., Nonat, A., Chaumont, D., Craievich, A. and Hanquet, B. ²⁹Si NMR and Small-Angle X-Ray Scattering Studies of the Effect of Alkaline Ions (Li⁺, Na⁺ and K⁺) in Silico-Alkaline Sols. *Journal of Physical Chemistry B*, V103 1999 pp. 2091-2099

104 Berra, M., Mangialardri T., and Paolini, E. Use of Lithium Compounds to Prevent Expansive of Alkali-Silica Reactivity in Concrete. *Advances in Cement Research*, V15 2003 No. 4 October pp. 145-154

105 Berube, M-A., Tremblay, C, Fournier, B., Thomas, M.D. and Stokes D.B. Influence of Lithium-Based Products Proposed for Counteracting ASR on the Chemistry of Pore Solution and Cement Hydrates. *Cement and Concrete Research*, V34 2004 pp.1645-1660

106 Whitmore, D. and Abbott, S. Use of an Applied Electric Field to Drive Lithium Ions

into Alkali-Silica Reactive Structures. *11th International Conference on Alkali-Aggregate Reaction*, Quebec, Canada 2000

107 Johnston D.P., Surdahl, R. and Stoke, D.B. A Case Study of a Lithium Based Treatment of an ASR-Affected Pavement. *11th International Conference on Alkali-Aggregate Reaction* , Quebec, Canada 2000